Universidade de Aveiro

Departamento de Electrónica, Telecomunicações e Informática

2014

Alícia Mafalda de Figueiredo Paiva João

Técnicas de equalização e pré-codificação para Sistemas MC-CDMA

Equalization and precoding techniques for future MC-CDMA systems

Universidade de Aveiro

Departamento de Electrónica, Telecomunicações e Informática

2014

Alícia Mafalda de Figueiredo Paiva João

Técnicas de equalização e pré-codificação para Sistemas MC-CDMA

Equalization and precoding techniques for future MC-CDMA systems

Dissertação apresentada à Universidade de Aveiro para cumprimento dos requisitos necessários à obtenção do grau de Mestre em Engenharia Electrónica e Telecomunicações, realizada sob a orientação científica do Professor Doutor Adão Silva (orientador), Professor Auxiliar e do Professor Doutor Atílio Gameiro (co-orientador), Professor Associado ambos do Departamento de Electrónica, Telecomunicações e Informática da Universidade de Aveiro.

“Para ser grande, sê inteiro: nada
Teu exagera ou exclui.

Sê todo em cada coisa. Põe quanto és
No mínimo que fazes.

Assim em cada lago a lua toda
Brilha, porque alta vive”

Ricardo Reis, *in “Odes”*

o júri / the jury

presidente / president

Professor Doutor António Luís Jesus Teixeira
Professor Associado c/ Agregação do Departamento de Electrónica, Telecomunicações e Informática
Universidade de Aveiro

vogais / examiners committee

Professor Doutor Paulo Jorge Coelho Marques
Professor Adjunto do Departamento de Engenharia Electrotécnica
Escola Superior de Tecnologia do Instituto Politécnico de Castelo Branco

Professor Doutor Adão Paulo Soares Silva
Professor Auxiliar do Departamento de Electrónica, Telecomunicações e Informática
Universidade de Aveiro

agradecimentos

"Teoria, poesia e prática" é o lema da Universidade de Aveiro, lar do Departamento de Electrónica, Telecomunicações e Informática. Ambos ficarão para sempre gravados na minha memória.

Encontro-me a terminar mais um ciclo da minha vida e é com grande alegria que agradeço a todas as pessoas que a enchem de cor, versos, rimas e estrofes.

Primeiramente, agradeço a todos os que embarcaram comigo nesta aventura: ao professor Adão Silva, pela sua orientação e disponibilidade ao longo deste ano, e aos meus colegas Francisco Oliveira e José Assunção, por estarem sempre disponíveis para me ajudarem.

Agradeço à minha mãe, ao meu pai e ao meu irmão, pela força, paciência e ânimo que sempre me transmitiram. Muito obrigada por me ampararem nas quedas e me impulsionarem nas subidas.

Gostaria ainda de agradecer a todos os Professores que entraram na minha vida. Muito obrigada por compartilharem comigo o vosso tempo, o vosso conhecimento e a vossa sabedoria. Ao amigo António Roldão, agradeço pela disponibilidade e compreensão ao longo destes meses.

Agradeço, também, a todos os meus amigos, por me trazerem o sol em dias de tempestade. Muito obrigada por me ouvirem e por me apoiarem incondicionalmente.

Por fim, agradeço, ainda, a todos, cujas suas histórias nos inspiram a trabalhar e a acreditar que o impossível se pode um dia tornar realidade.

palavras-chave LTE, LTE-Advanced, OFDM, MC-CDMA, MIMO, IA, IB-DFE, SIC

resumo

O número de dispositivos com ligações e aplicações sem fios está a aumentar exponencialmente, causando problemas de interferência e diminuindo a capacidade do sistema. Isto desencadeou uma procura por uma eficiência espectral superior e, consequentemente, tornou-se necessário desenvolver novas arquitecturas celulares que suportem estas novas exigências.

Coordenação ou cooperação multicelular é uma arquitectura promissora para sistemas celulares sem fios. Esta ajuda a mitigar a interferência entre células, melhorando a equidade e a capacidade do sistema. É, portanto, uma arquitectura já em estudo ao abrigo da tecnologia LTE-Advanced sob o conceito de coordenação multiponto (CoMP). Nesta dissertação, considerámos um sistema coordenado MC-CDMA com pré-codificação e equalização iterativas.

Uma das técnicas mais eficientes de pré-codificação é o alinhamento de interferências (IA). Este é um conceito relativamente novo que permite aumentar a capacidade do sistema em canais de elevada interferência. Sabe-se que, para os sistemas MC-CDMA, os equalizadores lineares convencionais não são os mais eficientes, devido à interferência residual entre portadoras (ICI). No entanto, a equalização iterativa no domínio da frequência (FDE) foi identificada como sendo uma das técnicas mais eficientes para lidar com ICI e explorar a diversidade oferecida pelos sistemas MIMO MC-CDMA. Esta técnica é baseada no conceito *Iterative Block Decision Feedback Equalization* (IB-DFE).

Nesta dissertação, é proposto um sistema MC-CDMA que une a pré-codificação iterativa do alinhamento de interferências no transmissor ao equalizador baseado no IB-DFE, com cancelamento sucessivo de interferências (SIC) no receptor. Este é construído por dois blocos: um filtro linear, que mitiga a interferência inter-utilizador, seguido por um bloco iterativo no domínio da frequência, que separa eficientemente os fluxos de dados espaciais na presença de interferência residual inter-utilizador alinhada. Este esquema permite atingir o número máximo de graus de liberdade e permite simultaneamente um ganho óptimo de diversidade espacial. O desempenho deste esquema está perto do filtro adaptado- *Matched Filter Bound* (MFB).

keywords LTE, LTE-Advanced, OFDM, MC-CDMA, MIMO, IA, IB-DFE, SIC

abstract

The number of devices with wireless connections and applications is increasing exponentially, causing interference problems and reducing the system's capacity gain. This initiated a search for a higher spectral efficiency and therefore it became necessary to develop new cellular architectures that support these new requirements.

Multicell cooperation or coordination is a promising architecture for cellular wireless systems to mitigate intercell interference, improving system fairness and increasing capacity, and thus is already under study in LTE-Advanced under the coordinated multipoint (CoMP) concept. In this thesis, efficient iterative precoding and equalization is considered for coordinated MC-CDMA based systems.

One of the most efficient precoding techniques is interference alignment (IA), which is a relatively new concept that allows high capacity gains in interfering channels. It is well known that for MC-CDMA systems standard linear equalizers are not the most efficient due to residual inter carrier interference (ICI). However, iterative frequency-domain equalization (FDE) has been identified as one of the most efficient technique to deal with ICI and exploit the inherent space-frequency diversity of the MIMO MC-CDMA systems, namely the one based on Iterative Block Decision Feedback Equalization (IB-DFE) concept.

In this thesis, it is proposed a MC-CDMA system that joins iterative IA precoding at the transmitter with IB-DFE successive interference cancellation (SIC) based receiver structure. The receiver is implemented in two steps: a linear filter, which mitigates the inter-user aligned interference, followed by an iterative frequency-domain receiver, which efficiently separates the spatial streams in the presence of residual inter-user aligned interference. This scheme provides the maximum degrees of freedom (DoF) and allows almost the optimum space-diversity gain. The scheme performance is close to the matched filter bound (MFB).

Table of Contents

List of Figures

List of Tables

Acronyms

1G	1st Generation
1xRTT	One Carrier Radio Transmission Technology
2G	2nd Generation
3G	3rd Generation
3GPP	3rd Generation Partnership Project
3GPP2	3rd Generation Partnership Project 2
4G	4th Generation
8-PSK	8 Phase Shift Keying
AMPS	Advanced Mobile Phone Services
AWGN	Additive White Gaussian Noise
BER	Bit Error Ratio
BPSK	Binary Phase-Shift Keying
BS	Base Station
CC	Component Carrier
CDD	Cyclic Delay Diversity
CDMA	Code Division Multiple Access
CoMP	Coordinated Multipoint Transmission
CP	Cyclic Prefix
CPU	Central Processing Unit
CRS	Common Reference Signal
CSI	Channel State Information
DM-RS	Demodulation Reference Signal
DoF	Degrees of Freedom
DS-CDMA	Direct Sequence CDMA
DS-SS	Direct Sequence Spread Spectrum
EDGE	Enhanced Data Rate For Global Evolution
EGC	Equal Gain Combining
eNB	Evolved Node B.
E-UTRA	Evolved UMTS Terrestrial Radio Access
EV-DO	Evolution Data Optimized
FDD	Frequency Division Duplexing
FDE	Frequency Domain Equalization
FDMA	Frequency Division Multiple Access
FFT	Fast Fourier Transform
FSTD	Frequency Shift Transmit Diversity
GSM	Global System for Mobile Communications
GPRS	General Packet Radio Service
HSCSD	High-Speed Circuit-Switched Data
HSDPA	High Speed Downlink Packet Access
HSPA	High Speed Packet Access

HSUPA	High Speed Uplink Packet Access
IA	Interference Alignment
IB-DFE	Iterative-Block Decision Feedback Equalization
IC	Interference Cancellation
ICI	Inter-carrier Interference
IFFT	Inverse Fast Fourier Transform
IL	Interference Leakage
IMT-Advanced	International Mobile Telecommunications-Advanced
ISI	Intersymbol Interference
ITU-R	International Telecommunications Union Radiocommunications sector
LAN	Local Area Network
LTE	Long Term Evolution
MAP	Maximum a Posteriori
MC-CDMA	Multicarrier - Code Division Multiple Access
MCS-L1	Mobile Communication System L1
MFB	Matched Filter Bound
MIMO	Multiple-Input Multiple-Output
MISO	Multiple-Input Single-Output
ML	Maximum Likelihood
MLSE	Maximum Likelihood Sequence Estimation
MMSE	Minimum Mean Square Error
MMSEC	Minimum Mean Square Error Combining
MRC	Maximal Ratio Combining
MUD	Multi-User Detection
MU-MIMO	Multiuser Multiple-Input Multiple-Output
NMT	Nordic Mobile Telephone
OFDM	Orthogonal Frequency Division Multiplexing
PAPR	Peak-to-Average Power Ratio
PIC	Parallel Interference Cancellation
PMI	Precoding Matrix Indicator
QAM	Quadrature Amplitude Modulation
QPSK	Quadrature Phase-Shift Keying
SC	Single Carrier
SC-FDE	Single Carrier Frequency Domain Equalization
SFBC	Space-Frequency Block Coding
SIC	Successive Interference Cancellation
SIMO	Single-Input Multiple-Output
SISO	Single-Input Single-Output
SM	Spatial Multiplexing
SNR	Signal-to-Noise Ratio
STBC	Space-Time Block Code
SUD	Single-User Detection
SVD	Singular Value Decomposition

TDMA	Time Division Multiple Access
TDD	Time Division Duplexing
TM	Transmission Mode
UE	User Equipment
UFR	Universal Frequency Reuse
UTRA	UMTS Terrestrial Radio Access
UTRAN	Universal Terrestrial Radio Access Network
WCDMA	Wideband Code Division Multiple Access
WLAN	Wireless Local Area Networks
ZFC	Zero Forcing Combining

1. Introduction

1.1. Evolution of Cellular Communications Systems

The first public telephone call placed on a portable phone took place on April 3 of 1973 by Martin Cooper. On its 30th anniversary, he said "People want to talk with other people – not a house, or an office, or a car. Given a choice, people will demand the freedom to communicate wherever they are, unfettered by the infamous cooper wire. It is that freedom we sought to vividly demonstrate in 1973" [1]. Perhaps this is the main reason behind the widely spreading of cell phones among the world population.

At first, they were considered luxury items and the voice quality was poor when the access existed at all. Nowadays mobile phones are an integral part of our life, being used in everyday situations like communication, navigation, multimedia, and entertainment [2]. This incredible device allows us to be in connection with everyone in any place at any time. It changed us and the way we are brought together. For example, if we are running late for a meeting it is expected from us to inform others [3]. However, cell phones were voted the most hated invention that Americans cannot live without beating alarm clocks, television, razors, microwave ovens, computers, and answering machines [2]. In Figure 1.1, we can see the four generations and some technologies that represent them.

1st generation (1G) systems were characterized by their analog voice transmission nature. First commercial 1G cellular systems appeared between 1979 and 1983. In this period were introduced Mobile Communication System L1 (MCS-L1) in Japan, Nordic Mobile Telephone (NMT) in Northern Europe and Advanced Mobile Phone Services (AMPS) in U.S. [2]. These systems are similarly advanced and worked fairly based on the same rules but they were incompatible with each other. This means that every user was assigned to their operator and their cell phone would not properly function outside the operator's cover area (except for NMT) [4].

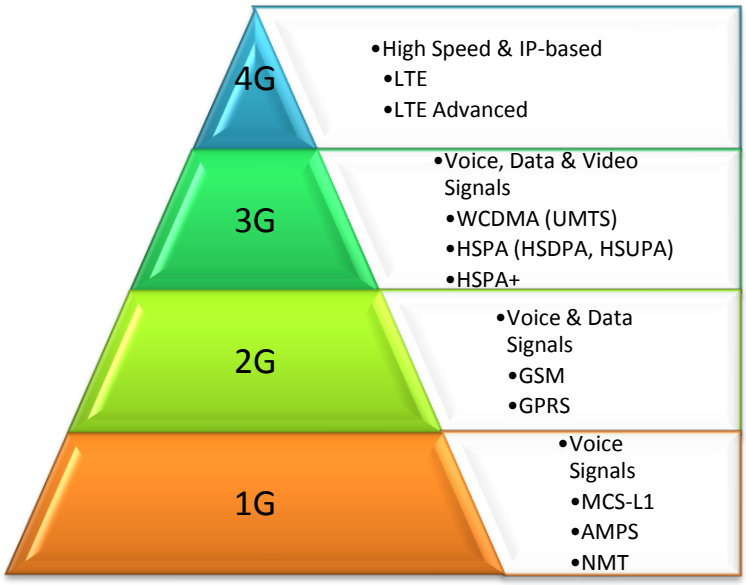

Figure 1.1: Illustration of generations and technologies

In 1990s, the first generation was gradually replaced by the 2nd generation (2G). These new systems were digital, offering better voice quality and providing the first data services [2]. To solve the roaming problem, European Union created a working group that had the task of formulating the objectives and standards of a common cellular system. And so was born Global System for Mobile Communications (GSM) [4]. GSM is the most widely used wireless technology in the world, and it is available in more than 219 countries [5]. We can observe in Figure 1.2, 65% of total cellular connections were GSM at the end of 2013 [6].

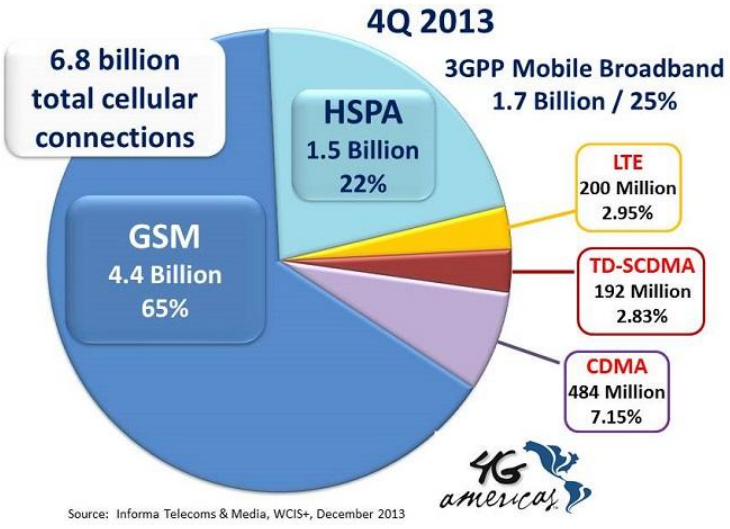

Figure 1.2: Mobile Market Shares by Technology [6]

GSM technology uses Frequency Division Duplex (FDD), meaning that downlink (transmission from base station to mobile station) and uplink (transmission from mobile station to base station) have different frequency bands. GSM can also use both Frequency Division Multiple

Access (FDMA) and Time Division Multiple Access (TDMA) in order of supporting multiple users [4]. Another large 2G system widely used by 1996 was CDMAOne or standard IS-95A. The main difference between these two systems is IS-95A based systems which allow simultaneous transmissions in the same frequency band. This feature was achieved by using direct sequence spread spectrum (DS-SS) techniques and by assigning each user a unique pseudorandom noise code. Between codes there was low correlation. The spectral inefficiency caused by both voice and data transmissions triggered an evolution to what is called a 2.5G. General Packet Radio Service (GPRS) is a GSM extension which allowed data ratings from 10 to 115 kbps and average around 40 kbps [2]. Even though these were moderated data ratings, there was still the need to increase them thus resulting in the arising of Enhanced Data Rate for Global Evolution (EDGE). It has a data rate three times higher than GSM because it uses 8-PSK modulation, meaning that for each data symbol three bits were transmitted [4]. EDGE also introduced High-Speed Circuit-Switched Data (HSDCSD) service which allowed transferring more data in each time slot. In packet-switched mode, the data transmission speed was up to 384 kbps [7].

In this endless pursuit of higher data transfer ratings it was introduced the 3rd generation (3G). 3G uses different techniques for radio transmission a reception to achieve more efficiency in spectrum's use. We were able to achieve bit rates up to 2 Mbps and multiplexing various services with different requirements on one channel [8]. At first, its appearance was quite unsuccessful due to high performance expectations and only after 3.5G introduction its performance was sufficed [9]. The International Telecommunication Union – Radiocommunication sector created the IMT-2000 standard which had the purpose of unifying all wireless systems in the same frequency bands, including cellular, Wireless Local Area Networks (WLAN), satellite networks and fixed wireless links. WLAN and fixed wireless links were removed from the original IMT-2000 because of higher data rates in unlicensed bands and better operation on higher frequencies, respectively. In order to establish a universal set of specifications two major competitive concepts were created, both based on CDMA techniques: Wideband Code Division Multiple Access (WCDMA) and CDMA 2000 [2].

3GPP was responsible for the release of 3G technology called Universal Mobile Terrestrial System (UMTS), which incorporated WCDMA as its air-interfaced technology. UMTS system has channel bandwidth of 5MHz for uplink and downlink. Also, in Europe, it presented seven unpaired channels within 1900-1920 MHz and 2010-2025 MHz. In USA and Japan, at least one of these bands was already occupied preventing European and Japanese systems from operating in the USA, for example [8]. Due to this problem the 3GPP2 was created, which managed the CDMA2000 specifications [2]. It was an evolution from IS-95, called CDMA2000 One Carrier Radio Transmission Technology (1xRTT) deployed in 2000. It has a bandwidth of 1.25MHz. Unlike UMTS, it is backwards compatible with the previous technology (IS-95) and separates onto different carrier frequencies data and voice. Eventually both technologies were enhanced to a 3.5G, UMTS became High Speed Packet Access (HSPA) and 1xRTT became Evolution Data Optimized (EV-DO) [9]. HSPA actually represents different advances in both downlink (HSDPA, High Speed Downlink

Packet Access) and uplink (HSUPA, High Speed Uplink Packet Access) directions. HSPA's networks elements are similar to those used by its predecessor WCDMA but it needs a different User Equipment (UE). HSPA enhancement allowed peak data rates increasing to 14 Mbps downlink and 5.8 Mbps uplink. On the other hand, EV-DO provides high speed data services to both mobile and broadband subscribers. On its later releases it offered multicast services allowing the same information to be transmitted to an unlimited number of users. MP3files and files are among the transmitting applications circulating over the network [8].

Although through the evolution of mobile phones its data traffic was slowly increasing, is with the introduction of Apple iphone in 2007 and Google's Android operating system a year later that data traffic became relevant and dominant (at the end of 2009). In order to increase the system capacity, it was proposed to improve the communication technology so we can exploit a higher SINR and a greater bandwidth. Moreover, 2G and 3G had two distinct core networks: one circuit switched domain for voice and the packet switch domain for data. It was an objective to transport voice calls over packed switched networks by using voice over IP (VoIP), merging both networks in one and reducing capital and operational costs. 3G had the additional problem of latency because those networks introduced a delay of the order of 100 milliseconds for data applications transference which is almost unacceptable for voice and real-time interactive games. LTE, Long Term Evolution, presented itself as a solution for these problems [9].

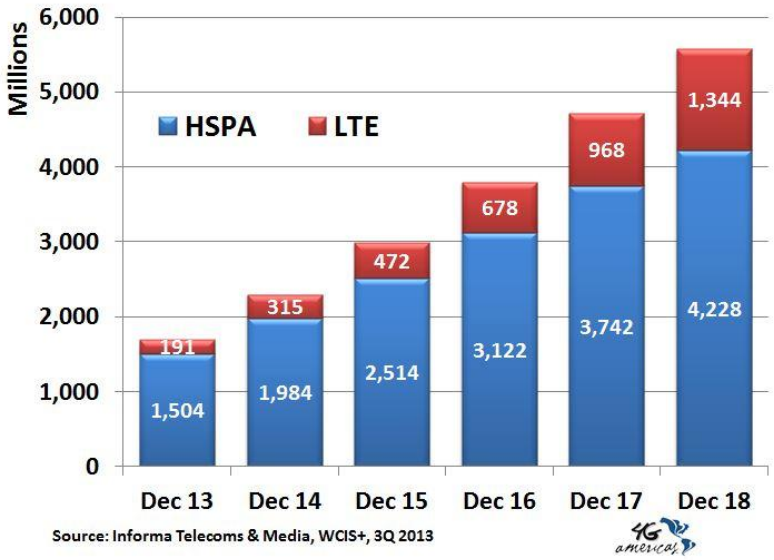

Figure 1.3: Global HSPA-LTE Forecast [10]

LTE is currently on the market and it was introduced in 3GPP Release 8 which was frozen in December 2008. LTE is a milestone in wireless communications history because for the first time a wide-area wireless network is universally deployed. From the beginning, LTE provided the highest rates, smallest radio network delay and significant spectral efficiency increase. Moreover, the operational cost is smaller than its predecessors because its architecture was designed to shorten

the operations. LTE systems support Frequency Division Duplex (FDD) and Time Division Duplex (TDD), allowing a different spectrum allocation [11]. LTE was required to have a peak data rate of 100 Mbps in the downlink and 50 Mbps in the uplink [12] but this performance was exceeded because today's system has peak data rates of 300 Mbps and 75 Mbps respectively [13]. In Figure 1.3 we can see that the number of LTE users will probably increase exponentially in the coming years.

The International Telecommunications Union Radiocommunication Sector (ITU-R) introduced the International Mobile Telecommunications Advanced (IMT-Advanced) list. This list was intended to recognize new cellular system and begin a brand new generation. Since 2009, 3GPP tried to perform enhancements in LTE technology in order to meet the IMT-Advanced requirements. Later that year, it was proposed a new ITU system, represented by LTE release 10 or LTE-Advanced. Besides using LTE's spectrum bands, it also uses some bands predicted by IMT-Advanced. LTE-Advanced aims to achieve a peak data rate of 1 Gbps in downlink and 500 Mbps in the uplink in a cost efficient way [11] [13] [14]. Both LTE and LTE-Advance will be presented with more detail in chapter 3.

1.2. Multicarrier Based Systems

The basic principle behind multicarrier systems is dividing a stream of data in sub-streams in parallel, which are transmitted in different frequencies or subcarriers. Digital systems promoted data transmission over several carriers, becoming the technique of choice for wireless communication systems [15]. The main reasons for this success are the equalization simplicity and robustness in multipath propagation scenarios. Most of multicarrier commercial systems are based on OFDM modulation [15] [16] [17] [18]. The multicarrier option is an integral part of the 4G technology specifications.

The spread spectrum techniques (namely the Direct Sequence CDMA (DS-CDMA) adopted in UMTS) and the OFDM success created the conditions needed for the merger of the two technologies, resulting in three different schemes: MC-DS-CDMA, Multitone CDMA (or MT-CDMA) and MC-CDMA. The first is a series-parallel conversion of the original data symbols in sub-streams and, then spread in time with a specific code for each user. The MT-CDMA can be considered a special case of MC-DS-CDMA, where carriers are overlapping. The spreading is done in the time domain too and it also uses a small number of overlapping carriers with a large bandwidth. The last scheme is made by a large number of orthogonal subcarriers with reduced bandwidth, and typically has an OFDM based modulation. Unlike the previous schemes, the spreading is done in the frequency domain, i.e., the spread data symbols are transmitted on different subcarriers. MC-CDMA benefits from OFDM characteristics such as high spectral efficiency and robustness against multi-path propagation, while CDMA allows a flexible multiple access with good interference

properties [19] [20]. However, the user capacity of MC-CDMA system is essentially limited by interference. The MC-CDMA scheme will be presented with more detail in subchapter 2.3.

1.3. Motivation and Objectives

Long Term Evolution (LTE) is considered to be the beginning of the 4th generation of mobile technology. LTE transmission rates are higher than 3G systems [9]. However, as we could observe in Figure 1.3, the number of 4G users is expected to increase exponentially, increasing the demand for broadband services, rendering the actual cellular architecture obsolete. By reducing the cell size, thus reducing propagation losses, it is possible to achieve higher transmission rates. This solution is not perfect because it produces a considerable increase on the user interference at cells borders due to the unitary frequency reuse, degrading system performance. In today's systems, eliminating inter-cell interference is done by assigning different frequencies to adjacent cells and thus wasting system capacity. Universal frequency reuse (UFR) is crucial to achieve high system's capacity but this requires new architectures to efficiently eliminate the interference between mobile terminals at cell's borders. Multicell cooperation or coordination is a promising architecture for cellular wireless systems to mitigate intercell interference, improving system fairness and increasing capacity, and thus is already under study in LTE-Advanced under the coordinated multipoint (CoMP) concept.

To achieve the high bit rates needed to meet the quality of service requirements of future multimedia applications, multi-carrier code division multiple access (MC-CDMA) has been considered as good air-interface candidate, especially for the downlink [21]. However, as discussed in previous section MC-CDMA is essentially limited by the interference. This interference can be mitigated by employing precoding techniques [22] and/or iterative block decision feedback equalization (IB-DFE) based receivers [23].

Conventional frequency domain equalization (FDE) schemes employ a linear FDE optimized under the minimum mean square error (MMSE) criterion. However, the residual interference levels might still be too high, leading to performance that is still several dB from the matched filter bound (MFB) [24]. Nonlinear frequency domain equalizers (FDEs) are known to outperform linear equalizers and are known to have good performance-complexity tradeoffs [25]. For this reason, there has been significant interest in the design of nonlinear FDEs, with the IB-DFE being the most promising nonlinear FDE [24].

Recently, analysis of interference channels has shown that each user's capacity on an interference channel is one half the rate of its interference-free capacity in the high transmit power regime, regardless of the number of users [26]. One interesting scheme to efficiently eliminate the inter-user interference and achieve a linear capacity scaling is interference

alignment (IA) [26]. This recent technique allows the transmitters to align in the unwanted users' receive signals in any dimension, through the use of precoders. With this strategy more interferers can be completely cancelled than with other interference cancellation methods, thus achieving the maximum degrees of freedom (DoF) [27]. Applications of IA include cellular networks, two-way communication networks, cooperative communication networks, cognitive radio networks, etc. [28].

In this thesis we consider MIMO MC-CDMA systems with iterative IA precoding at transmitter and iterative frequency-domain receivers based on the IB-DFE concept. The main motivation to consider this combination, is that IA based techniques achieve the maximum DoF in MIMO interference channels. However, they cannot by themselves efficiently exploit the space-frequency diversity inherent of the MIMO MC-CDMA systems. On the other hand, IB-DFE based receivers are well known to be one of the most efficient techniques to exploit this space-frequency diversity. Therefore, this combination allows us to design a system that is able to achieve maximum DoF (number of spatial stream per subcarrier) and exploit the high diversity order inherent to these systems. In this work the joint IB-DFE parallel interference cancellation (PIC) and IA scheme, recently proposed to MC-CDMA systems [29], is extended to IB-DFE successive interference cancellation (SIC). The results of the proposed IB-DFE SIC based approach are compared with the IB-DFE PIC one. The results have shown that the proposed receiver structure is robust to the residual inter-user aligned interference and quite efficient to separate the spatial streams, while allowing a close-to-optimum space-diversity gain, with performance close to the MFB with only a few iterations of the equalizer.

1.4. Contributions

The main results of this thesis were recently published in an international conference,

Alícia João, José Assunção, Adão Silva, Rui Dinis and Atílio Gameiro, “IB-DFE SIC based Receiver Structure for IA-Precoded MC-CDMA Systems”, in proceedings of the 22nd European Signal Processing Conference (EUSIPCO 2014), Lisbon, Portugal.

1.5. Outline

After the introduction about the evolution of mobile systems until today, the motivation and objectives, we present the following chapters:

In chapter 2, it is presented the OFDM/OFDMA and MC-CDMA multicarrier systems. We will overview their characteristics and some useful techniques against interference such as orthogonality and introduction of a cyclic prefix. Later in this chapter, we will also see some detection techniques both in single user case and multi-user case.

In chapter 3, we will start to discuss the three multiple antenna formats, the different types of diversity, spatial multiplexing and beamforming. In this chapter is also presented LTE system as a product of the combination of different technologies presented in the previous chapters. We will start with general network architecture, followed by an overview of LTE physical layer and an abbreviated description of LTE MIMO transmission modes in downlink. Later in this chapter is presented LTE-Advanced, where we will briefly discuss some technologies (like carrier aggregation, MIMO enhancements and CoMP) that were introduced in order to fulfill IMT-Advanced goals.

Following, in chapter 4, it is studied the interference alignment (IA) and the iterative equalization concepts. In this chapter is presented some interference alignment applications, such as index coding, X channel and, more importantly the closed form interference alignment for three users. After, we will present the iterative equalization for single carrier systems, focusing on IB-DFE concept.

In chapter 5, it is presented the IB-DFE SIC based receiver structure with IA-precoded MC-CDMA systems. Firstly, it is described the system model of an IA-precoded MC-CDMA based system. We will study in some detail the signal processing at the receiver and at the transmitter. We will present, analyze and compare the Bit Error Ratio (BER) obtained with precoding IA and with IB-DFE PIC/SIC based procedure with different parameters.

The last chapter is chapter 6, where it is presented work conclusions and some possible future research guidelines.

It is important to note that in this thesis, it will be used the following notation: Lowercase letters, boldface lowercase letters and boldface uppercase letters are used for scalars, vectors and matrices, respectively. $(.)^H$ and $(.)^T$ represents the complex conjugate transpose and transpose operators, $\mathrm{E}[.]$ represents the expectation operator, $\mathbf{I}_N$ is the identity matrix of size $N \times N$, $\mathrm{CN}(.,.)$ denotes a circular symmetric complex Gaussian vector, and $\{a\}$ represents a L-length block.

2. Multicarrier Systems

In a Single Carrier (SC) transmission, the information is modulated in only one carrier, adjusting phase, amplitude or frequency. If a system has a high data rate, it has a high symbol rate in a digital system meaning that its bandwidth is also high [30]. In a multicarrier transmission, the transmitted high-data-rate is divided into many different sub streams which are sent through many different sub-channels. In ideal case, the sub-channels would be orthogonal. Because of the division in the high-data-rate, the data rate of each sub-channel will be lower than the total data rate, and the corresponding sub-channel bandwidth is also lower than the total system bandwidth. The number of sub-channels is chosen so each sub-channel has a bandwidth smaller than the coherence bandwidth. Moreover, the sub-channels don't need to be contiguous, being efficiently implemented digitally [31]. In this chapter, it will be presented an overview of some multicarrier systems like OFDM, OFDMA and MC-CDMA. Later it will be also presented the detection techniques.

2.1. Orthogonal Frequency Division Multiplexing (OFDM)

OFDM is a modulation technique that is used for high-data-rate transmission in delay-dispersive environments and it is a multicarrier system. Figure 2.1 shows a conversion of a high-data-rate into a number of low-rate streams that are transmitted over parallel narrowband channels. This decrease in data rate makes the equalization a lot less complex [32].

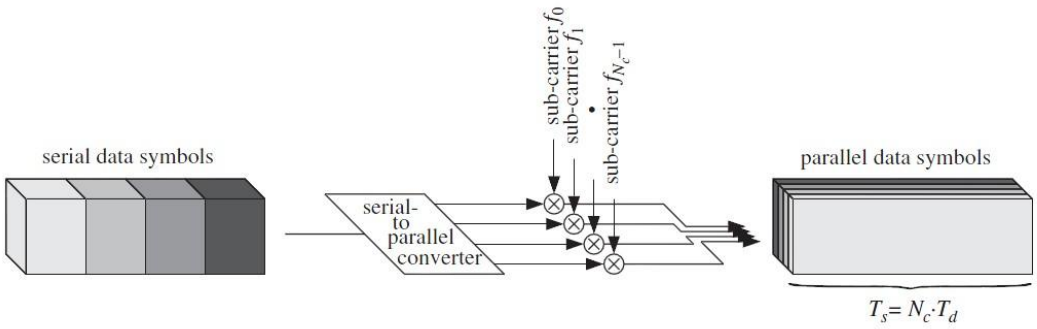

Figure 2.1: Multi-carrier modulation with N_c =4 sub-channels [33]

In an OFDM system with N_C subcarriers will be transmitted N_c data symbols in parallel, each modulated into a different subcarrier. The duration of an OFDM symbol is:

$$T_S = N_C T_d. \quad (2.1)$$

The spacing between subcarriers is given by:

$$\Delta f = \frac{1}{T_S} \quad (2.2)$$

and the frequency of each subcarrier is:

$$f_n = n\Delta f \quad (2.3)$$

where $n = 0, \dots, N_C - 1$.

So, each carrier is modulated by a data symbol, meaning that an OFDM is composed by the addiction of the different symbols in different subcarriers [30] [33].

Assuming that the OFDM symbol is periodic and all requirements about minimum sampling rates and word lengths are met, we can use Fast Fourier Transform (FFT) and Inverse Fast Fourier Transform (IFFT). This mathematical tool allows us to move back and forth between time and frequency domains on the receiver and transmitter without loss of information [30].

2.1.1. Modulation

The modulation of a multicarrier system starts by dividing the bit stream into N_C substreams. Each substream is modulated with bandwidth of B/N_C, where B is the bandwidth of the signal in a single carrier modulation. These are sent in separate subcarriers in separated subchannels. As we saw previously, the space between carriers is given by (2.2) which, for flat fading (and no ISI), lower than coherence band.

Basically, what we accomplish with using a multicarrier instead of a single carrier is a higher duration symbol for the same baud rate. For example, in a single carrier system with a baud rate, in symbols/s, the duration of a symbol is $T_d|_{SC} = 1/R$. On the other hand, for the same R, the duration of a multicarrier symbol is $T_d|_{MC} = N_C/R$.

As we can see, if we increase the number of subcarriers, the duration of the symbol will also increase, resulting in a more robust transmission to channel distortion, fading, and noise and reducing ISI [34].

2.1.2. Orthogonality

Other types of modulation (e.g. FDMA) require a guard band which causes loss of efficiency because there is a part of the spectrum we are not using. OFDM allows the overlapping of the subcarriers, transmitting additional subcarriers in a tight frequency space without interference from each other. We can conclude that all subcarriers are orthogonal between themselves, transmitting pulses at a rate $1/T$ within a bandwidth $1/(2T)$ without ISI [35]. Mathematically, considering Figure 2.2

$$\int_{-\infty}^{\infty} \operatorname{sinc}\left(\frac{t-lT}{T}\right) \operatorname{sinc}\left(\frac{t}{T}\right) dt = 0 \ \forall l. \qquad (2.4)$$

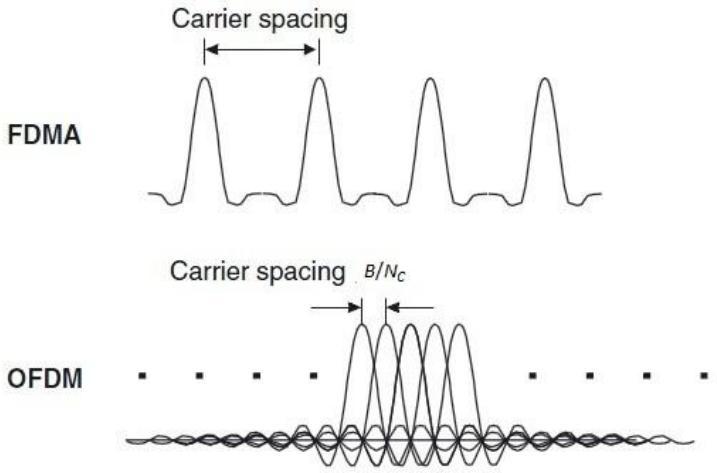

Figure 2.2: Principle behind OFDM: N_c carriers within a bandwidth of B [32]

Because each carrier is in the spectral null of all other carriers, the data streams of any two subcarriers will not interfere as long as the receiver does the appropriate demodulation [32]. Is this characteristic of allowing lining up the peak of one subcarrier with the nulls of the adjacent subcarriers that makes OFDM such practical system.

2.1.3. Cyclic Prefix

OFDM subcarriers can lose their orthogonality by passing a time-dispersive channel. OFDM symbols are no longer confined to a time slot, expanding to the neighboring slots causing ISI. So, the duration of the OFDM symbol is now $T_S + \tau_{max}$, where τ_{max} is maximum path delay. One solution to this problem is introducing a cyclic prefix (CP) [36]. Assuming that CP is longer than the channel impulse response and it is added in the transmitter, the effect on the adjacent symbol is minimized by CP removal at the receiver.

Cyclic prefix is a copy of the last part of the symbol and attaching it to the beginning. Also, it is a guard time, which should be bigger than the delay spread (maximum time delay of different radio channels path) caused by multipath effect [30].

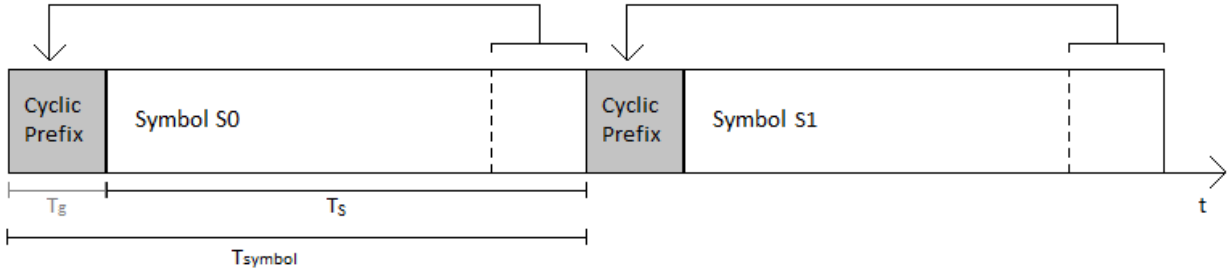

Figure 2.3: Cyclic prefix addition

In Figure 2.3 is represented the consequences of introducing the CP. By adding a time guard (T_g) to the OFDM symbol period without CP (T_S), in each OFDM symbol, the overall period of the symbol is given by:

$$T_{symbol} = T_g + T_S. \quad (2.5)$$

So, if $T_g > \tau_{max}$ OFDM system is inter-symbolic interference free but CP utilization implies loss of spectral efficiency because it reduces transmission rate.

When the amplitude and phase of the subcarriers are not constant, the nulls of the OFDM spectrum are shifted into other frequencies, thus causing inter-carrier interference (ICI) and loss of orthogonality. If $\Delta f \gg 2f_{D,max}$, i.e., subcarrier spacing is bigger than two times the maximum Doppler shift, there is no ICI.

A particular wireless communication system has assigned a particular frequency band to a specific service. Spectrum is thus a scarce resource which forces us to place the maximum number of users within a given bandwidth. Multiple access methods allow multiple users to communicate to a single base station (BS) [32].

2.2. OFDM System

In Figure 2.4, we can observe the basic transmitter and receiver of an OFDM system. The transmitter receives a stream of bits and converts them into symbols using a modulation scheme (for example QPSK). Each symbol is mixed with one of the subcarriers by the serial-to-parallel converter [9]. The IFFT block creates the signal where each of its inputs is one subcarrier and is modulated independently of the others. At the end of the transmitter, it is introduced the cyclic prefix to avoid ISI like we saw previously [30].

The information can now be sent through the channel. At the receiver, CP is removed and the FFT brings the signal back to frequency domain. Although CP prevents corruption of the data due to ISI, it doesn't protect the information against channel's impact in individual subcarriers caused by changes in phase and amplitude. So, it became necessary to introduce pilot symbols to help with channel's estimation. These reference symbols are placed in time and frequency domains, allowing receiver to interpolate the effect of the channel into the different subcarriers. One of the main solutions is performing a frequency domain equalizer [30].

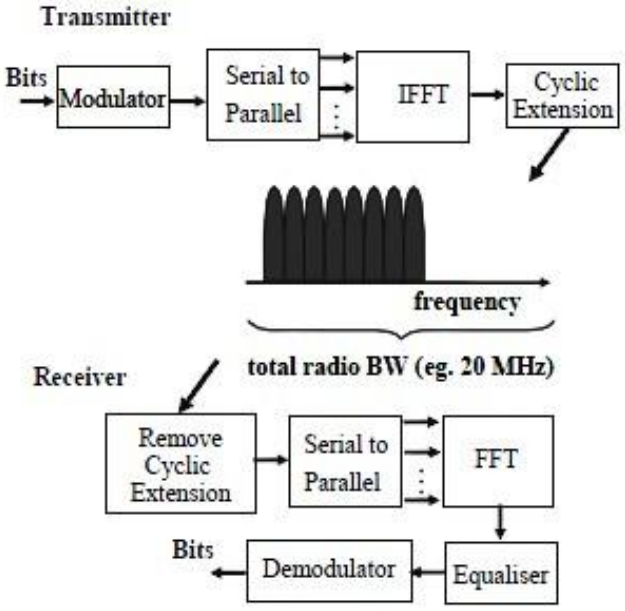

Figure 2.4: OFDM transmitter and receiver block diagram [30]

OFDM can also be used as multiple access scheme, referred as Orthogonal Frequency-Division Multiple Access (OFDMA). In OFDMA, the base station shares its resources with multiple users by communicating to the mobiles at different times and frequencies, distributing a different set of subcarriers to different users at the same time. In Figure 2.5, we have one possible distribution of four users in an OFDMA system. For example, UE 1 is receiving a voice over IP stream, which has low data rate and uses a constant number of subcarriers. UE 2 is receiving a stream of non real time packet data. In this case, the data come in bursts needing a vary number of subcarriers. In case of frequency fading, UE 3 and 4, the base station allocates the subcarriers

that receive a stronger signal from the mobile. Allocating the resources according to the needs of the transmitted signals reduces the impact of time and frequency fading [9].

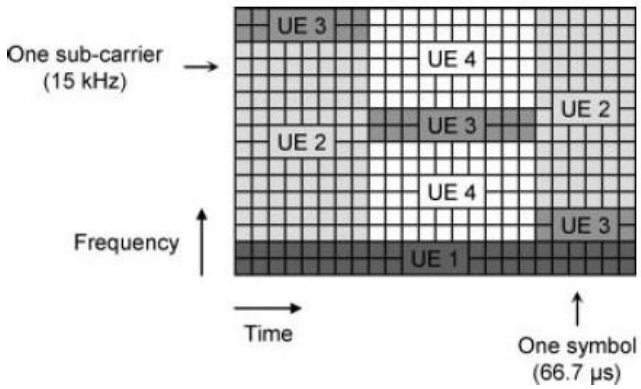

Figure 2.5: OFDMA - Multiple access implementation in time and frequency [9]

Being able to assign unequal numbers of subcarriers to the users revels how flexible OFDMA systems are. Moreover, it allows a user specific subcarrier distribution and chose power allocation. As we can see in Figure 2.5, OFDMA allows allocating several consecutives subcarriers to be assigned to different users. If the scheduling of a user's subcarrier is done arbitrarily over the available frequency spectrum, the subcarrier mapping is called distributed. If the all the subcarriers of a single user are adjacent, the subcarrier mapping is called localized [37]. The Figure 2.6 offers a visual comparison between localized and distributed subcarrier mapping.

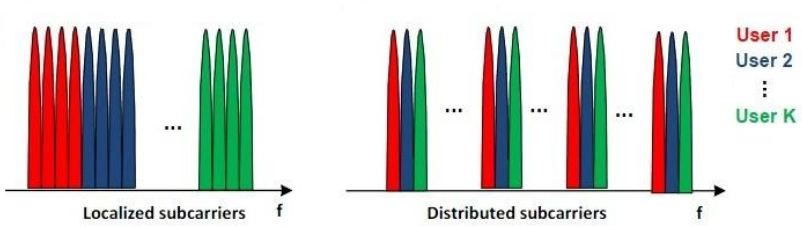

Figure 2.6: Types of subcarrier mapping [35]

The main drawback of OFDMA is high peak-to-average ratio (PAPR) due to non-constant envelop of the modulated signal. A high PAPR require expensive power amplifiers with linearity requirements that increase power consumption. This feature becomes a big problem if the sender is fed by a battery, since it would run out quickly. If the sender is a BS there is no problem [38]. That's why OFDMA is used in LTE's downlink and SC-FDMA in LTE's uplink.

2.3. MC-CDMA

Multicarrier Code-Division Multiple Access (MC-CDMA), merges the best of OFDM with the best of CDMA. Like OFDM, it has high spectral efficiency, robustness against multipath propagation and simple frequency equalizers. As CDMA, it allows a flexible multiple accesses with good interference properties [39]. From this reasoning, we can say that MC-CDMA is a combination of a multicarrier transmission and spreading in the frequency domain [37].

Figure 2.7 shows a MC-CDMA transmitter. In downlink, this transmitter is located in the base station. In this scheme, each k user will have their data symbols spread by a L length orthogonal code and, for simplicity sake, it is assumed that the number of subcarriers is equal to the spreading code length ($N_C = L$).

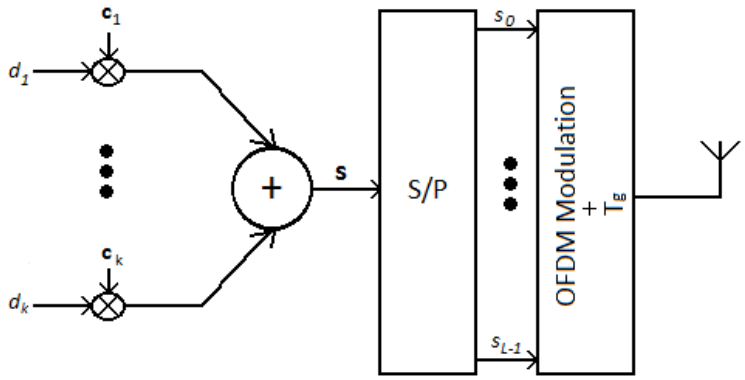

Figure 2.7: MC-CDMA - downlink transmitter generic block diagram

It is more computationally efficient to add the spread signals of the users before the OFDM operation, performing IFFT only one time. The multi-user signal of L subcarriers after the series-to-parallel conversion is given by:

$$\mathbf{s} = \sum_{k=1}^{K} d_k \, \mathbf{c}_k = [s_0 \quad s_2 \quad \cdots \quad s_{L-1}]^T \qquad (2.6)$$

Each user has a single unique spreading code that allows the transmission of all users simultaneously using the same range of frequencies, i.e., the user signal's separation is carried out in the code domain at the receiver. $\mathbf{c}_k$ is a Walsh-Hadamard code, which is a orthogonal code, and it has a dimension of $L \times 1$.

$$\mathbf{c}_k = \frac{1}{\sqrt{L}} \left[c_{k,0} \quad c_{k,1} \quad \cdots \quad c_{k,L-1} \right]^T. \qquad (2.7)$$

The term $1/\sqrt{L}$ ensures that the spread symbol power is equal to the original symbol power. The chip rate of the code $\mathbf{c}_k$ before serial-to-parallel conversion is given by:

$$\frac{1}{T_S} = \frac{L}{T_d} \qquad (2.8)$$

From (2.8), we can observe that the chip rate is L higher than the symbol rate $1/T_d$. Because $N_C = L$, the symbol duration, with guard interval, is [33]

$$T_{symbol} = T_g + LT_S. \qquad (2.9)$$

The equation (2.6) may be rewritten in matrix form

$$\mathbf{s} = \mathbf{Cd}, \qquad (2.10)$$

where $\mathbf{d} = [d_1 \;\; d_2 \;\; \cdots \;\; d_K]^T$ represents the transmitted data symbol vector of the K active users and $\mathbf{C} = [\mathbf{c}_1 \;\; \mathbf{c}_2 \;\; \cdots \;\; \mathbf{c}_K]$ is the K code matrix. It has the dimension of $L \times K$ and its columns represent the different codes for different users.

Before transmission, we still need to build the OFDM symbol by distributing $\mathbf{s}$ components through the N_C subcarriers and it is introduced the time guard interval. As it was previously mentioned, choosing the appropriate time guard interval and the appropriate number of subcarriers ensure robustness against frequency selective fading and ISI.

Note that considering that $L < N_C$, i.e., the number of subcarriers is greater than the code's length, it is possible to divide the frequency spectrum into (N_C/L) blocks of length L. Then, each symbol L chips may be mapped in L adjacent positions or in separate positions within the OFDM symbol. This last mapping method is called frequency interleaving.

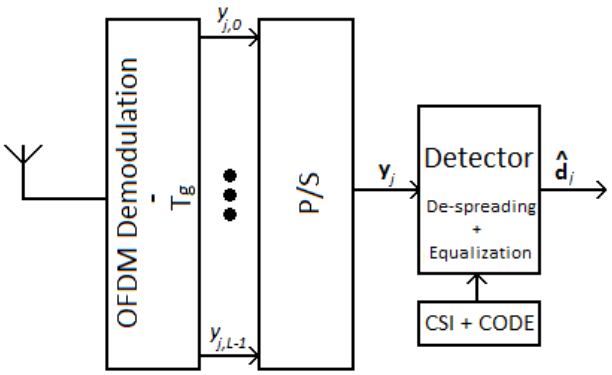

Figure 2.8: MC-CDMA - downlink receiver generic block diagram

Figure 2.8 illustrates a MC-CDMA receiver block diagram. In downlink this receptor is in UE. At first, is performed an OFDM demodulation (or one FFT) and it is removed the time guard that was introduced in the transmitter. Then it is performed the detection, which is a simple equalizer in the downlink and is made the de-spreading operation. After the equalization we obtain a soft estimate of the transmitted data symbols $\hat{\mathbf{d}}$.

In the downlink, all users transmitted from a BS to an UE j pass through the same channel. The multipath channel can be represented by a single complex coefficient in each position of the OFDM symbol in the frequency domain, if the fading is not selective on each subcarrier. The signal received by UE j after performing OFDM procedure and removing the T_g is given by:

$$\mathbf{y}_j = \mathbf{H}_j\mathbf{C}\mathbf{d} + \mathbf{n}, \tag{2.11}$$

where $\mathbf{n}$ is the AWGN noise in each subcarrier and $\mathbf{H}_j = \mathrm{diag}\{h_{j,0} \quad h_{j,1} \quad \cdots \quad h_{j,L-1}\}$ is a diagonal matrix with dimensions $L \times L$ and its nonzero elements are the channel's complex coefficients between the BS and the UE j. In some multi-user detection techniques is useful rewrite (2.11) as

$$\mathbf{y}_j = \mathbf{A}_j\mathbf{d} + \mathbf{n}. \tag{2.12}$$

These previous equations assume that the received subcarriers are orthogonal between themselves but by passing through a channel they will be affected by fading, which may cause the loss on the orthogonality. So, the signal obtained after the de-spreading operation is given by the sum of the desired signal with the other $K-1$ users' signal interference and the noise. The symbol estimate in UE *j* is given by:

$$\hat{d}_j = \mathbf{q}_j^T\mathbf{y}_j. \tag{2.13}$$

Replacing (2.11) in (2.13) we get

$$\hat{d}_j = d_j\mathbf{q}_j^T\mathbf{H}_j\mathbf{c}_j + \sum_{k=1,k\neq j}^{K} d_k\,\mathbf{q}_j^T\mathbf{H}_j\mathbf{c}_k + \mathbf{q}_j^T\mathbf{n}_j \tag{2.14}$$

where $\mathbf{q}_j = \begin{bmatrix} q_{j,0} & q_{j,1} & \cdots & q_{j,L-1} \end{bmatrix}^T$ is a vector with dimension $L \times 1$, which represents the equalization and de-spread proceedings and it may be written by:

$$\mathbf{q}_j = \mathbf{G}_j\mathbf{c}_j^*. \tag{2.15}$$

and $\mathbf{G}_j = \mathrm{diag}\{g_{j,0} \quad g_{j,1} \quad \cdots \quad g_{j,L-1}\}$ is a diagonal matrix of dimension $L \times L$ its nonzero elements are the equalizer coefficients.

The average SNR per subcarrier at the receiver input is defined by:

$$\gamma_c = \frac{\mathrm{E}\left[\left|h_{j,l}s_l\right|^2\right]}{\sigma_n^2} \tag{2.16}$$

where σ_n^2 is the noise variance. If the channel is normalized (i.e., $\mathrm{E}\left[\left|h_{j,l}s_l\right|^2\right] = 1$) and that s_l is statistically independent from $h_{j,l}$ for all l, the average SNR per subcarrier is

$$\gamma_c = \frac{\mathrm{E}[|s_l|^2]}{\sigma_n^2} \quad (2.17)$$

This expression may be further manipulated assuming that all users are transmitted with the same average energy $\mathrm{E}[|d_k|^2]$ in the downlink. We can establish a relation between the SNR per data symbol (γ_s) and the average SNR per subcarrier (γ_c):

$$\gamma_s = \frac{L}{K}\gamma_c = \frac{\mathrm{E}[|d_k|^2]}{\sigma_n^2}. \quad (2.18)$$

From (2.18) is possible to conclude that γ_c may be obtained by dividing γ_s by the code's length, due to the data symbol spreading, and multiplied by the total number of users because K signals overlap. Assuming that average power of the transmitted data symbols is one ($\mathrm{E}[|d_k|^2] = 1$), it is possible to write:

$$\frac{1}{\gamma_c} = \frac{L}{K}\sigma_n^2. \quad (2.19)$$

and the average SNR per bit (γ_b) is related to the average SNR per symbol by the following expression

$$\gamma_b = \frac{\gamma_s}{Rm_b}. \quad (2.20)$$

where $m_b = \log_2 M_c$ is the number of bits per data symbol, M_c is the constellation length and R is channel coding rate and is defined by:

$$R = \frac{number\ of\ information\ bits}{number\ of\ encoded\ bits}. \quad (2.21)$$

In a system without channel encoding $R = 1$.

2.4. Detection Techniques

In general, detection techniques may be classified into Single-User Detection (SUD) and Multi-User Detection (MUD). In SUD techniques, the signal is detected excluding the interference effect that other users cause, i.e., excluding inter-user interference. In MC-CDMA systems and assuming that the subcarrier fading is not selective, this technique use simple equalizers, where is performed a complex multiplication in each subcarrier. On other hand, in MUD techniques, the detection is preformed taking into account the effects of inter-user interference. As we can imagine, this implies an increase in complexity. For example, with an optimum detector, the complexity increases exponentially with the increase in the number of users [40]. One of the most

successful MUD detection techniques is the interference cancellation (IC) because they present a better relation between performance and complexity. IC techniques allow two types of schemes: Parallel Interference Cancellation (PIC) and Successive Interference Cancellation (SIC).

2.4.1. Single-User Detection

In a MC-CDMA system is possible to use the following equalizers:

- *Maximal Ratio Combining (MRC)*

The scheme the equalizer coefficients are obtained from the complex conjugate of the channel's frequency response,

$$g_{j,l} = h_{j,l}^{*}, \;\; l = 0, \;\; \cdots \;\; , \;\; L-1. \qquad (2.22)$$

This is the optimum scheme for the case of only one active user in the system [41]. In a uncorrelated fading channel in each subcarrier, the performance of MRC equalizer is equal to the one obtained with a AWGN channel, when $L \to \infty$ [25]. In a multi-user scheme, the MRC equalizer performance degrades greatly if the number of users increases because the orthogonality between subcarriers is destroyed by the inter-user interference, which is caused by the channel's coefficients variations.

- *Equal Gain Combining (EGC)*

This scheme only compensates for the phase rotation caused by the channel. Theirs coefficients are

$$g_{j,l} = \frac{h_{j,l}^{*}}{\left|h_{j,l}\right|}, \;\; l = 0, \;\; \cdots \;\; , \;\; L-1. \qquad (2.23)$$

By using this technique, the UE only needs to estimate the channel's phase coefficients, allowing the use of less complex system in the downlink.

- *Zero Force Combining (ZFC)*

The equalizer's coefficients are obtained by inverting the channel in this scheme.

$$g_{j,l} = \frac{h_{j,l}^{*}}{\left|h_{j,l}\right|^{2}}, \;\; l = 0, \;\; \cdots \;\; , \;\; L-1. \qquad (2.24)$$

The idea behind the use of this scheme is by restoring the orthogonality, we force the inter-user interference to zero. However, this scheme amplifies the noise, especially in low amplitude channels.

- *Minimum Mean Square Error Combining (MMSEC)*

In this scheme, the coefficients are obtained by minimizing the mean square error between the transmitted signal, before OFDM modulation, and the equalizer's output signal in each subcarrier. So, the error and the mean square error are given (respectively) by:

$$\varepsilon_{j,l} = s_l - g_{j,l} y_{j,l}, \tag{2.25}$$

$$J_l = \mathrm{E}\left[\left|\varepsilon_{j,l}\right|^2\right]. \tag{2.26}$$

The mean square error may be minimized using the orthogonality principle, which states that the mean square error J_l is minimum if the equalizer coefficient $g_{j,l}$ is chosen so that the error $\varepsilon_{j,l}$ is orthogonal to the received signal, or in other words, $\mathrm{E}\left[\varepsilon_{j,l} y_{j,l}^*\right] = 0$. From (2.16), (2.25) and (2.26), the coefficients are given by:

$$g_{j,l} = \frac{h_{j,l}^*}{\left|h_{j,l}\right|^2 + 1/\gamma_c}, \quad l = 0, \quad \cdots \quad , \quad L-1. \tag{2.27}$$

If $\gamma_c \to \infty$, the component $1/\gamma_c \to 0$ and the MMSEC equalizer is equal to the ZFC. Replacing (2.19) in (2.27), we have:

$$g_{j,l} = \frac{h_{j,l}^*}{\left|h_{j,l}\right|^2 + \frac{K}{L}\sigma_n^2}, \quad l = 0, \quad \cdots \quad , \quad L-1, \tag{2.28}$$

and it shows that the MMSEC coefficients require the estimation of the noise variance. This step increases UE complexity. This parameter can be estimated from pilot symbols, used to estimate the channel and synchronization, or from the transmission of null symbols. Null symbols are OFDM symbols that have no information in the beginning of each frame [42]. The MMSEC has a better performance than ZFC because it allows a trade-off between noise enhancement and interference, while ZFC only enhances noise [43].

2.4.2. Multi-User Detection

In this case, the optimum detector may be designed using one of two criterion: the Maximum a Posteriori (MAP) criteria or the Maximum Likelihood (ML) criteria [25] [40]. In this section is presented the algorithm based on its criteria called Maximum Likelihood Sequence Estimation (MLSE). From the MLSE sequence estimator is possible to extend it for the MAP sequence estimator, using the probability of the transmitted sequence. If all transmitted sequences have the same probability a posteriori, the estimator based on MAP criteria is identical to the one built upon ML criteria. Assuming that the constellation length M_c is the same to all K

users, the number of possible transmitted data vectors $\mathbf{d}_\mu$, $\mu = 0, \cdots, (M_c)^K - 1$ is equal to $(M_c)^K$.

Maximum Likelihood Sequence Estimation

The MLSE minimizes the error probability of the data symbols vector, or equivalently, maximizes the conditional probability $P\{\mathbf{d}_\mu|\mathbf{y}\}$, which means that probability of $\mathbf{d}_\mu$ being transmitted when the received vector is $\mathbf{y}$. The data estimation vector is given by:

$$\hat{\mathbf{d}} = \arg\max_{\mathbf{d}_\mu} P\{\mathbf{d}_\mu|\mathbf{y}\}, \quad (2.29)$$

where arg represents the function argument. In the particular case of Gaussian noise, (2.29) is equivalent to find the data symbol vector that minimizes the square of the Euclidean distance between the received signal and all possible transmitted sequences.

$$\Delta^2(\mathbf{d}_\mu, \mathbf{y}) = \|\mathbf{y} - \mathbf{A}\mathbf{d}_\mu\|^2, \quad (2.30)$$

So, the estimated transmitted data vector is obtained by

$$\hat{\mathbf{d}} = \arg\min_{\mathbf{d}_\mu} \Delta^2(\mathbf{d}_\mu, \mathbf{y}). \quad (2.31)$$

The disadvantage of this method is if we increase the number of users the complexity also increases, due to evaluation of $(M_c)^K$ square Euclidean distances for the estimation of the data symbol vector. Therefore, these detectors won't be used in real-time systems.

Linear Detection

The linear multi-user detection is suboptimal but less complex. It is based on the knowledge of the matrix $\mathbf{A}_j$ in the receiver. The K users coefficients are obtained from the calculation of the matrix $\mathbf{Q}_l = [q_{1,l} \;\; q_{2,l} \;\; \cdots \;\; q_{K,l}]$, which has the dimension $L \times K$. In each column of matrix $\mathbf{Q}_l$ is each user L's coefficients. The estimated vector $\hat{\mathbf{d}} = [\hat{d}_1 \;\; \hat{d}_2 \;\; \cdots \;\; \hat{d}_K]^T$ is given by:

$$\hat{\mathbf{d}} = \mathbf{Q}_l^T \mathbf{y}_l = \mathbf{Q}_l^T \mathbf{A}_j \mathbf{d} + \mathbf{Q}_l^T \mathbf{n}. \quad (2.32)$$

To compute the coefficient matrix there is two schemes: ZF-MUD and MMSEC-MUD. They both are an extension from the ZF-SU and MMSEC-SU equalizers. The equations that will give the coefficient matrix are:

$$\text{ZF-MUD: } \mathbf{Q}_l^T = \left(\mathbf{A}_j^H \mathbf{A}_j\right)^{-1} \mathbf{A}_j^H \quad (2.33)$$

$$\text{MMSEC-MUD: } \mathbf{Q}_l^T = \left(\mathbf{A}_j^H \mathbf{A}_j + \sigma^2 \mathbf{I}_\mathrm{K}\right)^{-1} \mathbf{A}_j^H \quad (2.34)$$

In the first case, the interference is removed by selecting $\mathbf{Q}_l^T$ equal to the pseudo-inverse of the matrix $\mathbf{A}$ [44]. In the second case, the coefficients are obtained by minimizing the MSE between the estimated data vector and the transmitted data vector. While the first case still enhances the noise, the second is a compromise between the interference cancelation and the noise enhancement, maximizing the signal-interference plus noise rate (SINR). These multi-user schemes don't have a practical interest in the downlink, because it is necessary to invert the a matrix with dimensions $K \times K$, increasing the complexity of the UE.

Interference Cancellation

IC techniques establish a good compromise between performance and complexity. The basic idea behind these techniques is estimate the inter-user interference and then subtracts it to the received signal. The two main ways to estimate the multiple access interference are: PIC and SIC. There are several schemes that bring together PIC and SIC, they are called IC hybrid [45]. These cancellation techniques allow the use of several cancellation stages, reducing successively the inter-user interference. With each stage, symbols' estimation of all users is improved.

Figure 2.9 shows the PIC's block diagram and the first stage of interference cancellation. The PIC detector estimates and subtracts in parallel all inter-user interference and this scheme is used when all transmitters are operating with a similar power. It is important to notice that, in stage zero, the signal is only detected, therefore, there is no interference cancellation.

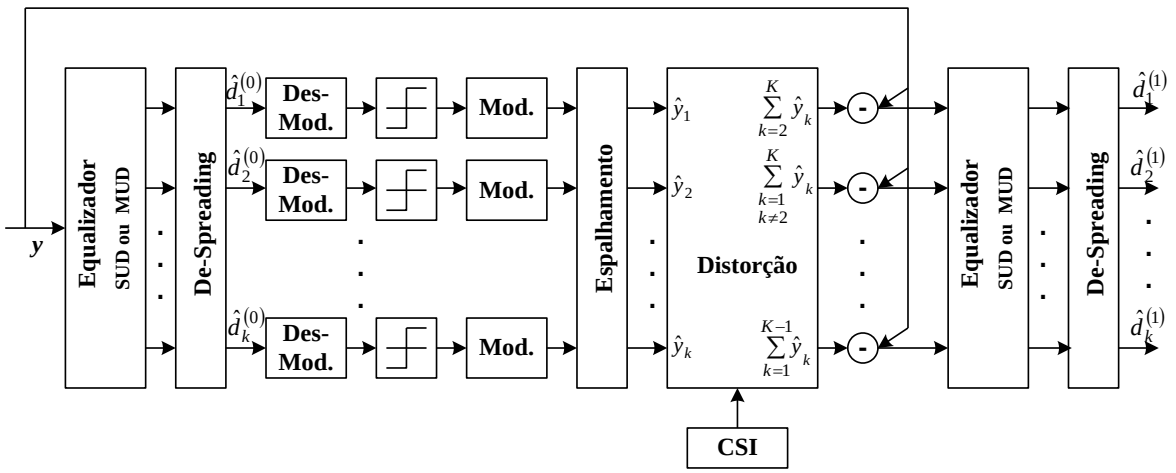

Figure 2.9: PIC's block diagram

Referring to Figure 2.9, initially, all users are detected in parallel by using a single-user or multi-user equalizer. Then is carried out the de-spreading and it is obtained the soft estimates of all users $\hat{d}_k^{(0)}$. From the estimated symbols, the received signals of all users are regenerated $\hat{y}_k$ by using the channel's estimations of different users. For each user, it is summed all $K-1$ regenerated signals, which is then subtracted, obtaining an estimate of the received signal for each user. This last estimation of the received signal has smaller inter-user interference than the

regenerated signals from the previous stages. The estimated signal for a given k user, considering N_{iter} stages, is given iteratively by:

$$\hat{d}_k^{(i)} = \mathbf{c}_k^H \mathbf{G}_k^{(i)} \left(\mathbf{y} - \sum_{j=1, j\neq k}^{K} \mathbf{H}_j \mathbf{c}_j d_j^{(i-1)} + \mathbf{n} \right), \qquad i = 1, \cdots, N_{iter} \tag{2.35}$$

The previous expression is not valid to the zero stage. The detection techniques presented in the previous subsection may be used in each stage [46] [47]. In the initial detection is used a MUD detector in order to obtain an accurate first data estimate. In the posterior stages, the detector MRC-SU presents the best results. The main problem of PIC techniques is if the first estimate is poor, the errors will be propagated through all the following stages.

While in PIC scheme, all users are detected simultaneously determined and regenerated, the SIC scheme detects, regenerates and subtracts one user at a time, thus the remaining users experience less inter-user interference. So, this last scheme is used when the users have different powers. Firstly, it is detected the user with higher power and the last user detected is the one with lower power. The result of this algorithm is that a user with higher power does not benefit from any reduction of interference but other users have a considerable reduction in the inter-user interference. Thus, the SIC detector effectively reduces the near-far effect.

The performance of these detectors may be improved by combining them with an array of antennas [48] [49]. These schemes may also use channel coding to estimate the data at each stage, decreasing propagation errors and increasing their performance [50].

3. Multiple Antenna Systems

Even though the previous techniques were developed in order to improve spectrum efficiency, robustness against multipath fading and allow multiple accesses with reasonable interference, it is still not enough. There is still a growing demand for higher data rates with better quality of service (QoS). Multiple antennas at the transmitters and receivers became an innovative technique that promised higher data rates at larger distances without consuming extra bandwidth or transmit power [51].

There are three multi-antenna formats, which differ from each other in the number of transmitter and/or receiver antennas and in level of complexity. Figure 3.1 illustrates the different configurations. Besides these three, it also shows the SISO to compare.

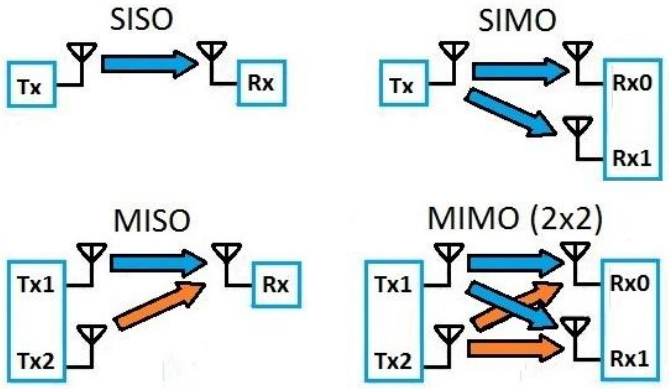

Figure 3.1: Multi-antenna formats SIMO 1x2, MISO 2x1 and MIMO 2x2 [52]

The first configuration is Single-Input Multiple-Output or SIMO. In this configuration, the receiver has multiple antennas (M_R) while the transmitter remains with only one. It is also known as receive diversity because receives signals from a number of independent sources. SIMO has a relatively simple implementation but the levels of processing are limited by size, cost and battery drain. The second configuration is Multiple-Input Single-Output (MISO) and it has multiple antennas at the transmitter (M_T) and only one at the receiver. It is also called as transmit

diversity because the data is transmitted redundantly by different antennas. The receiver can receive the best signal to reconstruct the original data. The best feature of this format is all the processing that occurs at the receiver in SIMO is transferred to the transmitter in MISO. This becomes very important because it reduces the power consumption at the receiver, allowing user equipments to be mobile. The last configuration is MIMO (Multiple-Input Multiple-Output) which has M_T transmitter antennas and M_R receiver antennas. It is used to improve channel robustness and data throughput capacity [53].

Finally, multiple antennas configurations allow different users to share the same resources. Multiuser MIMO (MU-MIMO) needs extra hardware and increases the cost of the overall system but doesn't need bandwidth increase [54].

3.1. Diversity

The idea behind multiple antennas is sending same information through different independent paths and combining them to mitigate fading effects. This principle is called diversity, which can be present with different forms. In time diversity, it is used time interleaving and channel coding. Channel coding ensures redundancy and interleaving ensures that the bits associated with a specific codeword are time separated, so they can undergo different channel fading. In frequency diversity, the signal is sent on different frequencies that induce different structures in the multi-path environment. The receiver gets some of the replicas, allowing redundancy in the frequency domain. Both these diversity techniques have drawbacks. While the first one has a decrease in data rate (due to coding repetition), the second one requires higher bandwidth (due to carriers separation). In spatial diversity, redundancy comes from replicas of the transmitted signal sent and received by multiple antennas spatially separated [33].

3.1.1. Receive Diversity

In this scheme, there are multiple antennas at the receiver and the spacing between them is wide enough so the mutual correlation between antennas is small. Because of this channels are independent and it is increased diversity gain [55]. Figure 3.2 illustrates a signal received by two antennas. We can observe that the fading occurs at different times because antennas process or filter the multipath in different ways allowing deep fade reducing by combination of two signals received by two antennas. The fades shown in Figure 3.2 are typical in narrowband systems such as GSM.

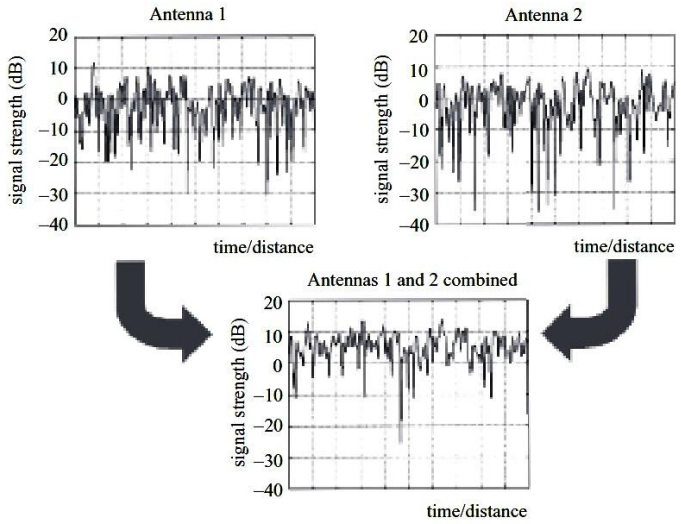

Figure 3.2: Reducing fading by using a combination of two uncorrelated signals [56]

So, how can we successfully combine multiple signals? There are four diversity combining methods, which are organized from worst to the best in the following list [56]:

- **Switched Combining:** In this method only one antenna is used at a time because the second is only used when the received signal falls below a certain value.
- **Selection Combining:** A selection algorithm compares the instantaneous amplitude of each channel and chooses the antenna branch with the highest amplitude, ignoring the other signal antennas'.
- **Equal Gain Combining:** Here the signals are co-phased on each branch and then summed.
- **Maximal Ratio Combining:** Each received signal is individually co-phased and weighted on their SNR before summing. This scheme is also known as Matched Filter.

3.1.2. Transmit Diversity

Transmit diversity uses two or more antennas at the transmitter and, thus reducing fading. It may seem, at first, quite similar to the receive diversity but to use this scheme it is necessary to solve one important problem. Let's assume that the transmitter has two antennas (for simplicity). When sending the same information from both antennas, the signals will be added together at the receive antenna and if no coding/precoding is done the diversity cannot be achieved. There are two ways to solve this problem: closed loop transmit diversity and open loop transmit diversity.

In the closed loop form, the transmitter applies a phase shift in one or both signals before sending them through different antennas. At the receiver, both signals will be in phase without

destructive interference. The phase shift is calculated by the receiver and fed back to the transmitter as a precoding matrix indicator (PMI), so the transmitter has prior knowledge of the channel state. This means that the transmitter has channel sate information (CSI) [57]. In a radio channel, the phase shifts occur in the frequency domain and they depend on the wavelength of the carrier, thus PMI comes as function of frequency too. The best choice PMI also depends on the mobile's position. The faster the mobile moves, more frequently will PMI change. The drawback of the closed loop is the delay introduced by the feedback loop: fast moving mobiles may use an inappropriate PMI, making this technique suitable to relatively slowly moving mobiles. For fast moving mobiles, one should consider the open loop technique [9].

In the open loop form, diversity can be achieved by space-time codification. Space-time codes have several advantages: they reduce transmitted power, don't require CSI and they are robust against non-ideal conditions (like antenna correlation, channel estimation errors, and Doppler effects). There are mainly two types of space-time codes: trellis and block codes. Block codes are characterized by space-time block code (STBC) and space-frequency block code (SFBC). [57] [9].

Figure 3.3 shows Alamouti's block diagram and the whole process before transmitting. The first step is to modulate the information bits, using an *M*-ary modulation (e.g QAM) thus forming symbols. The transmitted signal matrix for a code block composed only by s_1 and s_2 is:

$$\mathbf{S} = \begin{bmatrix} s_1 & -s_2^* \\ s_2 & s_1^* \end{bmatrix} \quad (3.1)$$

The matrix first row represents the symbols sent by Tx_1 and the second represents the symbols sent by Tx_2. So, firstly, Tx_1 transmits s_1 and Tx_2 sends s_2, after they send $-s_2^*$ and s_1^* respectively.

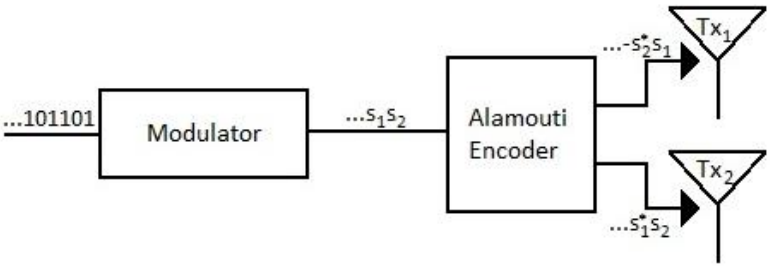

Figure 3.3: Block diagram of the Alamouti space-frequency encoder [58]

If we perform the operation $\mathbf{S} \times \mathbf{S}^H = \begin{bmatrix} |s_1|^2 + |s_2|^2 & 0 \\ 0 & |s_1|^2 + |s_2|^2 \end{bmatrix}$, we prove that $\mathbf{S}$ matrix is orthogonal and independent of s_1 and s_2 [43]. Because of this we can rewrite equation (3.1):

$$\mathbf{S} = \begin{bmatrix} s_n & -s_{n+1}^* \\ s_{n+1} & s_n^* \end{bmatrix} \quad (3.2)$$

Figure 3.4 illustrates the Alamouti's decoder.

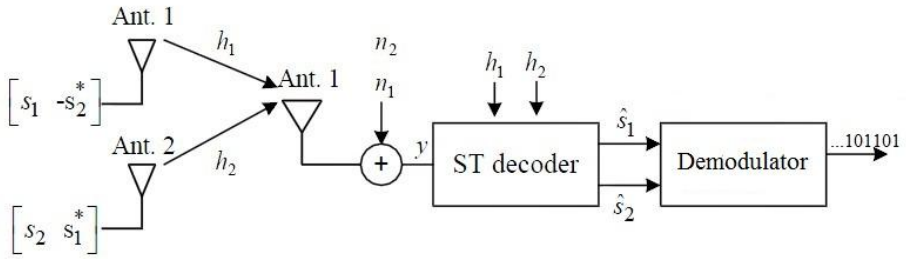

Figure 3.4: Alamouti's decoder [59]

Considering $\mathbf{h} = [h_1 \quad h_2]$ as the channel matrix and $\mathbf{n} = [n_1 \quad n_2]$ is the additive white Gaussian noise, the received signal is given by:

$$\mathbf{y} = \frac{1}{\sqrt{2}}\mathbf{hS} + \mathbf{n} \quad (3.3)$$

Each symbol is multiplied by a factor of $1/\sqrt{2}$ in order to normalize the power per symbol to the unity. Also, the equation (3.3) may be written in the following form:

$$\begin{cases} y_n = \frac{1}{\sqrt{2}}h_{1,n}s_n - \frac{1}{\sqrt{2}}h_{2,n}s_{n+1}^* + n_n \\ y_{n+1} = \frac{1}{\sqrt{2}}h_{1,n}s_{n+1} + \frac{1}{\sqrt{2}}h_{2,n}s_n^* + n_{n+1} \end{cases}. \quad (3.4)$$

Assuming now that the channels between two adjacent frequencies or instants are highly correlated, $h_{k,n} = h_{k,n+1}$, the estimated symbols after deciding are given by:

$$\begin{cases} \hat{s}_n = \frac{1}{\sqrt{2}}h_1^* y_n + \frac{1}{\sqrt{2}}h_2 y_{n+1}^* + n_n \\ \hat{s}_{n+1} = -\frac{1}{\sqrt{2}}h_1 y_n^* + \frac{1}{\sqrt{2}}h_2 y_{n+1}^* + n_{n+1} \end{cases}, \quad (3.5)$$

which means that the soft decision are given by

$$\hat{\mathbf{s}} = \mathbf{h}_{eq}^H \mathbf{y} \quad (3.6)$$

$$\hat{s}_n = \frac{1}{2}(h_1^* h_1 + h_2 h_2^*)s_n + \frac{1}{\sqrt{2}}h_1^* n_n + \frac{1}{\sqrt{2}}h_2 n_{n+1}^* \quad (3.7)$$

where $\mathbf{h}_{eq}^H \mathbf{h}_{eq} = (|h_1|^2 + |h_2|^2)\mathbf{I}_2$.

From (3.7), interference caused by $n+1$ data symbol is eliminated, thus its SNR is

$$SNR = \frac{1}{2}\frac{(|h_1|^2 + |h_2|^2)}{\sigma_n^2}. \quad (3.8)$$

These previous equations may be extended to a system with four antennas: two antennas in the transmitter and other two in the receiver. For example, instead of only having one system of equations in (3.4), it would present two systems of equation representing both antennas [43].

3.2. Spatial multiplexing

Another important possibility that arises from the use of multiple antennas is the spatial multiplexing. This technique tried to achieve maximum multiplexing gain, thus achieving also maximum capacity [43].

If the transmitter and receiver have multiple antennas, it is possible to send multiple parallel data streams between them, increasing data rate. A system with M_T transmit and M_R receive antennas, also described as $M_T \times M_R$, has a data rate proportional to $\min(M_T, M_R)$ [9].

Unlike Alamouti scheme, the information transmitted by different antennas will interfere with each other. To correctly separate them, the number of receive antennas has to be greater or equal to the number of transmit antennas, i.e. $M_R \geq M_T$ [57]. In Figure 3.5, shows the block diagram of spatial multiplexing system. In the transmitter the data symbols are precoded into the different antennas. The precoders are computed based on the channel information that should be feed backed from UEs to the BS, considering FDD mode, or estimated in the uplink if the TDD mode is assumed (channel reciprocity).

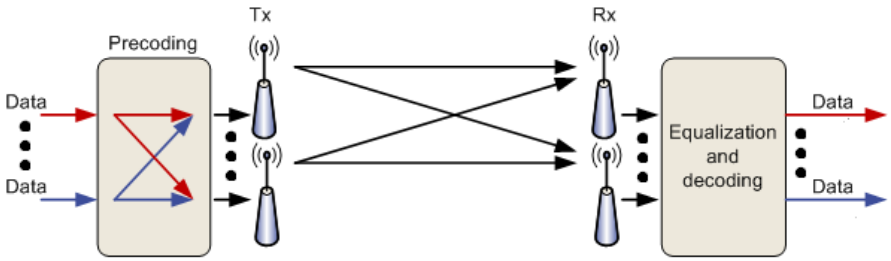

Figure 3.5: Spatial Multiplexing System [60]

Assuming that $\mathbf{H} = \begin{bmatrix} h_{11} & \dots & h_{1M_T} \\ \vdots & h_{ij} & \vdots \\ h_{M_R1} & \dots & h_{M_RM_T} \end{bmatrix}, i = 1, \dots, M_R; j = 1, \dots, M_T$ is the channel matrix, $\boldsymbol{s}$ is the data vector and $\boldsymbol{n}$ is the noise vector (exactly like in section 2.1), the signal received $\mathbf{y} = [y_1 \dots y_{M_R}]^T$ at receiver is given by:

$$\mathbf{y} = \mathbf{Hx} + \mathbf{n} \quad (3.9)$$

where $\mathbf{x} = \left[x_1 \dots x_{M_T}\right]^T$ is the transmitted signal vector.

Another way to describe the channel matrix is using the singular value decomposition (SVD). In this way all MIMO channels are considerate a set of parallel channels and $\mathbf{H}$ is written:

$$\mathbf{H} = \mathbf{UDV}^T \quad (3.10)$$

where $\mathbf{U}$ and $\mathbf{V}$ are unitary matrices of size $M_R \times r$ and $M_T \times r$ respectively, $r = rank(\mathbf{H}) \leq \min(M_T, M_R)$, and $\mathbf{D}$ is the diagonal matrix composed by non-negative real numbers,

$$\mathbf{D} = \begin{bmatrix} \lambda_1 & 0 & 0 \\ 0 & \ddots & 0 \\ 0 & 0 & \lambda_r \end{bmatrix}. \quad (3.11)$$

Now, setting the precoding matrix as

$$\mathbf{W} = \mathbf{VP}^{1/2} \quad (3.12)$$

with size $M_T \times r$, and $\mathbf{P}$ is a square diagonal power allocation matrix of size $r \times r$.

$$\mathbf{P} = \begin{bmatrix} p_1 & 0 & 0 \\ 0 & \ddots & 0 \\ 0 & 0 & p_r \end{bmatrix} \quad (3.13)$$

Setting the equalizer matrix as

$$\mathbf{G} = \mathbf{U}^H. \quad (3.14)$$

The transmitted signal is

$$\mathbf{x} = \mathbf{Ws}. \quad (3.15)$$

Replacing in (3.9) by the equations (3.10), (3.12), and (3.15):

$$\mathbf{y} = \mathbf{UDV}^T\mathbf{VP}^{1/2}\mathbf{s} + \mathbf{n}. \quad (3.16)$$

The estimated data symbols are obtained by

$$\hat{\mathbf{s}} = \mathbf{Gy} = \mathbf{U}^H\mathbf{UDV}^T\mathbf{VP}^{1/2}\mathbf{s} + \mathbf{n} \quad (3.17)$$

$$\hat{\mathbf{s}} = \mathbf{DP}^{1/2}\mathbf{s} + \tilde{\mathbf{n}}. \quad (3.18)$$

The soft estimate at r^{th} data symbol is

$$\hat{s}_i = \lambda_i\sqrt{p_i}s_i + \tilde{n}_i, i = 0, \dots, r \quad (3.19)$$

Another important thing to notice is: we can combine diversity and multiplexing in a system but it is impossible to construct a system with their full benefits. To have full diversity on a 2×2 system, each symbol must pass through two independent channels so diversity is two $(d = 2)$. Because the symbols are repeated the multiplexing gain is one $(r = 1)$. Now, to have full multiplexing on the same system, each channel is used by only one data stream $(r = 2)$. Exactly because of this there is no repetition of the symbols so the diversity is one $(d = 1)$. In the diversity, the data rate is constant and the BER decreases as the SNR increases and, in multiplexing, BER is constant while the data rate increases with SNR [43].

We can apply spatial multiplexing in MU-MIMO scenario. This combination is very useful in uplink. Various mobiles can transmit at the same time to the same base station and on the same carrier. Uplink MU-MIMO does not increase peak data rate of each mobile but increases cell throughput and can be implemented in non-expensive mobiles with only one antenna. MU-MIMO is the technique considered in LTE Release 8. In the downlink, it is also possible to apply MU-MIMO usually referred as beamforming.

3.3. Beamforming

Beamforming is a multiple antenna technique, which appeared in order to increase cell coverage and/or capacity. Firstly, let's imagine that only user 1 is active and is on a line of sight with the base station (BS). The signals of each antenna will reach user 1 in phase, interfering with each other constructively, thus the received signal power is high. On other hand, user 2 is at an oblique angle and it receives signals from alternate antennas that are $180°$ out of phase, interfering destructively, thus the power received is low. This scheme is a synthetic antenna beam, which has a main beam pointing to user 1 and not user 2. The whole power is focused on only one user because of the narrow beamwidth, which is narrower than a single antenna.

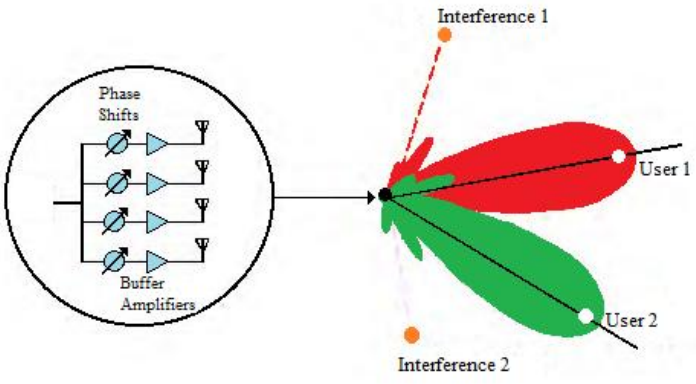

Figure 3.6: Beaforming with 4 transmit antennas [61]

Figure 3.6 shows an example of this technique with four transmitter and two users. When applying phase shifters to the transmitted signal, it can change the direction at which constructive interference arises. What is actually been done is focusing the synthetic antenna beam towards the intended users at any direction. By applying the suitable set of antenna weights, it is possible to adjust amplitudes and phases of the transmitted signals. In a system with M_T antennas, it is possible to adjust the direction of the main beam up to $M_T - 2$ nulls or sidelobes [9]. As we can see, in Figure 3.6, with four antennas it is possible to have two nulls and 2 sidelobes.

In OFDMA, the different subcarriers are processed using different set of antennas weights, allowing creating synthetic beams pointing in different directions. This allows communicating with several different mobiles at the same time in completely different locations.

While spatial multiplexing and diversity work best if the antennas are far apart and the signals are uncorrelated, beamforming works better if the antennas are close together. They should be separated only by the radio's wavelength, ensuring the signals sent or received are highly correlated. So it is possible to have two sets of antennas on a single BS: one set provides beamforming and the second provides diversity and/or spatial multiplexing [9].

3.4. LTE

LTE is currently on the market and it was introduced in 3GPP Release 8 which was frozen in December 2008. The new standard is based on the ODFM and MIMO principles discussed in the previous sections. The core network architecture designed is called system architecture evolution (SAE) and LTE covers the radio access network, air interface and mobile. The whole system is known by Evolved Packet System (EPS). EPS is IP based, meaning that real-time services and datacom services are carried by the IP protocol. The IP address is allocated when the mobile phone is turned on and released when is turned off. This advance allowed 3GPP and non-3GPP radio access technologies to be compatible [9] [38]. Another LTE innovation is the Evolved UMTS Terrestrial Radio Access (E-UTRA), which is a brand new radio interface built upon E-UTRAN physical structure. E-UTRA main specifications are presented in Table 3.1 [62].

	MIMO	Multiple Access	Modulation	Duplexing	Channel Coding	Bandwidth (MHz)
Downlink	2x2 4x2 4x4	OFDM	QPSK 16-QAM 64-QAM	FDD TDD	Turbo Coding	1.25 2.5 5 10 15 20
Uplink	1x2 1x4	SC-FDMA				

Table 3.1: E-UTRA Specifications [62]

Although LTE acronym refers only to the air interface evolution, it became colloquial name for the whole system [9] [38]. It is possible to observe that LTE greatly upgraded the previous 3G systems by developing a new flat architecture IP-based. It also allowed 3GPP and non-3GPP radio access technologies to be compatible. In the Table 3.2, is possible to compare some of the parameters from both generations [62] [63] [64] [13].

		Downlink Peak Transmission Rate (Mbps)	Peak Spectral Efficiency (bps/Hz)	Latency (ms)	Mobility (km/h)
3G HSDPA Release 6		14,4	3	50	250
4G LTE FDD 20 MHz 64-QAM	1x1	100	>5	5	350
	4x4	326			

Table 3.2: Performance comparison between 3G HSDPA and 4G LTE [62]

The LTE communication protocol is founded in the physical layer (PHY). PHY is means by which the base station is connected to the mobile. A poor wireless connectivity means calls drop, fail downloads and stall videos. Also, it interacts with both media access control layer (MAC) and the radio resource control layer (RRC), transporting data services to higher layers. PHY is responsible for the channel coding, PHY hybrid automatic repeat request (HARQ) processing, modulation, multi-antenna processing, and mapping of the signal to the appropriate physical time-frequency resources [65].

3.4.1. Physical Layer in LTE

In Figure 3.7, we can observe the major blocks in processing the transport blocks. Firstly, when LTE downlink PHY processing accepts the transport blocks from the MAC layer, the processing begins with calculation of the cyclic redundancy check (CRC) and attaching it to the data or control stream.

In case that block size is greater than maximum allowed, it is preformed the code block segmentation in order to adapt the size for the turbo coding and the CRC is recalculated and attached in every code block before encoding. Then is the turbo encoding, which provides forward error correction in a reliable transmission. The rate matching is responsible for puncturing in order to adapt the code rate and the HARQ provides a retransmission when the user fails to receive the data correctly. The scrambling uses a pseudo-random gold sequence to reduce interference between cells. Modulation performs QPSK, 16-QAM or 64-QAM, which are used in LTE layer mapping, and precoding. These modulation schemes allow multi-antenna transmission. Finally, the resource elements of OFDM symbols are mapped to each antenna [65]. In LTE, the

OFDM signal depends of the bandwidth because LTE specifies flexible channel bandwidths from 1.4 MHz up to 20 MHz.

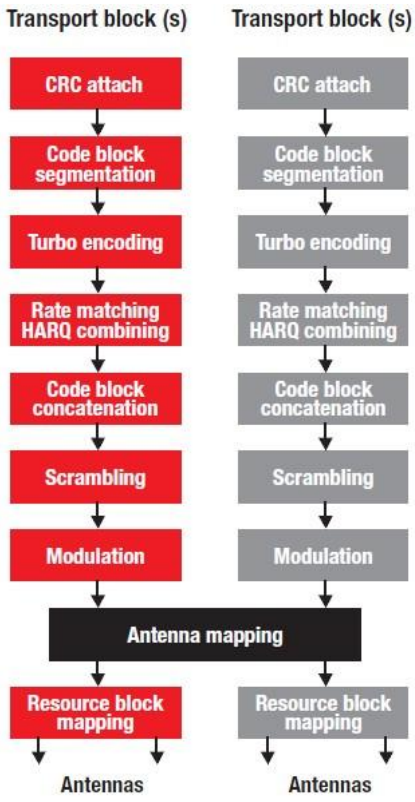

Figure 3.7: LTE downlink major functional blocks in transport processing [65]

In Table 3.4 is presented some of the parameters according to each bandwidth case. It is possible to notice that the downlink bandwidth efficiency is around 90% (except for 1.25 MHZ), thus only 10% of the available band is composed by guard subcarriers. These subcarriers will be converted by IFFT into zeros in the correct locations [62] [66].

Bandwidth (MHz)	**1.25**	**2.5**	**5**	**10**	**15**	**20**
FFT size N_C	128	256	512	1024	1536	2048
Subcarrier Spacing Δf **(kHz)**	15					
Sampling frequency $f_{N_C} = N_C \Delta f$	1.92	3.84	7.68	15.36	23.04	30.72
Guard Subcarriers	52	105	211	423	635	847
Occupied Subcarriers	76	151	301	601	901	1201
Occupied Band (MHz)	1.140	2.265	4.515	9.015	13.515	18.015
Downlink Bandwidth Efficiency	77.1%	90%	90%	90%	90%	90%

Table 3.3: LTE's OFDM Parameters [66]

3.4.2. Frame Structure

LTE also supports FDD and TDD, allowing a flexible spectrum deployment, so its air interface needs to be studied in both time and frequencies domains. LTE's frame structure has two types: type 1 for FDD and type 2 for TDD. Even though down and uplink have different multiple access schemes, they use the same frame structure.

It is the frame structure which defines frame, subframe, slot and symbol in the time domain, where its time length is expressed in time units T_s. So,

$$T_s = \frac{1}{15000 \times 2048} = 32.55\ ns, \qquad (3.20)$$

which correspond to the 30.72 MHz sample clock for the 2048 point FFT used in 20 MHz bandwidth system [67].

Also, the time of a frame and the time of a sub-frame are given by:

$$T_{frame} = 307200 T_s = 10\ ms \qquad (3.21)$$

$$T_{subframe} = 30720 T_s = 1\ ms \qquad (3.22)$$

because each frame has 10 ms and it consists of 10 subframes.

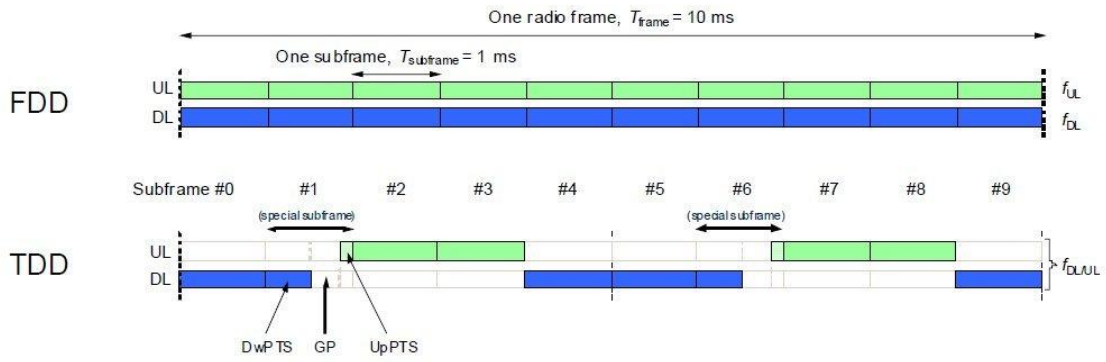

Figure 3.8: LTE frame structure both in FDD and TDD [68]

- *FDD frame structure*

In Figure 3.8, we can observe that there are two carrier frequencies: one for uplink transmission (f_{UL}) and the other for downlink transmission (f_{DL}). Thus it is possible to occur downlink and uplink simultaneously (assuming full duplex), with ten subframes for downlink and others ten for uplink.

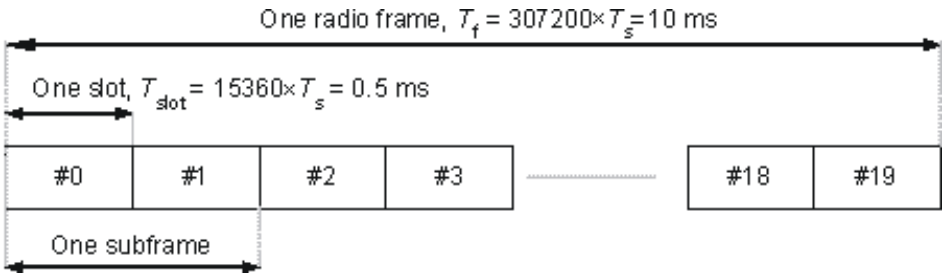

Figure 3.9: FDD structure [69]

Figure 3.9 shows the type of frame applicable to FDD transmissions. It also shows that each radio frame is composed by 20 slots numbered from 0 to 19. It is possible that those 20 slots are designated to downlink or to uplink but it is also possible to divide each slot in half and designate a half to downlink transmissions and the other half to uplink transmissions achieving full duplex.

- *TDD frame structure*

Figure 3.8 also shows TDD operation. In this case, there is a single carrier frequency and uplink and downlink transmissions are separated in time.

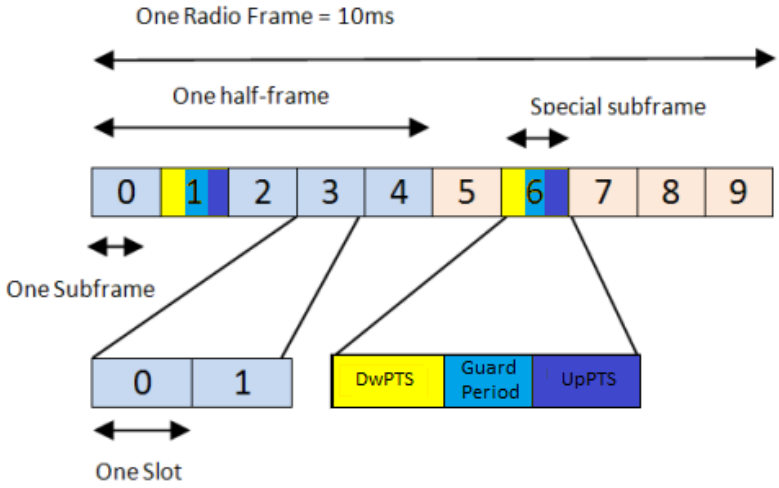

Figure 3.10: TDD structure [70]

As we can see in Figure 3.10, each frame is divided in two half frames of 5 ms each and each half frame has five subframes. Also, one of the subframes is a special subframe (in Figure 3.10 are subframes 1 and 6), which has three special fields: downlink pilot timeslot (DwPTS), Guard Period (GP), and uplink pilot timeslot (UpPTS). The total length of these three fields is 1 ms. The slot 0 and DwPTS are reserved for downlink transitions in a similar manner slot 1 and UpPTS are reserved for uplink transmissions. This flexible assignment in a single frame allows downlink and uplink to occur with asymmetric data rates [12].

3.4.3. Slot Structure

OFDM based systems have one remarkable advantage: ability to protect against multipath delay spread. As discussed in section 2.1, the introduction of a guard period, or CP, between each symbol eliminates ISI due to multipath delay spread [12].

With a subcarrier spacing of 15 kHz, the useful symbol time is approximately of 66,7 μs, so the overall OFDM symbol time is the sum of the useful symbol time and the CP length. LTE has two cyclic prefix lengths: the normal and the extended, which have seven and six OFDM symbols per slot respectively. Normal cyclic prefix of $144 \times T_s$, or 4.69 μs, protects multipath delay spread to >1.4 km [12]. A longer CP is less efficient but it may be very useful in large coverage cells.

- *Resource Element and Resource Block*

The smallest unit in the physical layer is called resource element (RE), which corresponds to one OFDM subcarrier during a single OFDM symbol interval. It can be seen has a time-frequency grid where each hole is an RE and, moreover, in case of multi-antenna transmission, there a grid per antenna. The smallest unit for scheduled transmission is the resource block (RB), which physically occupies 0.5 ms or one slot and 180 kHz. The number of subcarriers per resource block (N_{sc}^{RB}) and the number of symbols per resource block (N_{OFDM}) depend of the CP length and subcarrier spacing. In downlink [12]:

Configuration	Subcarrier Spacing (kHz)	N_{sc}^{RB}	N_{OFDM}
Normal CP	15	12	7
Extended CP	15		6
	7,5	24	3

Table 3.4: Resource block parameters for the downlink [12]

From the Table 3.4, we see that N_{sc}^{RB} depends on the number of OFDM symbols in a downlink slot, which means that it depends on CP length and the subcarrier spacing.

3.4.4. Muti-antenna modes for LTE

Spectral efficiency in MIMO systems is achieved by the creation of “spatial layers” in a wireless channel. In fact, they are born due to multipath and scattering between transmitters and receivers. Their numbers also depend on the number of transmitter and receiver antennas [71]. LTE physical layer is responsible for adapting the MIMO Transmission Mode (TM) according to the operating environment of a specific user. In other words, the channel condition will determine which TM will be used by the user. There are seven LTE transmission modes and they can fit three

categories: spatial multiplexing mode, the diversity mode and the beamforming mode. Table 3.5 shows a brief overview of the seven downlink transmission modes [62] [71] [72].

TM	Description	Advantages/Disadvantages and Applications
1	Single transmit antenna. A single data stream is transmitted on one antenna and received by one or more antennas.	Doesn't allow spatial multiplexing (SM), transmit diversity, nor beamforming. Reduced throughput rates and cell coverage. Small cells sites for services where high speed is not required by the user.
2	Transmit diversity is the default MIMO mode. May use 2 or 4 antennas Transmission of the same information stream on multiple antennas. Each antenna stream uses different coding and different frequency resources. For 2 antennas is used a SFBC Alamouti code. For 4 antennas is used combination of SFBC and frequency shift transmit diversity (FSTD).	Systems where SM can't be used. Improves the SNR and makes the transmission robust.
3	Open loop SM with cyclic delay diversity (CDD) Two information streams are transmitted over 2 (up to 4) antennas. No precoding matrix indicator (PMI) is included. Uses 3 precoding matrices, which are cyclic shifted according to the used subcarrier index, creating frequency diversity.	Achieves higher data rates. Requires less UE feedback. Provides better peak throughput than TM2. Is used when the channel rapidly changes, i.e., user is moving with high velocity.
4	Closed loop SM Two information streams are transmitted over two code words from N antennas (up to 4). PMI is fed back from the UE to the BS, allowing the transmission optimization over the wireless channel. BS transmits specific reference signals, distributed over various RE and over various timeslots, allowing the channel's estimation at the receiver. The UE sends a response regarding the channel situation, including the information about which precoding is preferred from the codebook.	Achieves higher data rates. The signals at the receiver are easily separated into the original streams. Increases the data throughput for UE with low mobility and channel's variations are slow.
5	MU-MIMO Similar to TM4 but the SM is used to serve several UEs at the same RE, sharing the same resources. The users are separated in the space domain and, if they are not orthogonal to each other, they will experience inter-user interference.	Overall network data rate is improved. The correct precoding allows to UEs to recover their data interference with low interference.
6	Close loop SM using a single transmission layer and is a special case of TM4.	BS to acquire CSI sends the downlink reference signals.

	Uses feedback signals and codebook set of TM4 but only rank 1 matrices are selected by the BS for precoding. In other words, a single codeword is sent over a single spatial layer. Beamforming mode is performed by a codebook set of matrices.	Then it waits for the UE to perform the necessary computations to select and feedback the precoding matrix index. Used in LTE-FDD system.
7	Single layer beamforming The BS directly performs a channel estimation using the reference signals received from UE in the uplink, performing the desired precoding. Then, a specific UE reference signal is coded and transmitted, using the same weights on data precoding. Because the UE only needs one specific reference signal, the UE assumes that the transmission was made by a single antenna.	BS just needs to receive the uplink reference signal to obtain a precise channel response. Suited to perform beam transmissions in the LTE-TDD variant. Increases the cell coverage in order to reach users located at the cell edge, directing the main lobe.

Table 3.5: Overview of the seven downlink transmission modes in LTE

3.5. LTE-Advanced

LTE-Advanced is considered an enhancement of the LTE technology and it may be deployed in a spectrum occupied by its predecessor without causing compatibility problems. In fact, LTE-Advanced is applying spectrum bands from LTE along with the future bands of IMT-Advanced [11]. LTE-Advanced requirements were set to match or even enhance the ones proposed by IMT-Advanced. In Table 3.6 is presented a comparison between requirements of LTE and LTE-Advanced for downlink.

Targets	Antenna Configuration	LTE Release 8	LTE-Advanced
Peak Data Rate	8x8	300 Mbps	1 Gbps
Peak Spectrum Efficiency (bps/Hz)	8x8	15	30
Capacity (bps/Hz/cell)	4x2	1.87	2.6
Cell-edge User Throughput (bps/Hz/cell/user)	4x2	0.06	0.09

Table 3.6: LTE and LTE-Advanced performance targets for downlink [13].

The list of specifications also includes compatibility between other cellular systems, UE suitable for worldwide use and roaming capability. In order to fulfill these ambitious goals, it will

consider new technologies. Some of these enabling technologies are presented in this subchapter [13] [73].

3.5.1. Carrier Aggregation

The simplest way of increasing capacity is by increasing the bandwidth [14]. The carrier aggregation makes it possible to have bandwidth up to 100 MHz, while preserving the compatibility with the LTE. So, LTE-Advanced groups several LTE component carriers (CCs). Each component can have a bandwidth from 1.4 up to 20 MHz and a maximum of five component carriers can be aggregated [13] [14]. In other words, LTE-Advanced devices are able to use a greater bandwidth while LTE devices still consider the spectrum to be composed by separate component carriers. Also the number of aggregated carriers can be different in downlink and uplink but the number of uplink components is smaller than the number of downlink components [14]. Another advantage of using this technique is the increase in peak data rates: 1 Gbps in the downlink and 500 Mbps in the uplink [73] [74].

There are three carrier allocation scenarios: contiguous intra-band, non-contiguous intra-band and non-contiguous inter-band aggregation. In Figure 3.11, it is presented the three alternatives.

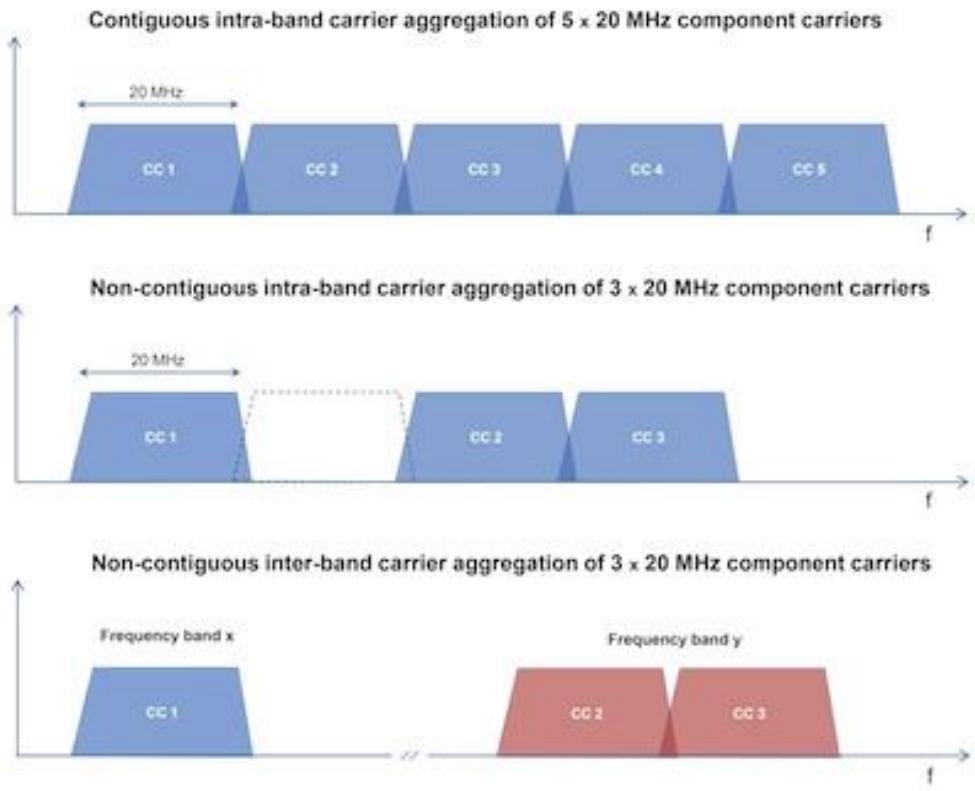

Figure 3.11: Different carrier aggregation scenarios [75]

In the first scenario, the component carriers are located in different bands. This fact allows a different cell's coverage for each band and forces different radio components to support each band at the UE. In this scenario, the component carrier's separation is a multiple of 100 kHz. The second scenario is the non-contiguous intra-band aggregation. As we can see in Figure 3.11, the component carriers are located in the same band but different devices can coexist. Finally, the third scenario is non-contiguous inter-band aggregation. In this scheme, the component carriers of the same device are adjacent to each other and different devices have different bands. They are separated by a multiple of 300 kHz and each band is orthogonal to the others, providing a free interference system [73] [14] [74] [75].

3.5.2. MIMO Enhancements for LTE-Advanced

MIMO allows to increase the overall bit rate through several different data streams on two or more antennas and using the same resources in both frequency and time [14]. As we saw in chapter 3.1, it also allows beamforming and spatial multiplexing techniques. Enhancing these techniques it will allow the increase the peak data rates, the system performance improvement and the support of various transmissions schemes with a universal structure [73] [74]. One problem that arises from using these is: they require the channel's state information (CSI) knowledge. However a significant performance improvement can be obtained by adapting the system to the radio channel conditions at the base station. In TDD systems, CSI is gathered from the uplink because the same carrier frequency is used for both transmission and reception. In FDD systems, it is necessary to feedback information through the reverse link. As one can imagine, having a full CSI knowledge might cause an excessive overhead and it may be more desirable to use a statistical or quantization CSI. Another drawback is possibility for terminal mobility because it corrupts the information arriving to the base station [13].

LTE-Advanced introduced the support for dual layer beamforming. In this technique, the BS transmits to two receive antennas located in one or two mobiles, providing full support for downlink users MIMO. It also increases the BSs antenna ports number to eight, supporting 8x8 configurations on downlink and 4x4 on uplink [73]. Moreover, LTE-Advanced has three main operating modes and they are represented in Figure 3.12. In Single User MIMO (SU-MIMO), it is possible to use transmit diversity and spatial multiplexing techniques in combination with beamforming, increasing substantially the peak user data rates. In Multi-User MIMO (MU-MIMO), a different number of streams reach each user, increasing the cell average data rate. This scheme is very appealing because it offers the best complexity/performance trade off. Lastly is the Cooperative MIMO. In this technology, the cell-edge user throughput is boosted by coordinating the transmission and the reception of signals among base stations, reducing inter-cell interference. These techniques are also known as Coordinated Multipoint (CoMP) transmission and they will be presented in the next section [13].

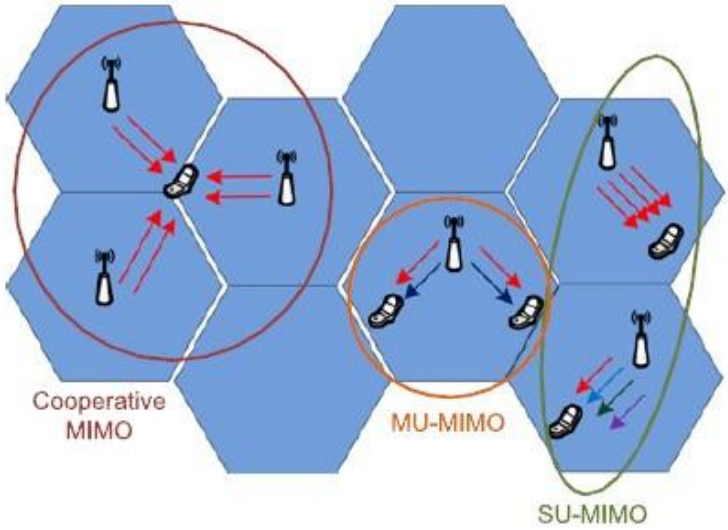

Figure 3.12: LTE-Advanced MIMO main modes [13]

3.5.3. Coordinated Multipoint transmission - CoMP

Coordination between base stations promises to reduce inter-cell in both downlink and uplink, especially in urban areas due to larger rate demands that impose high number of BS. In downlink, CoMP is applied by performing a coordinated transmission from the BS. In uplink, the interference may be mitigated by a coordinate reception in BS. The most common CoMP approaches need scheduling information regarding the users at different base stations. This information is well known by them and forces the use of very-low-latency links, allowing exchanging information between them in the order of milliseconds [13]. Figure 3.13 compares tradition MIMO downlink spatial multiplexing with coordinated multipoint. The most obvious difference is that in a coordinated multipoint system both BS do not need to be physically co-located but they are connected through a high speed data connection. This connection enables both base stations to exchange information [76]. In other words, they coordinate their coding or decoding operations based on the global channel state and the user data information exchange over the backhaul links among several cells [73] [77].

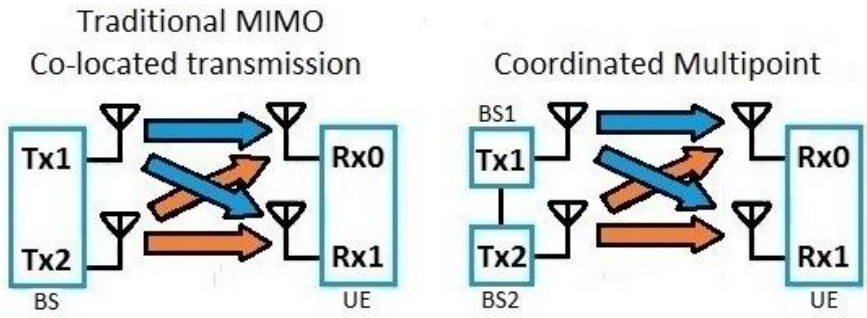

Figure 3.13: Comparison of traditional downlink MIMO and coordinated multipoint [76]

The most important CoMP schemes are: the coordinated scheduling/beamforming and joint processing.

- *Coordinated Scheduling/Beamforming (CS/CB)*

In this scheme only one BS transmits data to the UE but different BS still share control information. The BS responsible for transmitting the data to the user is called anchor cell. To improve sum throughout and reduce interference, it is used coordinated beamforming with precoding at each base station. Figure 3.14 is an architectural illustration of this transmission scheme. One thing that we should notice is that each eNB scheduler makes its decisions independently. However, to achieve optimum scheduling, each eNB takes into account CSI from other users.

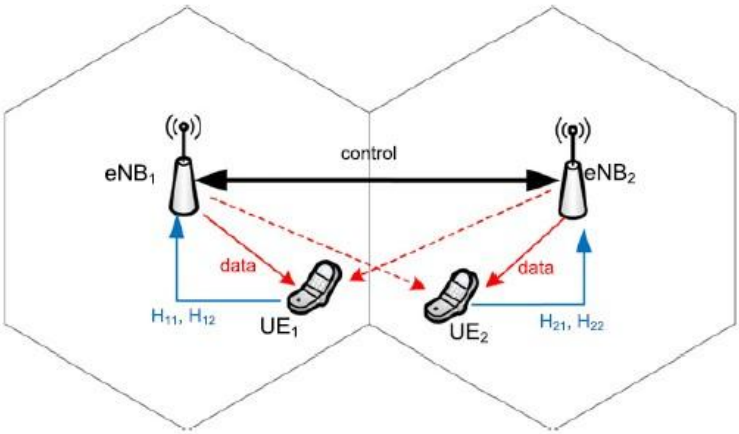

Figure 3.14: Coordinated Scheduling/Beamforming transmission scheme [13]

Using the example from the Figure 3.14, the operation of CS/CB system has four basic steps. At first, the eNBs determine which UEs are attached to both eNBs. Then they request the users to feed back channel information for CoMP mode operation in order to coordinate precoding and UE pairing. In the second step, the UE estimate the downlink channel quality of the anchor cell and the interfering cell. It should be used different reference signals for link adaptation measurements and demodulation purposes. UE may use the reference signals to perform demodulation and link adaptation. Having specific common reference signals (CRS) do not ensure orthogonality for each coordinating eNB. Another concern is the overhead because UE near to the eNB may not benefit from CoMP. LTE-Advanced solves both problems by using an UE specific demodulation reference signals (DM-RS). Also, it doesn't have a codebook, allowing a flexible precoding. Thirdly, UE feeds back to its anchor eNB two types of information: its channel information and the interfering channels information. The second UE repeats this step. Finally, Precoding matrices are calculated based on throughput maximization and fairness limitations and the final UE selection or pairing. Then, the transmission is performed. One significant advantage of this scheme is the generalization of this procedure is straightforward, i.e., it is relatively simple extend this scenario to a larger number of base stations [13].

- *Joint Processing (JP)*

In this scheme, one UE data is jointly transmitted from multiple eNBs to improve the received signal quality and cancel interference. In other words, the data and CSI are shared between different cells to be jointly processed at these cells [13] [73]. The principle behind these techniques is: the number of independent channels is the same as the product of transmitting and receiving antennas. For this to work all antennas must be uncorrelated with each others. There are two different JP methods: joint transmission and dynamic cell selection. In both cases, it is necessary a very fast link interconnecting eNBs, allowing them to share user data [13].

Firstly, let's focus on the joint transmission. In this method, the data is transmitted simultaneously from several sites and the cluster of base stations must jointly decide on the transmission scheme of a signal to the UE. Precoding is done by using DM-RS among the coordinating cells. Serving eNBs (or eNB cluster) determination is performed by either the network, the UE or adaptively between the UE and the network. Also, a cluster may be formed by a fixed set of serving cells or by a flexible set. In a fixed set, users performing CoMP (users at the cell edge) have different frequency zones. Serving UE or not with CoMP mode is done by evaluating the SINR before the scheme is applied. If the UE is served with CoMP mode, the UE is schedule to a preconfigured frequency zone jointly scheduled with other CoMP users. After, all the cluster cells will serve the UE simultaneously. One problem arises from this condition. Forcing all cells in the cluster to serve a single UE causes waste of resources because some clusters eNBs have very weak signal strength. In these cases, a flexible scheduling solution is much easier to implement than changing the size or the number of elements of the CoMP cluster [13]. The received signals at one particular UE may be coherently or non-coherently added together [73]. In a coherent transmission, the network obtains CSI from all cooperating eNBs. The receiver then combines every received signal at symbol level coherently because the phase of the transmitted signal can be adjusted to the CSI. Two possible coherent implementations are: different phase correction applied to each cell and global precoding matrix based on all CSI between cooperating cells and the UE. In the last one, each cell precoders is actually a part of the global precoding matix. In a non-coherent transmission, the network doesn't possess the information regarding the relationship of the channels in the cooperating cells. This means that it is impossible to coherently combine the received signals that arrived at the UE. So the cell edge users calculate the channel quality and send them to only their serving cells without providing channel phase information. One widely used example of a non-coherent approach is the SU-MIMO, where the systems overhead is simplified and the backhaul capacity is increased but a coherent approach produces greater gains than a non-coherent one [13].

In the dynamic cell selection, a transmission for one particular UE is performed from one point at a time. This point is chosen from the cooperating CoMP that serves the same UE. This method allows switching the transmission point on a subframe-by-subframe basis. The serving cell is responsible by the radio source management, packet scheduling and related common

channels. One advantage of this JP method is that there is no need for phase synchronization because there is no simultaneous eNB transmission [13].

4. Interference Alignment and Iterative Frequency Domain Equalization

This chapter presents the concepts of interference alignment and iterative frequency domain equalization, which are crucial to understand the work done in chapter 5. In section 4.1 the interference alignment technique recently proposed is discussed. The iterative frequency domain equalization originally proposed for single carrier (SC) system is presented.

4.1. Interference Alignment

Interference Alignment (IA) is a relatively new concept that arose from the analysis of the interface network capacity. Although most of the work developed was made under idealized assumptions, e.g., global channel knowledge and high signal strengths, the IA became an idea with increasing interest in communication, signal processing, networking and information theory communities. There are several types of IA schemes like spatial, lattice, asymptotic, asymmetric complex signal, opportunistic, ergodic, blind, retrospective, and aligned interference neutralization. These are based on coding and traditional Shannon theory, among other mathematical tools. Some IA applications [28]:

- Wireless interference networks
- Cellular networks
- Two-way communication networks
- Multicast and compound networks
- Multihop multiflow networks
- Tactical communication networks with secrecy and jamming issues
- Cognitive radio networks

- Distributed data storage network
- Index coding networks
- Wired multiple unicast networks
- Cooperative communication networks

4.1.1. Index Coding

One of the earliest interference alignment applications was introduced in [78]. In Example 7 of [78], it was considered a wireless broadcast channel with cognitive receivers, as shown in Figure 4.1.

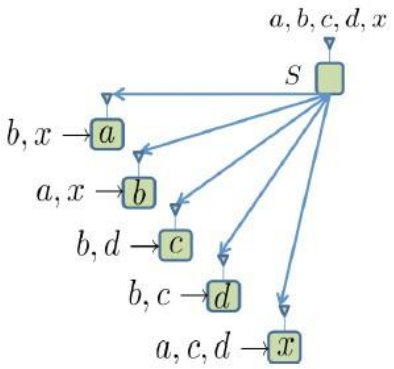

Figure 4.1: IA solution for a broadcast channel with cognitive receivers [28].

The broadcast channel has five independent information symbols or messages a, b, c, d, x, which have to be received by five separated receivers. The symbol that each one desires is labeled on them and each receiver knows some of the symbols that it does not want. This knowledge may come from previous transmissions of those messages that failed the desired node but were strong enough to be decoded in undesired one. For example, in Figure 4.1, the receiver that desires a (or receiver a) as already received and decoded b, x and the one that desires c (or receiver c), knows b and d. The solution proposed uses two signaling dimensions, i.e., two consecutive channels send the symbol $\mathbf{S}$, which is composed by:

$$\mathbf{S} = \begin{bmatrix}1\\0\end{bmatrix} a + \begin{bmatrix}1\\1\end{bmatrix} b + \begin{bmatrix}0\\1\end{bmatrix} c + \begin{bmatrix}0\\1\end{bmatrix} d + \begin{bmatrix}1\\0\end{bmatrix} x \qquad (4.1)$$

Now, let's see how the receiver recovers the information. Receiver a accesses to the two dimensional symbol $\mathbf{S}$ and has the information about b and x. Because the receiver knows b and x, it may remove them, leaving three remaining symbols a, c and d in a two dimensional space. The symbol that the receiver wants is a, so c and d will constitute interference and thus they must align. By analyzing (4.1) and in Figure 4.2: a), it is possible to conclude that c and d are seen along the interference beam $[0 \quad 1]^{\mathrm{T}}$ aligned in one-dimensional space, while a is along the beam $[1 \quad 0]^{\mathrm{T}}$. This fact allows to recover a without interference.

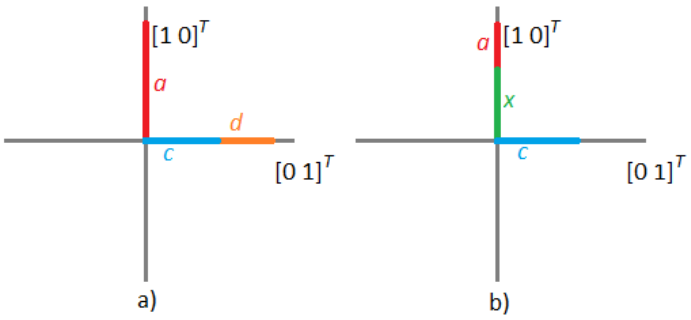

Figure 4.2: Interference alignment representation. In a) is represented receiver *a* IA and b) is receiver *c* IA.

Similarly, at receiver c, after removing the known symbols, there are three unknown ones, a, c and x in a two-dimensional space. As we can see in Figure 4.2 b), both a and x are aligned in a different dimension than c, allowing to recover the desired information. For the other receivers, the reasoning is done in the same way. The idea behind interference alignment is that not all information is necessary in all nodes [28].

4.1.2. X Channel

Several years later, Jafar and Shamai's presented in [79], the interface alignment scheme for a two user X channel. An X channel is a system with two transmitters and two receivers, each one with multiple antennas, where independent messages are sent over fixed channels from each transmitter to each receiver.

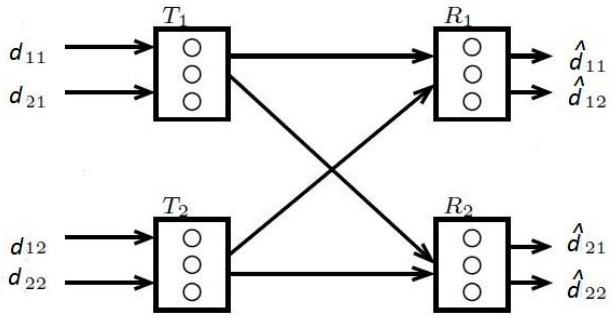

Figure 4.3: MIMO X channel [79]

Figure 4.3 illustrates a MIMO X channel with 2 pairs transmitter-receiver. Each transmitter and each receiver have three antennas ($M_R = M_T = M = 3$). The system is described by the input-output equations:

$$\mathbf{Y}^{[1]} = \mathbf{H}^{[11]}\mathbf{X}^{[1]} + \mathbf{H}^{[12]}\mathbf{X}^{[2]} + \mathbf{N}^{[1]} \quad (4.2)$$

$$\mathbf{Y}^{[2]} = \mathbf{H}^{[21]}\mathbf{X}^{[1]} + \mathbf{H}^{[22]}\mathbf{X}^{[2]} + \mathbf{N}^{[2]} \quad (4.3)$$

where:

- $\mathbf{Y}^{[1]}$ is the $M_{R1} \times 1$ output vector at receiver 1
- $\mathbf{Y}^{[2]}$ is the $M_{R2} \times 1$ output vector at receiver 2
- $\mathbf{X}^{[1]}$ is the $M_{T1} \times 1$ input vector at transmitter 1
- $\mathbf{X}^{[2]}$ is the $M_{T2} \times 1$ input vector at transmitter 2
- $\mathbf{N}^{[1]}$ is the $M_{R1} \times 1$ AWGN vector at receiver 1
- $\mathbf{N}^{[2]}$ is the $M_{R2} \times 1$ AWGN vector at receiver 2
- $\mathbf{H}^{[11]}$ is the $M_{R1} \times M_{T1}$ channel matrix between transmitter 1 and receiver 1
- $\mathbf{H}^{[12]}$ is the $M_{R1} \times M_{T2}$ channel matrix between transmitter 2 and receiver 1
- $\mathbf{H}^{[21]}$ is the $M_{R2} \times M_{T1}$channel matrix between transmitter 1 and receiver 2
- $\mathbf{H}^{[22]}$ is the $M_{R2} \times M_{T2}$channel matrix between transmitter 2 and receiver 2

Each transmitter has a single message to each receiver. In total we have four independent messages $(d_{11}, d_{12}, d_{21}, d_{22})$ to only three dimensions of interference alignment. Still this should be enough to receive correctly one symbol per message free from interference. This is done by aligning the two undesired symbols at each receiver along one given direction. Observing Figure 4.4, we can see how the alignment is done.

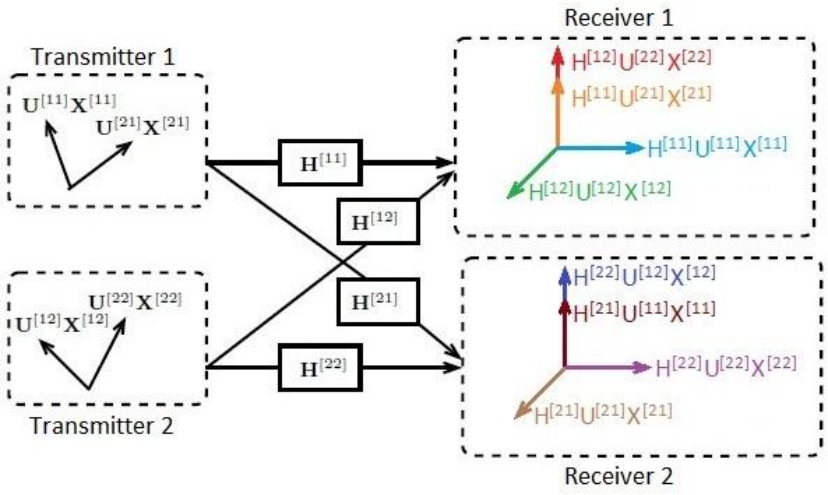

Figure 4.4: Interference Alignment on MIMO X channel [79]

As we can see, transmitter 1 sends independent code words $\mathbf{X}^{[11]}$ and $\mathbf{X}^{[21]}$ for messages d_{11} and d_{21} along the directions $\mathbf{U}^{[11]}$ and $\mathbf{U}^{[21]}$, respectively. As for transmitter 2, it sends the independent code words $\mathbf{X}^{[12]}$ and $\mathbf{X}^{[22]}$ for messages d_{12} and d_{22} along the directions $\mathbf{U}^{[12]}$ and $\mathbf{U}^{[22]}$, respectively.

At receiver 1, we can see that both desired signal vectors $\mathbf{H}^{[11]}\mathbf{U}^{[11]}\mathbf{X}^{[11]}$ and $\mathbf{H}^{[12]}\mathbf{U}^{[12]}\mathbf{X}^{[12]}$ are linearly independent and the interference vectors (signal vectors destined to receiver 2) are linearly dependent, occupying the same spatial dimension. The alignment done at receiver 2 is analogous. We can then conclude that, at each receiver, we have three linearly independent equations in four unknowns. Because two of the unknowns are desired, IA allows us to recover them by aligning the two undesired ones in the same direction.

The fact that channel matrices are generic guarantees there aren't any accidental alignments and being able to represent those alignments through a linear algebraic vector space means that interference alignment is a general principle [28].

The degrees of freedom can be obtained by [80]:

$$R = \frac{\max(M_T, M_R)}{\min(M_T, M_R)} \tag{4.4}$$

$$DoF = \begin{cases} \min(M_T, M_R)\, K, & K \leq R \\ \min(M_T, M_R)\, \dfrac{R}{R+1}, & K > R \end{cases} \tag{4.5}$$

The formula (4.5) can only be used if R is an integer. The DoF of this problem with two users is three.

4.1.3. Interference Channel with K>2 Users

Let's now consider IA for $K > 2$ users. In propagation delayed based alignment (Figure 4.5 a), each transmitter is active half of the time over odd time slots. At receiver, even delays are introduced in the desired signal while odd delays are introduced in the interfering signals. This method sets the desired signal, in each receiver, in the odd time slots and the interference signals in even time slots.

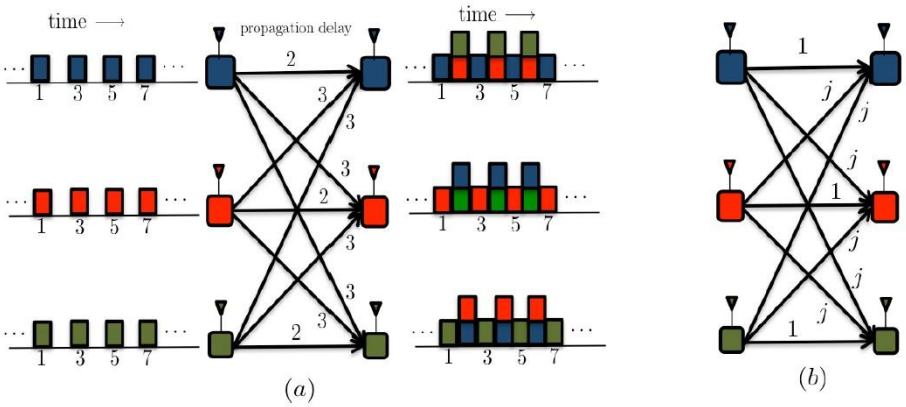

Figure 4.5: IA of three user interference channel: a) through propagation delays and b) through phase alignment [28]

Now, let's imagine that the delay introduced is random for random number of users. It is still possible to have IA propagation delay such that every user can send their signal free from interference for $1/2 - \varepsilon$ of the time. $\varepsilon > 0$ and it can be small has we want it to be, providing that we can have a symbol duration small enough. The price of having such small symbol duration is the bandwidth, which becomes arbitrarily large, but each user gets to use the channel free from

interference $1/2$ of the time. This phenomenon is called bandwidth scaling and, in K user interference channel, the bandwidth scales as $O(K^{2K^2})$.

In phase alignment (Figure 4.5 b), each transmitter sends only real signals. If the signal flows through a direct channel, there is no phase shift, while if it flows through a interfering channel, there is a $90°$ phase shift. Both these examples have a similar approach: they exploit differences in paths lengths. While the first one uses the knowledge of propagation delays, the second uses the phase of the channel coefficients.

- *K=3*

The problem of having three or more users is that each signal must satisfy more than one condition. In Figure 4.6 is presented a three user interference channel.

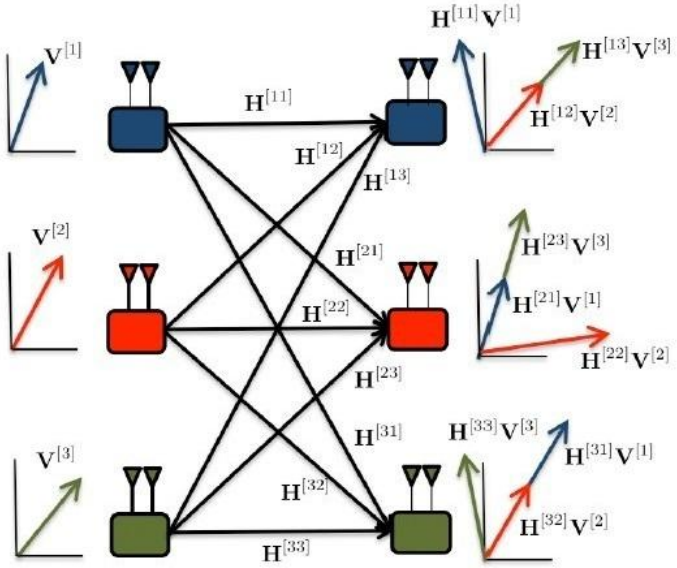

Figure 4.6: IA on the three user MIMO interference channel with two antennas [28]

For example:

- At receiver 1, transmitter 2's signal must be aligned with transmitter 3's signal, which can be described as

$$\mathbf{H}^{[12]}\mathbf{V}^{[2]} = \mathbf{H}^{[13]}\mathbf{V}^{[3]}$$
$$\Rightarrow \mathbf{V}^{[2]} = \left(\mathbf{H}^{[12]}\right)^{-1}\mathbf{H}^{[13]}\mathbf{V}^{[3]} \quad (4.6)$$

- At receiver 2, transmitter 1's and transmitter 3's signals must be aligned, which can be described as

$$\mathbf{H}^{[21]}\mathbf{V}^{[1]} = \mathbf{H}^{[23]}\mathbf{V}^{[3]} \quad (4.7)$$

$$\Rightarrow \mathbf{V}^{[1]} = \left(\mathbf{H}^{[21]}\right)^{-1}\mathbf{H}^{[23]}\mathbf{V}^{[3]}$$

- Finally, at receiver 3, transmitter 1's and transmitter 2's signals must be aligned, which can be described as

$$\mathbf{H}^{[31]}\mathbf{V}^{[1]} = \mathbf{H}^{[32]}\mathbf{V}^{[2]} \quad (4.8)$$

From (4.6) and (4.7), it's possible to rewrite (4.8) as

$$\mathbf{H}^{[31]}\left(\mathbf{H}^{[21]}\right)^{-1}\mathbf{H}^{[23]}\mathbf{V}^{[3]} = \mathbf{H}^{[32]}\left(\mathbf{H}^{[12]}\right)^{-1}\mathbf{H}^{[13]}\mathbf{V}^{[3]} \quad (4.9)$$

$$\mathbf{V}^{[3]} = \text{eigvec}\left(\left(\mathbf{H}^{[23]}\right)^{-1}\mathbf{H}^{[21]}\left(\mathbf{H}^{[31]}\right)^{-1}\mathbf{H}^{[32]}\left(\mathbf{H}^{[12]}\right)^{-1}\mathbf{H}^{[13]}\right). \quad (4.10)$$

This example allows 3 DoF, which is the maximum allowed in this channel. For example, in 2×2 TDMA MIMO, each user would send two symbols but only one user would be active at a time and not achieving more than 2 DoF. In IA scheme, each user sends only one symbol (offering half of its time) but all users are active at the same time.

This example cannot be extended to more than three users. Firstly, the number of alignment constraints increases with increasing number of interfering users. K user interference channel needs an alignment of $K-1$ interfering signal spaces at each K receiver, making a total of $\mathrm{O}(K^2)$ signal space alignment constraints. There are K signal space alignments to satisfy $\mathrm{O}(K^2)$ signal space alignment constraints. Secondly, the diversity of channels also imposes a limitation. Limited diversity does not allow interference alignment [28].

4.2. Iterative Equalization for SC systems

Iterative equalization was firstly considered in SC systems, usually referred as SC-FDE, i.e. single carrier systems with frequency domain equalization. The FDE block can be a linear equalization as discussed in chapter 3 or iterative based equalization. Although linear equalizers schemes have a reasonable complexity performance ratio, they still suffer from noise enhancement and residual ISI. Thus, a nonlinear approach outperforms the linear one [81] [82] [83]. One of the most popular nonlinear equalizers is built by implementing a feedback filter to the output of the feedforward block samples and establishing an iterative scheme. This provides an efficient way to of equalizing the received signals and provides a good tradeoff between complexity and performance [81].

In this section we present an iterative equalizer based on IB-DFE principles. We considered an uplink system with K users that transmit, using the same channel resources, to a BS equipped with M_R antennas. This means that the information from all UEs is transmitted at the same

frequency band [84] [85]. The main blocks of a SC-FDE based system is shown in Figure 4.7. The data block associated to the kth user is $\{d_{k,n}; k = 1, \dots, K,\ n = 0, \dots, N_c - 1\}$, where its constellation symbol (with $\mathrm{E}\left[\left|d_{k,n}\right|^2\right] = \sigma_d^2$) is selected from the data according to a given mapping rule, e.g., QPSK modulation with Gray mapping. In frequency domain, $d_{k,n}$'s become $\{d_{k,l}; k = 1, \dots, K,\ l = 0, \dots, N_C - 1\}$. If k UEs are transmitting simultaneous to M_R antennas in the receiver, the received signal in time domain will be $\{y_{k,n};\ k = 1, \dots, K, n = 0, \dots, N_c - 1\}$ or in the frequency domain $\{y_{k,l}; k = 1, \dots, K, l = 0, \dots, N_C - 1\}$ [85].

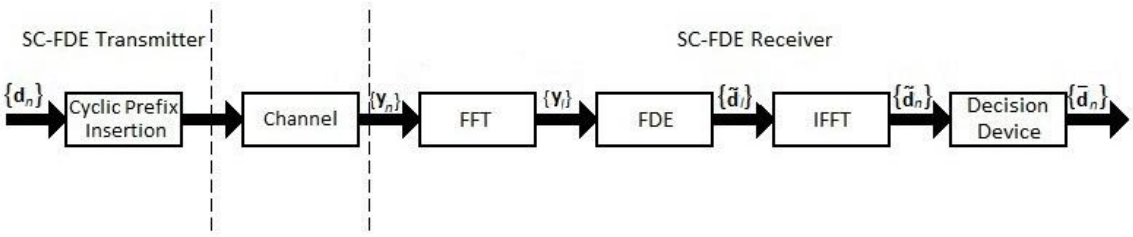

Figure 4.7: SC-FDE transmission block diagram

The received signal in the frequency domain, $\mathbf{y}_l$, on a subcarrier l and in the matrix form, is given by the expression:

$$\mathbf{y}_l = \mathbf{H}_{k,l}\mathbf{d}_{k,l} + \mathbf{n}_l \qquad (4.11)$$

where $\mathbf{y}_l = [\mathrm{y}_{l,1} \quad \cdots \quad \mathrm{y}_{l,M_R}]^T$, $\mathbf{H}_{k,l} = \begin{bmatrix} \mathrm{H}_{1,l,1} & \cdots & \mathrm{H}_{K,l,1} \\ \vdots & \ddots & \vdots \\ \mathrm{H}_{1,l,M_R} & \cdots & \mathrm{H}_{K,l,M_R} \end{bmatrix}$ is the UE's channel realizations, $\mathbf{d}_{k,l} = [\mathrm{d}_{1,l} \quad \cdots \quad \mathrm{d}_{k,l}]^T$ is the UE transmissions and $\mathbf{n}_l = [\mathrm{n}_{l,1} \quad \cdots \quad \mathrm{n}_{l,M_R}]^T$ is the channel Gaussian white noise described previously [85] [86].

So, the FDE block in Figure 4.7 will be replaced by an Iterative-Block Decision Feedback Equalization (IB-DFE) [83], which is an iterative DFE for SC-FDE. This new scheme is presented in Figure 4.8 for an ith iteration [85].

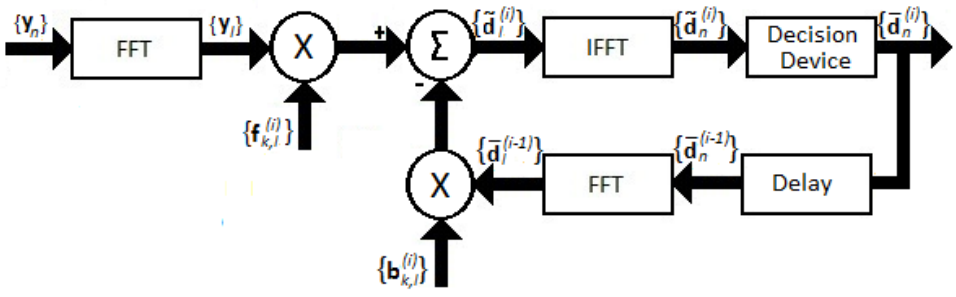

Figure 4.8: IB-DFE basic block diagram structure [85]

Firstly, the estimated frequency domain signal of user *k* on subcarrier *l* and *i*th itariation, $\tilde{d}_{k,l}^{(i)}$, for a particular iteration i and user k is given by:

$$\tilde{d}_{k,l}^{(i)} = \mathbf{f}_{k.l}^{(i)T}\mathbf{y}_l - \mathbf{b}_{k,l}^{(i)}\bar{\boldsymbol{d}}_l^{(i-1)}, \tag{4.12}$$

where $\mathbf{f}_{k,l}^{(i)} = \left[\mathrm{f}_{k,l}^{(i,1)} \quad \cdots \quad \mathrm{f}_{k,l}^{(i,M)}\right]^T$ are the feedforward coefficients, $\mathbf{b}_{k,l}^{(i)} = \left[\mathrm{b}_{k,l}^{(i,1)} \quad \cdots \quad \mathrm{b}_{k,l}^{(i,K)}\right]$ are the feedback coefficients. We should notice that both feedforward and feedback coefficients are in the frequency domain. $\bar{\mathbf{d}}_l^{(i-1)} = \left[\bar{d}_{1,l}^{(i-1)} \quad \cdots \quad \bar{d}_{K,l}^{(i-1)}\right]^T$ are the soft decisions estimates from the previous iteration for all users.

The feedforward and feedback coefficients are computed in order to minimizing the mean square error of the received samples of the kth user on the lth subcarrier $\mathrm{MSE}_{k,l}^{(i)} = \mathrm{E}\left[\left|\tilde{d}_{k,l}^{(i)} - d_{k,l}\right|^2\right]$. The BER can be approximately given by [84]:

$$\mathrm{BER}_k \approx \mathrm{Q}\left(\sqrt{\frac{1}{\frac{1}{N_C}\sum_{l=0}^{N_C-1}\mathrm{MSE}_{k,l}}}\right), \tag{4.13}$$

where $\mathrm{Q}(x)$ is the Gaussian function. Note that minimize the MSE is equivalent to minimize the BER. Mathematically, the optimization problem can be formuted as

$$\min_{\mathbf{f}_{k,l}\mathbf{b}_{k,l}} \mathrm{MSE}_{k,l}^{(i)} \text{ s.t. } \frac{1}{N_C}\sum_{l=0}^{N_C-1}\mathbf{f}_{k,l}\mathbf{h}_{k,l} = 1. \tag{4.14}$$

After some mathematical manipulations

$$\mathbf{f}_{k,l}^{(i)} = \left[\mathbf{H}_l^H\left(\mathbf{I}_K - \boldsymbol{\Psi}^{(i-1)^2}\right)\mathbf{H}_l + \frac{\sigma_n^2}{\sigma_d^2}\mathbf{I}_M\right]^{-1}\mathbf{H}_l^H\boldsymbol{\Omega}_l^{(i)}, \tag{4.15}$$

$$\mathbf{b}_{k,l}^{(i)} = \mathbf{H}_{k,l}\mathbf{f}_{k,l}^{(i)} - \boldsymbol{\Gamma}_k, \tag{4.16}$$

where $\boldsymbol{\Psi}^{(i)} = \mathrm{diag}\left(\psi_1^{(i)}, \ldots, \psi_K^{(i)}\right)$ and $\boldsymbol{\Omega}_l^{(i)} = \left(\mathbf{I}_K - \boldsymbol{\Psi}^{(i-1)^2}\right)\boldsymbol{\Gamma}_k - \frac{\mu_k^{(i)}}{\sigma_d^2}\boldsymbol{\Gamma}_k$, with $\mu_k^{(i)}$ is the Lagrange multiplier for the ith iteration regarding the kth user. $\boldsymbol{\Gamma}_k$ is an appropriate column vector with 0 in all positions except the kth position that is 1.The $\psi_k^{(i)}$ represents the correlation coefficient for the k user at iteration i, which is defined by

$$\psi_k^{(i)} = \frac{\mathrm{E}\left[\hat{d}_{k,l}^{(i)}d_{k,l}^*\right]}{\mathrm{E}\left[\left|d_{k,l}\right|^2\right]}, \quad l = 1, \ldots, L. \tag{4.17}$$

$\hat{\mathbf{d}}_{k,l}^{(i)}$ represents the hard decisions associated to the data estimates and it is related to the $\bar{\mathbf{d}}_{k,l}^{(i)}$ by the following expressions [85] [87]

$$\bar{\mathbf{d}}_{k,l}^{(i)} \simeq \boldsymbol{\Psi}^{(i)} \hat{\mathbf{d}}_{k,l}^{(i)}, \quad (4.18)$$

$$\hat{\mathbf{d}}_{k,l}^{(i)} = \boldsymbol{\Psi}^{(i)} + \boldsymbol{\Delta}_{k,l}, \quad (4.19)$$

where $\Delta_{k,l} = [\Delta_{1,l} \quad \cdots \quad \Delta_{K,l}]^T$ is a zero-mean error vector and it is independent from $\mathbf{d}_{k,l}$ vector. The correlation coefficient is a parameter of great importance in a good receiver performance because it ensures the estimates used in the feedback loop reliability [84].This loop takes into account the decisions for each block plus the overall block reliability, reducing error propagation.

Conventional IB-DFE receivers can be considered low complexity turbo equalizers because there is no need to perform the channel decoding in the feedback loop, employing the equalizer output instead the channel decoder output. We should notice that in the first iteration ($i = 1$), and to detect the first user, there is no information about $\mathbf{d}_n$, thus $\boldsymbol{\Psi}^{(0)}$ and $\mathbf{b}_{k,l}^{(0)}$ are a null matrix and vector, respectively.

5. Joint Iterative Frequency Domain Equalization and Interference Alignment for MC-CDMA

As it was previously stated, spectral resources are scarce and have to be managed with efficiency due to the increasing demand of wireless services. Future multimedia applications will need high bit rates in order to maintain a desirable quality of service. MC-CDMA has been proposed as a good air-interface in downlink [33] [88].

This scheme is a combination between OFDM and CDMA, bringing together the advantages of both schemes. For example, it has high spectral efficiency and robustness against multipath fading like OFDM based schemes and it has a flexible multiple access with good interference properties like CDMA based schemes [19] [20]. MC-CDMA system is mostly limited by interference, which can be reduced by employing precoding techniques and IB-DFE based receivers [22] [23].

On one hand, to reduce interference may be considered linear frequency domain equalization (FDE) with MMSE criterion. However, the residual interference level may still be relatively high, which causes degradation in the performance (still several dB from the matched filter bound, or MFB) [24]. Nonlinear time domain equalizers may outperform the linear ones [25]. One of the most promising nonlinear FDE is IB-DFE, which was extended for diversity scenarios, MIMO systems and MC-CDMA systems, among others [89] [90] [91]. IB-DFE can be seen as a low complexity turbo equalizer implemented in the frequency-domain and it doesn't require a channel decoder output in the feedback loop [25].

On the other hand, it is possible to remove interference and achieve a linear capacity scaling by introducing IA [26]. This technique allows maximum degrees of freedom (DoF) and, consequently, allowing a better performance than other interference cancellation methods [27]. As we saw in chapter 4, there is a closed-form solution for constant channels but it can only be

used in a very particular case: when the overall system supports only 3 users. If $K > 3$, the precoding vectors formulation is done by an iterative algorithm [26] [92] [93] .

In the present chapter, a joint iterative IA precoding at the transmitter with IB-DFE successive interference cancellation (SIC) based receiver structure for MC-CDMA systems is designed. In the considered scheme the chips are IA-precoded instead of the data symbols as in narrowband or OFDM-based systems as discussed in chapter 3. The receiver is designed in two steps: first a linear filter is used to mitigate the inter-user aligned interference, and then an iterative frequency-domain receiver is designed to efficiently separate the spatial streams in the presence of residual inter-user aligned interference at the output of the filter. The matrices for this non-linear space-frequency equalizer are obtained by minimizing the mean square error (MSE) of each user at each subcarrier. The receiver structure is explicitly designed taking into account the residual inter-user interference, allowing both an efficient separation of the spatial streams and a reduction in the number of iterations of the IA procedure. This is very important because it will allow reducing the information needed to be exchanged between the different transmitter-receiver pairs. The designed scheme achieves the maximum degrees of freedom provided by the IA precoding, while allowing an almost optimum space-diversity gain, with performance close to the matched filter bound (MFB).

In this chapter it will be used the following notation: $\mathrm{tr}(\mathbf{A})$ is the trace of matrix $\mathbf{A}$, $\nu_{\min}^{P}(\mathbf{A})$ is the matrix whose columns are the eigenvectors corresponding to the P smallest eigenvalues of matrix $\mathbf{A}$ and $\mathbf{e}_p$ is an appropriate column vector with 0 in all positions except the pth position that is 1.

5.1. System Model

The transmitter proposed in this work is an IA-precoded MC-CDMA based, where it is considered a K-user MIMO interference channel with constant coefficients on per-subcarrier basis. The same physical channel is shared by K transmitter-receiver pairs, where a given transmitter only intends to have its P_k spatial data symbols on each subcarrier decoded by a single receiver. Without loss of generality, it was considerate a symmetric case, where all transmitters and receivers have M antennas ($M_R = M_T = M$), and $P_k = P \ \forall k$. It is denoted by an (M, M, K) interference channel with P data symbols per-subcarrier.

For $K \leq 3$, the number of spatial DoF achievable is only $KM/2$ for an (M, M, K) interference channel. Although, for $K > 3$, the DoF achievable is $P_t = \sum_{k=1}^{K} P_k < 2M - 1$ [94]. So, our system has $KM/2$ and P_t spatial DoF per-subcarrier for $K \leq 3$ and $K > 3$, respectively.

Figure 5.1 shows the proposed kth MC-CDMA based transmitter. Firstly, the constellation symbols $d_{k,p,l}$ are selected according to given mapping rule with $\mathrm{E}\left[\left|d_{k,p,l}\right|^2\right] = \sigma_d^2$.

Secondly, each P L-length data symbol blocks, $\{d_{k,p,l}; k = 1, \dots, K, p = 1, \dots, P, l = 0, \dots, L-1\}$, is spread into L chips using orthogonal Walsh-Hadamard codes, forming the block $\{s_{k,p,l}; p = 1, \dots, P, l = 0, \dots, L-1\}$.

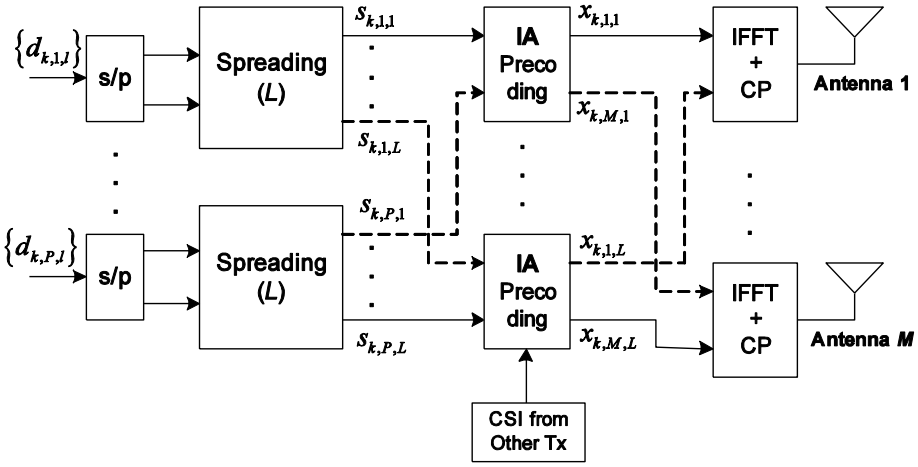

Figure 5.1: IA-precoded MC-CDMA based transmitter proposed

Thirdly, set of P chips (one of each block) is weighed by an IA-precoding matrix. The resulting signal at the kth transmitter subcarrier l is:

$$\mathbf{x}_{k,l} = \mathbf{W}_{k,l}\mathbf{s}_{k,l} \qquad (5.1)$$

where $\mathbf{s}_{k,l} = [s_{k,1,l} \quad \cdots \quad s_{k,P,l}]^T$ and $\mathbf{W}_{k,l} \in \mathrm{C}^{M \times P}$ is the linear precoding matrix calculated at the kth transmitter on subcarrier l, constrained to $\left\|\mathbf{W}_{k,l}\right\|_F^2 \leq T_P$. T_P is the transmit power at the transmitters. Finally, the precoding signals are mapped into an OFDM symbol and it is inserted the cyclic prefix.

At the receiver and after cyclic prefix removal and FFT operation, the received frequency-domain signal for the kth transmitter subcarrier l is given by

$$\mathbf{y}_{k,l} = \mathbf{H}_{k,k,l}\mathbf{W}_{k,l}\mathbf{s}_{k,l} + \sum_{\substack{j=1 \\ j \neq k}}^{K} \mathbf{H}_{k,j,l}\mathbf{W}_{j,l}\,\mathbf{s}_{j,l} + \mathbf{n}_{k,l} \qquad (5.2)$$

where $\mathbf{H}_{k,j,l}$ is a $M \times M$ matrix and denotes the overall channel between the transmitter j and receiver k on subcarrier l, and $\mathbf{n}_{k,l}$ is the additive white Gaussian noise (AWGN) vector at the receiver k on subcarrier l, in other words, $\mathbf{n}_{k,l} \sim \mathrm{CN}(0, \sigma_n^2\mathbf{I}_M)$. To obtain the equation (5.2), we assume that the CP is long enough to account for different overall cannel impulse responses between the transmitters and receivers, i.e., including transmit and receive filters, multipath

propagation effects and differences in the time-of-arrival for different transmitter-to-receiver links.

As it can be seen in Figure 5.2, the detection procedure is done by two different blocks. The first is a linear filter used to mitigate the aligned user's interference. The signal after this block is given by

$$\bar{\mathbf{y}}_{k,l} = \mathbf{\Phi}_{k,l}^{H}\mathbf{H}_{k,k,l}\mathbf{W}_{k,l}\mathbf{s}_{k,l} + \mathbf{\Phi}_{k,l}^{H}\sum_{\substack{j=1 \\ j\neq k}}^{K}\mathbf{H}_{k,j,l}\mathbf{W}_{j,l}\,\mathbf{s}_{j,l} + \mathbf{\Phi}_{k,l}^{H}\mathbf{n}_{k,l} \qquad (5.3)$$

where $\mathbf{\Phi}_{k,l}^{H} \in \mathrm{C}^{M\times P}$ corresponds to the first linear receiving filter.

The second is a non-linear equalizer based on IB-DFE principle, designed to separate the spatial P L-length data block.

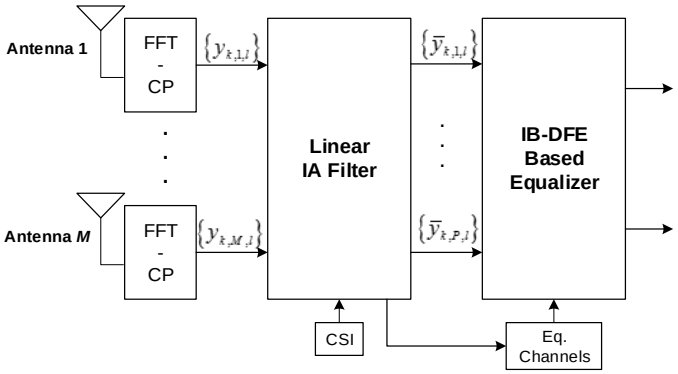

Figure 5.2: Proposed MC-CDMA receiver structure [29]

5.2. Precoding and Equalizer Design

In this section is presented iterative minimum interference leakage (IL) IA precoding algorithm considered in this work, followed by the proposed nonlinear iterative space-frequency equalizer.

5.2.1. IA Precoders

We considered an iterative approach to a general case because closed-form solutions have been found in few specific cases (e.g. $K \leq 3$) [93]. The objective of using this technique is to precode the signal at the transmitter j in a way that the interference caused by that specific transmitter won't affect in the receiver k. For $k \neq j$, the interference caused by transmitter j in

the receiver k is nearly orthogonal to the subspace of its receive space. This subspace has an orthonormal basis $\mathbf{\Phi}_{k,l}$ and it has precoders jointly designed to optimize an appropriate cost function.

The iterative interference leakage algorithm minimizes the total interference leakage (IL) that remains at each receiver after attempting to cancel the aligned interference. This step is done by left multiplication with $\mathbf{\Phi}_{k,l}^{H}$ for each user k (in equation (5.3)). The global function to optimize is

$$\Im_{IL} = \sum_{k=1}^{K} \sum_{\substack{j=1 \\ j \neq k}}^{K} \left\| \mathbf{\Phi}_{k,l}^{H} \mathbf{H}_{k,j,l} \mathbf{W}_{j,l} \right\|_{F}^{2} \qquad (5.4)$$

which is denoted by IL. The optimization problem can be formulated as

$$\min \Im_{IL}\left(\{\mathbf{W}_{j,l}\}, \{\mathbf{\Phi}\}\right) \text{s.t.} \begin{cases} \mathbf{W}_{\mathrm{j},l}^{H} \mathbf{W}_{j,l} = T_p \mathbf{I}_P, & j \in \{1, \ldots, K\} \\ \mathbf{\Phi}_{k,l}^{H} \mathbf{\Phi}_{k,l} = \mathbf{I}_P, & j \in \{1, \ldots, K\} \end{cases} \qquad (5.5)$$

One simple way to solve this problem is to use an alternating minimization procedure [93]. This iterative algorithm, at first, defines an arbitrary orthogonal basis $\mathbf{\Phi}_{k,l}$ for each receiver subspace on each subcarrier. Then finds the precoding matrix $\boldsymbol{W}_{j,l}$ such that each node has maximum squared Euclidean distance between it and the subspace spanned by the columns of each $\mathbf{\Phi}_{k,l}$ by using

$$\mathbf{W}_{j,l} = \upsilon_{\min}^{P} \left(\sum_{\substack{j=1 \\ j \neq k}}^{K} \mathbf{H}_{k,j,l}^{H} \mathbf{\Phi}_{k,l} \mathbf{\Phi}_{k,l}^{H} \mathbf{H}_{k,j,l} \right) \qquad (5.6)$$

and, then, updates the receiver orthonormal subspaces according to

$$\mathbf{\Phi}_{j,l} = \upsilon_{\min}^{P} \left(\sum_{\substack{j=1 \\ j \neq k}}^{K} \mathbf{H}_{k,j,l} \mathbf{W}_{j,l} \mathbf{W}_{j,l}^{H} \mathbf{H}_{k,j,l}^{H} \right) \qquad (5.7)$$

Equations (5.6) and (5.7) are repeated until convergence. This can be carried out until $\Im_{IL}(\mathrm{t}) < \varepsilon$ if feasibility conditions are met, or $|\Im_{IL}(\mathrm{t}-1) - \Im_{IL}(\mathrm{t})| < \varepsilon$ otherwise, for an arbitrary threshold ε.

The IA at receiver k on subcarrier l is ideally orthogonal to the subspace $\mathbf{\Phi}_{k,l}$ because each subspace is reserved for every single k's signal (i.e. for each user) on each subcarrier. After the interference aligned has been mitigated with left multiplication $\mathbf{\Phi}_{k,l}$, each receiver must be separated the desired spatial streams. It is possible to use a MMSE linear equalizer, so the linear

equalizer $\mathbf{G}_{k,l}$ is formed by multiplying $\mathbf{\Phi}_{k,l}^{H}$ and the linear spatial equalizer $\overline{\mathbf{G}}_{k,l}$ in a conventional receiver. $\overline{\mathbf{G}}_{k,l}$ neglects the inter-user interference aligned and equalizes only the intended signal: $\mathbf{G}_{k,l} = \overline{\mathbf{G}}_{k,l}\mathbf{\Phi}_{k,l}^{H}$. Then the vector $\tilde{\mathbf{s}}_{k,l} = \overline{\mathbf{G}}_{k,l}\bar{\mathbf{y}}_{k,l}$ is the estimate of the original transmit vector $\mathbf{s}_{k,l}$.

5.2.2. Iterative Equalizer Design

As discussed above, in MC-CDMA based systems, linear equalization is not efficient to separate the spatial streams due to residual inter-carrier interferences (ICI). Also, in an IA based system, it is neglected the inter-user aligned interference. One may access that a linear equalizer is not the best option. The subspace $\mathbf{\Phi}_{k,l}$ should be full orthogonal to interference aligned subspace but this is not possible for some practical scenarios [95] and/or requires a relatively high number of iterations [93]. To solve these problems it was developed a new non-linear receiver structure based on IB-DFE principles, accounting the residual inter-user interference and allowing the perfect alignment requirement to be more relaxed. This receiver separates, efficiently, the P L-length data symbol blocks even to systems that suffer from residual inter-user interference, not needing a perfect orthogonality.

- *Parallel Interference Cancellation (PIC)*

In the paper [29], it was proposed and IB-DFE PIC based equalizer used to separate the spatial streams for IA precoded MC-CDMA systems. In this section, we briefly review this schemes and the extension to the IB-DFE SIC is derived. Figure 5.3 illustrates the mains blocks of the IB-DFE PIC based procedure. In each iteration, it is detected all P L-length data block of the kth receiver in a parallel way. Most of the updated estimated of the transmit data symbols is used cancel the residual interference.

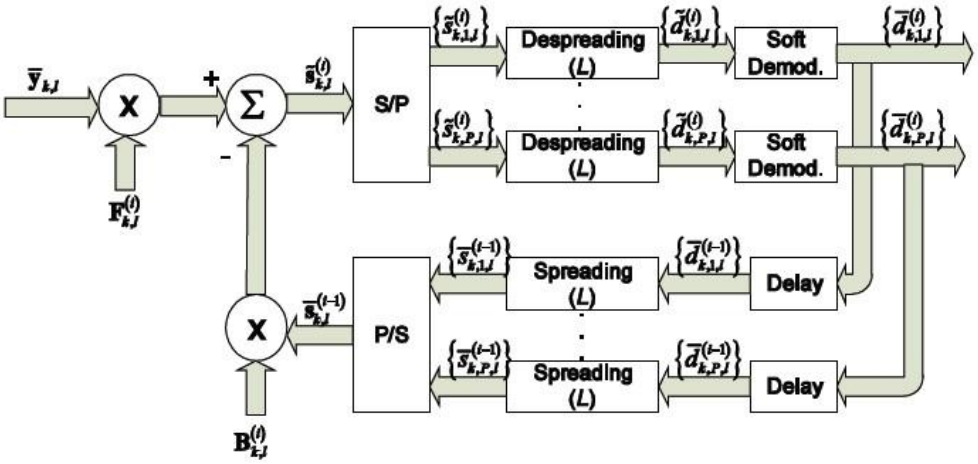

Figure 5.3: Iterative receiver PIC equalizer based on IB-DFE concept

At the ith iteration and before despreading, the signal at kth receiver on the lth subcarrier associated to the pth L-length data block is given by:

$$\tilde{\mathbf{s}}_{k,p,l}^{(i)} = \mathbf{F}_{k,l}^{(i)T} \bar{\mathbf{y}}_{k,l} - \mathbf{B}_{k,l}^{(i)T} \bar{\mathbf{s}}_{k,l}^{(i-1)} \quad (5.8)$$

where $\mathbf{F}_{k,l}^{(i)} \in \mathrm{C}^{P\times P}$ and $\mathbf{B}_{k,l}^{(i)} \in \mathrm{C}^{P\times P}$ and they denote both feedforward and feedback matrices coefficients on the pth data blocked applied on the lth subcarrier at the kth user, respectively, and $\bar{\mathbf{s}}_{k,p,l}^{(i-1)} = \left[\bar{\mathrm{s}}_{k,1,l}^{(i)}, \ldots, \bar{\mathrm{s}}_{k,p-1,l}^{(i)}, \bar{\mathrm{s}}_{k,p,l}^{(i-1)} \ldots, \bar{\mathrm{s}}_{k,P,l}^{(i-1)}\right]^T$.

Setting $\mathbf{H}_{k,j,l}^{eq} = \mathbf{\Phi}_{k,l}^{H} \mathbf{H}_{k,j,l} \mathbf{W}_{j,l}$, it is possible to rewrite the equation (5.3) as

$$\bar{\mathbf{y}}_{k,l} = \underbrace{\mathbf{H}_{k,k,l}^{eq} \mathbf{s}_{k,l}}_{desired\ signal} + \underbrace{\sum_{\substack{j=1 \\ j\neq k}}^{K} \mathbf{H}_{k,j,l}^{eq}\, \mathbf{s}_{j,l}}_{residual\ inter-user\ interference} + \underbrace{\mathbf{\Phi}_{k,l}^{H} \mathbf{n}_{k,l}}_{noise} \quad (5.9)$$

where $\mathbf{H}_{k,k,l}^{eq} \mathbf{s}_{k,l}$ denotes the desired signal, $\sum_{\substack{j=1 \\ j\neq k}}^{K} \mathbf{H}_{k,j,l}^{eq}\, \mathbf{s}_{j,l}$ is the residual inter-user interference, and $\mathbf{\Phi}_{k,l}^{H} \mathbf{n}_{k,l}$ is the noise. Also, $\mathbf{H}_{k,k,l}^{eq} \in \mathrm{C}^{P\times P}$ represents the equivalent channels after IA procedure. The block $\left\{\bar{s}_{k,p,l}^{(i-1)}; l = 0, \ldots, L-1\right\}$ is the spreading of the pth de-spreading block average values conditioned of the detector output $\left\{\bar{d}_{k,p,l}^{(i)}; l = 0, \ldots, L-1\right\}$ for each iteration i.

It could be written that $\bar{\mathbf{s}}_{k,l}^{(i-1)} \approx \mathbf{\Psi}_{k}^{(i-1)^2} \mathbf{s}_{k,l} + \mathbf{\Psi}_{k}^{(i-1)^2} \mathbf{\Delta}_{k,l}$, where the error $\mathbf{\Delta}_{k,l} = [\Delta_{k,1,l} \quad \ldots \quad \Delta_{k,P,l}]^{\mathrm{T}}$ has zero mean and $\mathbf{\Psi}_{k}^{(i)} = \mathrm{diag}\left(\psi_{k,1}^{(i)}, \ldots, \psi_{k,P}^{(i)}\right)$, with correlation coefficients defined as:

$$\psi_{k,p}^{(i)} = \frac{\mathrm{E}\left[\hat{d}_{k,p,l}^{(i)} d_{k,p,l}^{*}\right]}{\mathrm{E}\left[\left|d_{k,p,l}\right|^2\right]} \quad (5.10)$$

being a measure of the pth L-length block estimates reliability associated to the ith iteration.

Considering QPSK modulation $d_{k,p,l}$is $\hat{d}_{k,p,l}^{(i)} = \mathrm{sign}\left(\mathrm{Re}\left\{\tilde{d}_{k,p,l}^{(i)}\right\}\right) + \mathrm{jsign}\left(\mathrm{Im}\left\{\tilde{d}_{k,p,l}^{(i)}\right\}\right)$.

So, the iterative nonlinear equalizer is now characterized by $\mathbf{F}_{k,l}^{(i)}$ and $\mathbf{B}_{k,l}^{(i)}$ in a particular iteration on each receiver. The feedforward and feedback matrices are computed to minimize the overall MSE of the spreading samples $\mathrm{MSE}_{k,l}^{(i)} = \mathrm{E}\left[\left\|\tilde{\mathbf{s}}_{k,l}^{(i)} - \mathbf{s}_{k,l}\right\|^2\right]$, at each iteration.

Therefore, the optimization problem can be formulated as

$$\min_{\mathbf{F}_{k,l}^{(i)}\mathbf{B}_{k,l}^{(i)}} \mathrm{MSE}_{k,p,l}^{(i)} \ \text{s.t}\ \frac{1}{L}\sum_{l=0}^{L-1}\mathrm{tr}\left(\mathbf{F}_{k,l}^{(i)T}\mathbf{H}_{k,k,l}^{eqT}\right) = P \tag{5.11}$$

where $\mathbf{H}_{k,k,p,l}^{eqT} \in \mathrm{C}^{P\times P}$ is the equivalent channel associated to the pth data block. After some mathematical manipulations, the feedforward and feedback vectors can be obtained:

$$\mathbf{F}_{k,l}^{(i)} = \left(\mathbf{H}_{k,k,l}^{eqH}\left(\mathbf{I}_P - \mathbf{\Psi}_k^{(i-1)^2}\right)\mathbf{H}_{k,k,l}^{eq} + \sum_{j=1,j\neq k}^{K}\mathbf{H}_{k,j,l}^{eqH}\mathbf{R}_d\mathbf{H}_{k,k,l}^{eq} + \frac{\sigma_n^2}{\sigma_d^2}\mathbf{I}_P\right)^{-1}\mathbf{H}_{k,k,l}^{eqH}\mathbf{\Omega}_{k,p}^{(i)} \tag{5.12}$$

where $\mathbf{R}_d = \sigma_d^2\mathbf{I}_P$ and

$$\mathbf{B}_{k,l}^{(i)} = \mathbf{H}_{k,k,l}^{eqH}\mathbf{F}_{k,l}^{(i)} - \mathbf{I}_P \tag{5.13}$$

with

$$\mathbf{\Omega}_{k,p}^{(i)} = \left(\mathbf{I}_P - \mathbf{\Psi}_k^{(\mathrm{i}-1)^2}\right) - \frac{\mu_{k,p}^{(i)}}{\sigma_d^2 L}\mathbf{I}_P, \tag{5.14}$$

The Lagrangian multiplier is selected, at each iteration i, to ensure that the condition $\frac{1}{L}\sum_{l=0}^{L-1}\mathrm{tr}\left(\mathbf{F}_{k,l}^{(i)T}\mathbf{H}_{k,k,l}^{eqT}\right) = P$ is fulfilled. Also, it should be noticed that for the first iteration ($i = 1$) and for the first L-length data block to be detected $\mathbf{\Psi}_k^{(0)}$ is a null matrix and $\bar{\mathbf{s}}_{k,l}$ is a null vector.

- *Successive Interference Cancellation (SIC)*

Figure 5.4 illustrates the mains blocks of the IB-DFE SIC based procedure. In each iteration, it is detected all P L-length data block of the kth receiver in a successive way. Most of the updated estimated of the transmit data symbols is used to cancel the residual interference.

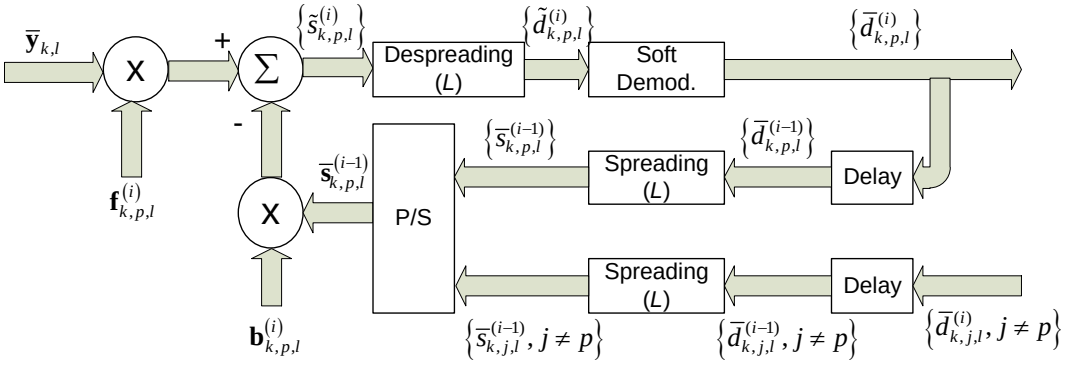

Figure 5.4: Iterative receiver SIC equalizer based on IB-DFE concept

At the ith iteration and before despreading, the signal at kth receiver on the lth subcarrier associated to the pth L-length data block is given by:

$$\tilde{\mathbf{s}}_{k,p,l}^{(i)} = \mathbf{f}_{k,p,l}^{(i)T}\bar{\mathbf{y}}_{k,l} - \mathbf{b}_{k,p,l}^{(i)T}\bar{\mathbf{s}}_{k,p,l}^{(i-1)} \quad (5.15)$$

where $\mathbf{f}_{k,p,l}^{(i)} \in \mathrm{C}^{P\times 1}$ and $\mathbf{b}_{k,p,l}^{(i)} \in \mathrm{C}^{P\times 1}$ and they denote both feedforward and feedback vectors coefficients on the pth data blocked applied on the lth subcarrier at the kth user, respectively, and $\bar{\mathbf{s}}_{k,p,l}^{(i-1)} = \left[\bar{\mathrm{s}}_{k,1,l}^{(i)}, \ldots, \bar{\mathrm{s}}_{k,p-1,l}^{(i)}, \bar{\mathrm{s}}_{k,p,l}^{(i-1)} \ldots, \bar{\mathrm{s}}_{k,P,l}^{(i-1)}\right]^T$. If we compare the equation (5.8) with the (5.15), they are undoubtedly similar. However, due to its series nature, the coefficients of feedforward and feedback are no longer matrices but vectors.

The iterative non-linear equalizer is characterized by the coefficients $\mathbf{f}_{k,p,l}^{(i)}$ and $\mathbf{b}_{k,p,l}^{(i)}$ in a particular iteration and at each receiver. Contrarily to the PIC approach, to compute these vectors, we need to minimize the MSE of the spreading samples associated to the pth L-length data block on lth subcarrier $\mathrm{MSE}_{k,p,l}^{(i)} = \mathrm{E}\left[\left|\tilde{s}_{k,p,l}^{(i)} - s_{k,p,l}\right|^2\right]$. The optimization problem can be formulated as

$$\min_{\mathbf{f}_{k,p,l},\mathbf{b}_{k,p,l}} \mathrm{MSE}_{k,p,l}^{(i)} \ \mathrm{s.t}\ \frac{1}{L}\sum_{l=0}^{L-1}\mathbf{f}_{k,p,l}^{(i)T}\mathbf{h}_{k,k,p,l}^{eqT} = 1 \quad (5.16)$$

where $\mathbf{h}_{k,k,p,l}^{eqT} \in \mathrm{C}^{P\times 1}$ is the equivalent channel associated to the pth data block. After some mathematical manipulations, the feedforward and feedback vectors can be obtained:

$$\mathbf{f}_{k,p,l}^{(i)} = \left(\mathbf{H}_{k,k,l}^{eqH}\left(\mathbf{I}_P - \mathbf{\Psi}_k^{(i-1)^2}\right)\mathbf{H}_{k,k,l}^{eq} + \sum_{j=1,j\neq k}^{K}\mathbf{H}_{k,j,l}^{eqH}\mathbf{R}_d\mathbf{H}_{k,k,l}^{eq} + \frac{\sigma_n^2}{\sigma_d^2}\mathbf{I}_P\right)^{-1}\mathbf{H}_{k,k,l}^{eqH}\mathbf{\Omega}_{k,p}^{(i)} \quad (5.17)$$

and

$$\mathbf{b}_{k,p,l}^{(i)} = \mathbf{H}_{k,k,l}^{eqH}\mathbf{f}_{k,p,l}^{(i)} - \mathbf{e}_p \quad (5.18)$$

with

$$\mathbf{\Omega}_{k,p}^{(i)} = \left(\mathbf{I}_P - \mathbf{\Psi}_k^{(\mathrm{i}-1)^2}\right)\mathbf{e}_p - \frac{\mu_{k,p}^{(i)}}{\sigma_d^2 L}\mathbf{e}_p \quad (5.19)$$

The Lagrangian multiplier is selected, at each iteration i, to ensure that the condition $\frac{1}{L}\sum_{l=0}^{L-1}\mathbf{f}_{k,p,l}^{(i)T}\,\mathbf{h}_{k,k,p,l}^{eqT} = 1$ is fulfilled. Also, it should be noticed that for the first iteration ($i = 1$) and for the first L-length data block to be detected $\mathbf{\Psi}_k^{(0)}$ is a null matrix and $\bar{\mathbf{s}}_{k,p,l}^{(0)}, p = 1$ is a null

vector. Lastly, the signal after filtering process is given by (5.9) and the correlation coefficients are computed using the equation (5.10).

5.3. Numerical Results

In this section, it is presented the performance results for the developed receiver structure, which was composed by an IA precoding with an IB-DFE based equalizer built upon the successive interference cancellation multi-user's detection. These results were obtained considering that: The channels between each transmitter and receiver pair are uncorrelated and severely time-dispersive, each one with rich multipath propagation and uncorrelated Rayleigh fading for different multipath components. Specifically, we assume a $Lp = 32$-path frequency-selective block Rayleigh fading channel with uniform power delay profile (i.e., each path with average power of $1/Lp$). The same conclusions could be drawn for other multipath fading channels, provided that the number of separable multipath components is high. Also, it was assumed perfect channel state information and synchronization.

The results are presented in terms of average bit error rate (BER) as a function of average bit energy per one-sided noise power spectral density (E_b/N_0). For the sake of comparisons, it is included the matched filter bound (MFB), and it was introduced the results for the standard linear IA MMSE scheme. In this case, the second IB-DFE based equalizer is not considered. Also, the results are compared with the IB-DFE PIC approach recently proposed in [29].

The FFT size was set at 128 with a QPSK constellation under Gray mapping rule. There were built two scenarios:

1. Four transmitter-receiver pairs ($K = 4$), each equipped with five antennas ($M = 5$), transmitting simultaneously two L-length data block ($P = 2$). This scenario is referred as (5, 5, 4) interference channel with $P = 2$.
2. Three transmitter-receiver pairs ($K = 3$), each equipped with four antennas ($M = 4$), transmitting simultaneously two L-length data block ($P = 2$). This scenario is referred as (4, 4, 3) interference channel with $P = 2$.

Figure 5.5 and Figure 5.6 show the results for (5, 5, 4), with $P = 2$ and 100 iterations in the IA procedure (this number was found enough to have free inter-user aligned interference) and it is presented the results for 1, 2 and 4 iterations of the IB-DFE SIC and PIC based equalizers, respectively. Firstly let's analyze the results of Figure 5.5. The first thing we notice is the results of the first IB-DFE iteration are already better than the standard linear MMSE equalization. This behavior happens because SIC-based structures to detect a given data block takes into account the previous detected ones, with the exception of the first data block. It is possible to see that

there is a significant improvement from the 1st iteration to the 2nd, with a BER of 10^{-5}, the difference is almost 8 dB and from the 2nd to the 4th there is an improvement of approximately 1,2 dB. The difference between the MFB and the 4th iteration is smaller than 0,5 dB for the same BER. From Figure 5.6 is possible to draw the same conclusions as for the results obtained in the previous scenario. However, we can observe that for this case the 1st iteration curve matches the linear standard IA MMSE curve (not presented in this plot for clarity) contrary to SIC based curves. This is caused by the parallel nature of the PIC equalizer. In the 1st iteration, $\boldsymbol{\Psi}_k^{(0)}$ is a null matrix and $\bar{\mathbf{s}}_{k,l}$ is a null vector, resembling only the linear receiver. Comparing the SIC and the PIC approach, it is clear that for the first and second iterations the SIC approach outperforms the PIC one. This is because the SIC based structure to detect a given user takes into account the previous detected ones, with the exception for the first user. However, when the number of iteration increases, the performance of the PIC approach tends to the one given by the SIC approach. We can observe that the BER performance of both approaches is basically the same for four 4 iterations.

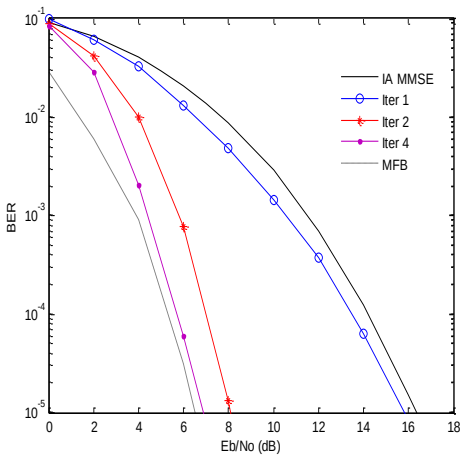

Figure 5.5: Proposed SIC receiver structure for (5, 5, 4) with *P*=2 and 100 IA iterations performance.

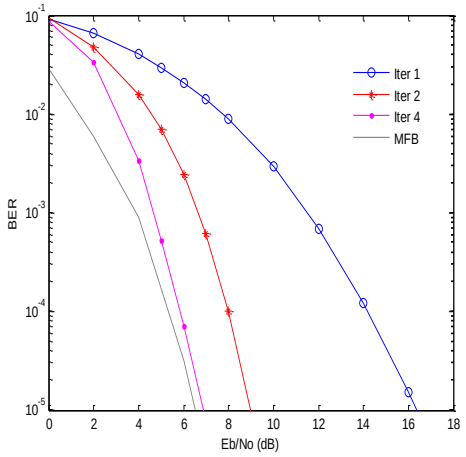

Figure 5.6: PIC receiver structure for (5, 5, 4) with *P*=2 and 100 IA iterations performance.

The results of Figure 5.7 and Figure 5.8 were obtained for the same parameters than Figure 5.5 and Figure 5.6, respectively, however the number of IA procedure iterations was set to 10. Because of this drastic reduction, we decided to include the 8th IB-DFE iteration. In this case the inter-user aligned interference cannot be neglected and may have a significant impact on the system performance. As we can observe in both figures, there is performance degradation. For BER of 10^{-5}, the difference between the MFB and the 8th IB-DFE iteration is almost 2 dB for both SIC and PIC. Comparing the 2nd iteration of Figure 5.6 and Figure 5.5 for a BER of 10^{-2}, there is a difference of almost 1 dB and, now comparing the 4th iteration for the same BER, the difference is 0,8 dB. This reduction allows us to conclude that the proposed scheme efficiently mitigates the residual inter-user interference.

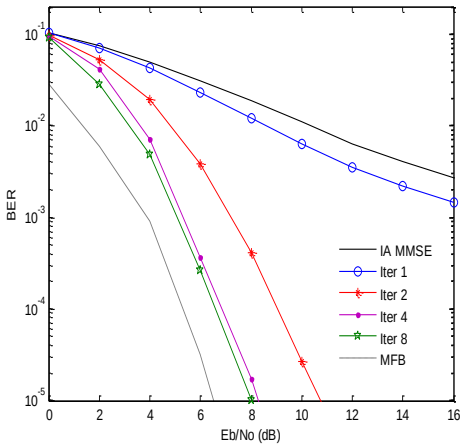

Figure 5.7: Proposed SIC receiver structure for (5, 5, 4) with *P*=2 and 10 IA iterations performance.

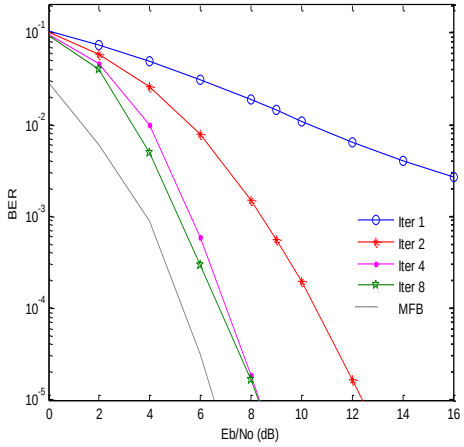

Figure 5.8: PIC receiver structure for (5, 5, 4) with *P*=2 and 10 IA iterations performance.

From Figure 5.9 and Figure 5.10, it is possible to draw the same conclusions as for the results obtained in the previous scenario. Decreasing the number of users to three with $P = 2$, forces to decrease the number of antennas to four, in order to fulfil the conditions for the alignment presented in section 5.2.2. This number of antennas decreases DoF, keeping the diversity at the same level as the scenario with $K = 4$. As it should be expected the performance is basically the same.

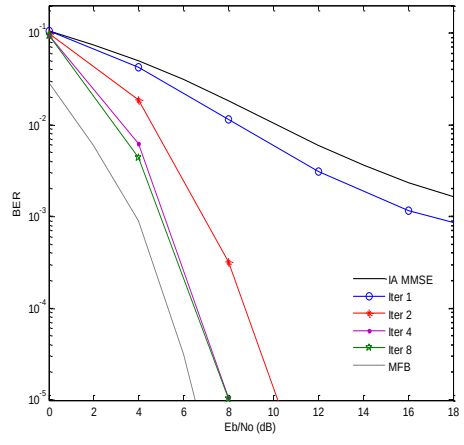

Figure 5.9: Proposed SIC receiver structure for (4, 4, 3) with *P*=2 and 10 IA iterations performance.

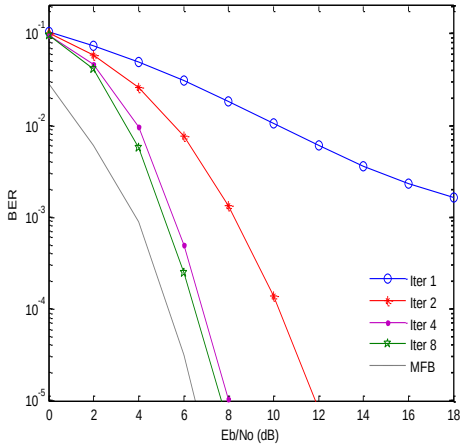

Figure 5.10: PIC receiver structure for (4, 4, 3) with *P*=2 and 10 IA iterations performance.

Another question arose, how does vary the system performance in function of the number of iterations in the IA procedure? Figure 5.11 presents the results for (5, 5, 4), both with $P = 2$, first and fourth iterations for the IB-DFE based equalizer and several iterations in the IA procedure (5, 10, 20, 50, 100).

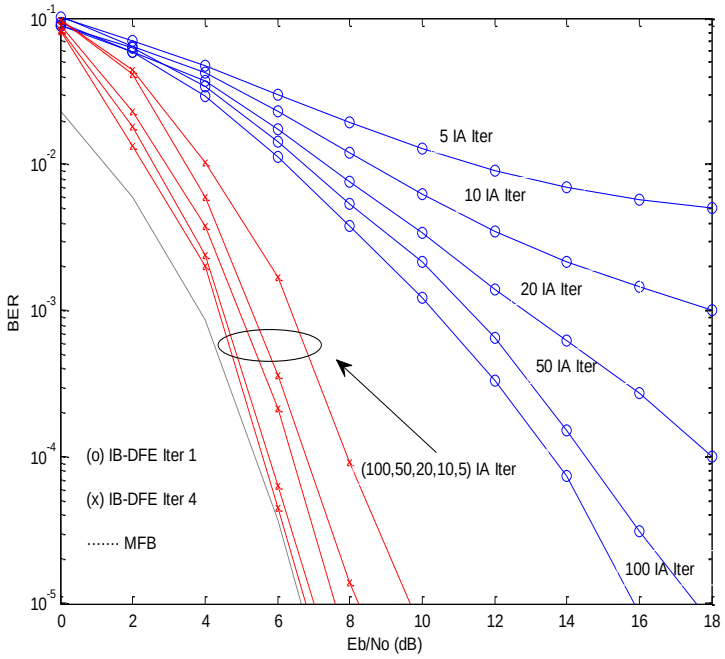

Figure 5.11: Proposed receiver structure for (5, 5, 4) with *P*=2 for several IA iterations performance.

From Figure 5.11, we can observe that if we increase the number of IA iterations the performance will be better. With four equalizer iterations, we can see that the performance degradation is relatively small. In other words, we almost have the same performance with 100, 50 and 20 IA iterations. This means that we can reduce the number of IA iterations and thus reducing the amount of information exchanged between the different transmitter-receiver pairs. However, if we have only one equalizer iteration, the number of IA iterations becomes extremely important. As we can see in the figure, there is significant performance degradation from 100 to 5 IA iterations because the residual inter-user interference increases as the number of IA iterations decreases.

The results in Figure 5.12 and Figure 5.13 were obtained for the same parameters in Figure 5.7 and Figure 5.8, respectively. Here, it is compared the performances of two approaches: Robust against Non-Robust. The Robust approach is the results of the proposed scheme. In the case of the Non-Robust, it is ignored the residual inter-user aligned interference, i.e., the term $\sum_{j=1,j\neq k}^{K} \mathbf{H}_{k,j,l}^{eqH} \mathbf{R}_d \mathbf{H}_{k,k,l}^{eq}$ in (5.17) is not considered. This figure shows the significant performance impact caused by the residual inter-user aligned interference; a Non-Robust scheme presents lower BER values. These results prove that the proposed receiver structure is robust to the inter-user aligned interference. Once again, the results obtain from the IB-DFE SIC receiver is better in the first iterations than the IB-DFE PIC receiver but by increasing the number of iteration the PIC response will approach the SIC.

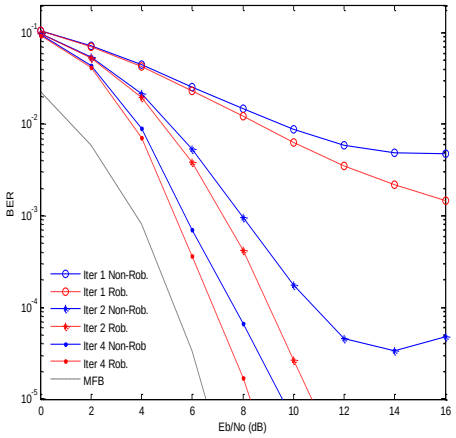

Figure 5.12: Proposed SIC receiver structure (Rob.) against the non-robust approach (Non-Rob) for (5, 5, 4) with *P*=2 for 10 IA iterations performance.

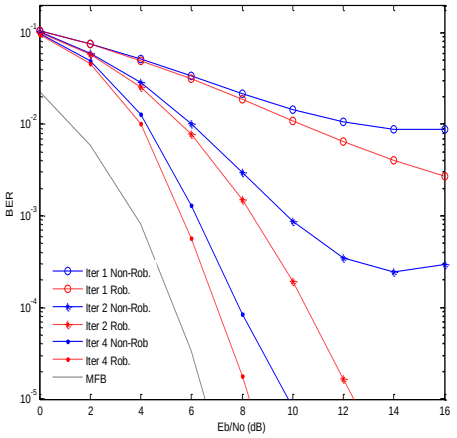

Figure 5.13: PIC receiver structure (Rob.) against the non-robust approach (Non-Rob) for (5, 5, 4) with *P*=2 for 10 IA iterations performance.

6. Conclusions and Future Work

In chapter 1, we could observe that mobile communications are growing and being develop at great pace. If we ask our parents if they had a mobile phone, sent SMS or had internet everywhere, when they were our age, they will most certainly say no. To be truthful, mobile phones invaded our lives and they came to stay. They are spread all over the world and the number of users is still increasing. Nowadays, these devices are much more than voice communication devices. They became our diaries, notebooks, photographic cameras, among so many others applications. This increase in services and users demanded the development and implementation of new technologies. While the reduction of the cell size reduces the propagation loss, the inter-user interferences present at cells edge increases. To solve this problem, it is assigned different frequencies to different cells, wasting system capacity. Multicell cooperation or coordination is a promising architecture that eliminates inter-users interference while improving systems fairness and increasing capacity.

In this thesis, we started by briefly presenting the evolution of cellular communications before LTE. The different generations are the milestones, which mark the evolution of cellular systems. The first generation had analog voice transmissions, while the second had already moved on to digital. With the third generation, it became possible to access multimedia data services. Nowadays we are living the concept of “Anywhere, anything, anytime” with LTE technology, which has a performance with higher data rates and higher user mobility. However the evolution did not stop at this stage, the LTE Release 10, or LTE-Advanced was frozen in April 2011.

In the second chapter, it was described the multiple carrier and multiple access schemes. It was presented, with some detail, OFDM/OFDMA systems and MC-CDMA. OFDMA was deployed in the downlink of LTE systems, assuming an important role in wireless communications. Although OFDM based systems have high spectral efficiency and robustness against multipath fading, by being combined with CDMA systems, they allow flexible multiple access and good interference properties, forming MC-CDMA scheme. So this scheme was proposed as the air-interface in

downlink because it allows achieving high bit rates. Later in this chapter, it was presented some detection techniques for single user and multi-user detection. In MUD, the detection takes into account the effects of inter-user interference. Interference cancellation techniques (PIC and SIC) are used because they provide a good relation between performance and complexity.

In chapter 3, it was introduced another solution to achieve high bit rates. The multiple antenna systems allow exploiting diversity, spatial multiplexing and beamforming in order to improve data rates. Later in this chapter, it was presented, with more detail, LTE and LTE-Advanced systems under the light of the previous technologies. We saw that LTE represent a great improvement over the 3G technologies but they are still unable to respond to the demands set by ITU. We focused our attention in LTE physical layer and multi-antenna modes. LTE-Advanced was proposed to match and enhance IMT-Advanced goals. Two technologies that allow increasing capacity and bit rates are the carrier aggregation and the coordinated multipoint.

In chapter 4, it was introduced the interference alignment techniques. These techniques allow to efficiently eliminate the inter-user interference, allowing achieving the maximum number of degrees of freedom. In this chapter, we focused our attention in the special case of $K = 3$ users closed form. Later in this chapter, it was presented iterative equalization for single carrier systems. Here we saw that linear equalizers have relatively low complexity but they still suffer from noise enhancement and residual ISI. This allowed us search for a nonlinear approach that outperforms the linear one. We studied an iterative equalizer based on the IB-DFE principles.

In chapter 5, it was considered a MIMO MC-CDMA system with IA precoding on each subcarrier at the transmitter and with IB-DFE based processing at the receiver. The receiver structure is composed by two parts: At first is a linear filter, which mitigates the inter-user aligned interference, and then an iterative frequency-domain equalizer, which separates the spatial streams. The results have shown that the proposed receiver structure is robust to the inter-user aligned interference and efficient to separate the spatial streams. The performance gets pretty close to MFB with few equalizer iterations. Also, the robust residual inter-user aligned interference allows a significant reduction on the iterations number of the IA process and thus reducing the information exchanged between the different transmitter-receiver pairs. It is also possible to conclude that both PIC and SIC approaches produce similar results, except with fewer equalizer iterations, where SIC's performance is a little better.

6.1. Future Work

Concerning the future work, we suggest the following improvements on the simulation platform:

- In this work, it was assumed a $(5,5,4)$ and $(4,4,3)$ interference channels with $P = 2$. It would be interesting to extend it in order to support even more users.
- It would be also interesting to compare these systems for a $P \neq 2$ data symbols per subcarrier.
- In this thesis' simulations was considered perfect channel information. It would be interesting to observe how the proposed system would behave with imperfect channel information.
- To compute the precoders it was used the IL algorithm, it would be interesting to combine other iterative IA algorithms with IB-DFE at the receiver.

7. References

[1] Newstream/Arraycomm, “Martin Cooper - History of Cell Phone,” [Online]. Available: http://inventors.about.com/cs/inventorsalphabet/a/martin_cooper.htm.

[2] M. L. Roberts, M. A. Temple, R. F. Mills and R. A. Raines, “Evolution of the Air Interface of Cellulares Communications Systems Toward 4G Realization,” *IEEE Communications Surveys & Tuturials,* vol. 8, no. 1, 2006.

[3] M. Ehrenkrona, “How mobile phones have changed our lives,” [Online]. Available: http://www.ericssonhistory.com/communication/how-the-telephone-changed-the-world/How-mobile-phones-have-changed-our-lives/.

[4] K. Wesolowski, Mobile Communication Systems, Chichester: John Wiley & Sons Ltd, 2002.

[5] “GSM: Global System for Mobile Communications,” [Online]. Available: http://www.4gamericas.org/index.cfm?fuseaction=page&sectionid=242.

[6] “Mobile Market Shares by Technology,” [Online]. Available: http://www.4gamericas.org/index.cfm?fuseaction=page&pageid=565.

[7] E. Seurre, P. Savelli and P.-J. Pietri, “Introduction to EDGE,” in *EDGE for Mobile Internet*, Boston, Artech House, 2003, pp. 51-52.

[8] A. R. Mishra, Cellular Technologies for Emerging Markets 2G, 3G and Byond, Chichester: John Wiley & Sons Ltd, 2010.

[9] C. Cox, An Introduction to LTE, Chichester: John Wiley & Sons Ltd, 2012.

[10] “Global HSPA-LTE Forecast,” [Online]. Available: http://www.4gamericas.org/index.cfm?fuseaction=page&pageid=1940.

[11] G. A. Abed, M. Ismail and K. Jumari, “The Evolution to 4G Cellular Systems: Architecture and Key Features of LTE-Advanced Networks,” *International Journal of Computer Networks and Wireless Communications,* vol. 2, no. 1, pp. 21-26, 2012.

[12] M. Rumney, LTE and the Evolution to 4G Wireless, Padstow: John Wiley & Sons Ltd, 2009.

[13] I. F. Akyildiz, D. M. Gutierrez-Estevez and E. C. Reyes, “The evolution to 4G cellular systems: LTE-Advanced,” *Physical Communication,* vol. 3, pp. 217-244, 2010.

[14] J. Wannstrom, “LTE-Advanced,” 3GPP, June 2013. [Online]. Available: http://www.3gpp.org/technologies/keywords-acronyms/97-lte-advanced.

[15] J. A. C. Bingham, "Multicarrier Modulation for Data Transmission: An Idea Whose Time Has Come," *IEEE Communications Magazine,* vol. 25, no. 5, Feb. 2002.

[16] S. B. Weinstein and P. M. Ebert, “Data Transmission by Frequency Division Multiplexing Using Discrete Fourier Transformer,” *IEEE Transactions on Communications Technology,* vol. 19, Oct. 1971.

[17] M. Engles, Wireless OFDM Systems: How to Make Them Work?, Kluwer Academic Publishers, 2002.

[18] S. Kaiser, Multi-Carrier CDMA Mobile Radio System - Analysis and Optimization of Detection, Decoding and Channel Estimation, Ph. D. Thesis, ISBN 3-18-353110-0, Düsseldorf, 1998.

[19] S. Hara and R. Prasad, “Overview of Multicarrier CDMA,” *IEEE Communications Magazine,* vol. 35, no. 12, Dec. 1997.

[20] L. Hanzo, M. Münster, B. J. Choi and T. Keller, OFDM and MC-CDMA for Broadband Multi-user Communications, WLANs and Broadcasting, West Sussex: Jonh Wiley & Sons Ltd., 2004.

[21] K. Fazel and S. Kaiser, Multi-Carrier and Spread Spectrum Systems, New York: John Wiley & Sons Ltd, 2003.

[22] A. Silva and A. Gameiro, “Transmission Strategies for MISO downlink MC-CDMA Mobile Systems,” *Wireless Personal Communication,* vol. 54, no. 3, pp. 521-541, Aug. 2010.

[23] P. Silva and R. Dinis, “Joint Turbo Equalization and Multiuser Detection of MC-CDMA Signals With Strongly Nonlinear Transmitters,” *IEEE Trans on Vehicular Technology,* vol. 58, no. 5, pp. 2288-2298, Jun 2009.

[24] N. Benvenuto, R. Dinis, D. Falconer and S. Tomasin, “Single Carrier Modulation with Non Linear Frequency Domain Equalization: An Idea Whose Time Has Come – Again,” *IEEE Proceedings,* vol. 98, no. 1, pp. 69-96, Jan. 2010.

[25] J. Proakis, Digital Communications, New York: MacGraw-Hill, 3rd edn, 1995.

[26] V. Cadambe and S. Jafar, "Interference alignment and degrees of freedom of the K-user interference channel," *IEEE Transactions on Information Theory,* vol. 54, no. 8, pp. 3425-3441, Aug. 2008.

[27] M. A. Maddah-Ali, A. S. Motahari and A. K. Khandani, "Communicating over MIMO X channels: Interference alignment, decomposition, and performance analysis," *IEEE Transactions on Information Theory,* vol. 54, no. 8, pp. 3457-3470, Aug. 2008.

[28] S. A. Jafar, "Interference Alignment - A New Look at Signal Dimensions in a Communication Network," *Foundations and Trends in Communications and Information Theory,* vol. 7, no. 1, 2010.

[29] A. Silva, S. Teodoro, R. Dinis and A. Gameiro, "Iterative Frequency-Domain Detection for IA-Precoded MC-CDMA Systems," *IEEE Transactions on Communications,* vol. 62, no. 4, pp. 1240 - 1248, April 2014.

[30] H. Holma and A. Toskala, LTE for UMTS – OFDMA and SC-FDMA Based Radio Access, Chichester: John Wiley & Sons Ltd, 2nd edn, 2009.

[31] A. Goldsmith, Wireless Communications, Cambridge University Press, Aug. 2005.

[32] A. F. Molisch, Wireless Communications, Chichester: John Wiley & Sons Ltd, 2nd edn, 2011.

[33] K. Fazel and S. Kaiser, Multi-Carrier and Spread Spectrum Systems, Chichester: John Wiley & Sons Ltd, 2nd edn, 2008.

[34] H. Hosseini, N. Fisal and S. K. Syed-Yusof, "Wavelet Packet based Multicarrier Modulation for Cognitive UWB Systems," *Signal Processing – An International Journal (SPIJ),* vol. 4, no. 2, 2010.

[35] A. Silva and A. Gameiro, *OFDM /OFDMA, SC-FDMA and MC-CDMA Techniques,* University of Aveiro: Comunicações Sem Fios Lecture, 2013/14.

[36] V. Mittal and S. Mittal, "A Cyclic Prefix OFDM System with BPSK Modulation," *Global Journal of Researches in Engineering Electrical and Electronics Engineering,* vol. 12, no. 7, July 2012.

[37] E. Krouk and S. Semenov, Modulation and Coding Techniques in Wireless Communication, Chichester: A John Wiley and Sons Ltd, 2011.

[38] M. Nohrborg, "LTE Overview," 3 GPP, [Online]. Available: http://www.3gpp.org/technologies/keywords-acronyms/98-lte.

[39] A. M. Tulino, L. Li and S. Verdú, "Spectral Efficiency of Multicarrier CDMA," *IEEE Transactions on Information Theory,* vol. 51, 2 February 2005.

[40] S. Verdú, Multiuser Detection, Cambridge University, 2001.

[41] D. G. Brennan, "Linear Diversity Combining Techniques," *Proceedings of the IRE,* vol. 47, Jun. 1959.

[42] K. Fazel, S. Kaiser, P. Robertson and M. J. Ruf, "A Concept of Digital Terrestrial Television Broadcasting," *Wireless Personal Communications,* vol. 2, 1995.

[43] A. Sibille, C. Oestges and A. Zanella, MIMO From Theory to Implementation, Academic Press, 2011.

[44] G. H. Golub and C. F. Van Loan, Matrix Computation, Johns Hopkins University Press, 1996.

[45] A. Silva, Técnicas de Cancelamento PIC para o Sistema UMTS-TDD, Master Thesis, Aveiro, April 2002.

[46] J. Y. Baudais, J. F. Herald and J. Citerne, "An Improved Linear MMSE Detection Technique for Multi-Carrier CDMA Systems: Comparison and Combination with Interference Cancelation Schemes," *European Transactions on Telecomunications,* vol. 11, no. 6, Nov./Dec. 2000.

[47] D. N. Kalofonos and J. G. Proakis, "Performance of the Multistage Detector for MC-CDMA System in a Rayleigh Fading Channel," in *IEEE Proceedings of GLOBECOM*, 1996.

[48] J. Bastos and A. Gameiro, "Multisensor Interference Cancellation Performance in Asynchronous Uplink on MC-CDMA Systems," in *Proceedings of the 11th Asia-Pacific Conference on Communications (APCC)*, 2005.

[49] J. Bastos, A. Silva and A. Gameiro, "Performance Evaluation of Multisensor Parallel Interference Cancellation for the Uplink on MC-CDMA Systems," in *7th International Symposium on Wireless Personal Multimedia Communications*, 2004.

[50] S. Kaiser and J. Hagenauer, "Multi-Carrier CDMA with Iterative Decoding and Soft-Interference Cancellation," in *IEEE Proceedings of GLOBECOM*, 1197.

[51] S. Sandhu, R. Nabar, D. Gore and A. Paulraj, "Introduction to Space-Time Codes," [Online]. Available: web.stanford.edu/group/sarg/sandhu062503.pdf.

[52] "Transforming MIMO Test With Fast, Accurate Signal Creation and Channel Emulation," 1 Oct. 2008. [Online]. Available: http://www.agilent.com/about/newsroom/tmnews/background/2008/01oct2008_pxb.html.

[53] I. Poole, “MIMO Formats - SISO, SIMO, MISO, MU-MIMO,” [Online]. Available: http://www.radio-electronics.com/info/antennas/mimo/formats-siso-simo-miso-mimo.php.

[54] D. Gesbert, M. Kountouris, R. W. Heath Jr., C.-B. Chae and T. Sälzer, “From Single User to Multiuser Communications: Shifting the MIMO Paradigm,” *IEEE Signal Processing Magazine,* 2007.

[55] M. Mohaisen, Y. Wang and K. Chang, “Multiple Antenna Technologies,” 2009. [Online]. Available: arxiv.org/ftp/arxiv/papers/0909/0909.3342.pdf.

[56] Y. Huang and K. Boyle, Antennas From Theory to Practice, Chichester: A John Wiley and Sons Ltd, 2008.

[57] E. Biglieri, R. Calderbank, A. Constantinides, A. Goldsmith, A. Paulraj and H. V. Poor, MIMO Wireless Communications, Cambridge: Cambridge University Press, 2007.

[58] “MIMO Wireless Communications,” 26 October 2005. [Online]. Available: http://www.eng.newcastle.edu.au/eecs/fyweb/Archives/2005/c2104305/mimo.html.

[59] A. Silva and A. Gameiro, *Multiple Antenna Systems,* University of Aveiro: Comunicações Sem Fios Lecture, 2013/14.

[60] Mprical, “Key HSPA+ Throughput Feature,” 13 September 2011. [Online]. Available: http://www.mpirical.com/blog/article/171.

[61] TELETOPIX.ORG, “Beamforming in LTE,” 27 December 2011. [Online]. Available: http://www.teletopix.org/4g-lte/beamforming-in-lte/.

[62] G. M. C. d. Anjos, MIMO Processing Techniques for 4G Systems, Master Thesis, Aveiro, 2013.

[63] S. Sesia, I. Toufik and M. Baker, LTE - The UMTS Long Term Evolution, Chicago: John Wiley & Sons Ltd, 2009.

[64] E. Dahlman, S. Parkvall, J. Sköld and P. Beming, 3G Evolution, Oxford: Elsevier Ltd, 2008.

[65] Z. Lin and G. Wood, “TMS320TCI6618 - TI’s high-performance LTE physical layer solution,” *White Paper,* 2011.

[66] Telesystem Innovations, “LTE in a Nutshell,” *White Paper,* 2010.

[67] J. Zyren, “Overview of the 3GPP Long Term Evolution Physical Layer,” *White Paper,* 2007.

[68] Z. Ghadialy, “Interoperability between LTE FDD/TDD network,” 18 November 2011. [Online]. Available: http://blog.3g4g.co.uk/search/label/TD-LTE.

[69] Agilent Technologies, “SC-FDMA Frame Structure,” [Online]. Available: http://wireless.agilent.com/wireless/helpfiles/n7624b/Content/Main/SC-FDMA_Frame_Structure.htm.

[70] T. Zacharopoulou, “An Introduction to LTE,” 25 June 2012. [Online]. Available: http://0el70lte.wordpress.com/2012/06/25/hello-world/.

[71] Telesystem Innovations, “The seven Modes of MIMO in LTE,” *White Paper,* 2009.

[72] Rohde & Schwarz GmbH & Co., “LTE Transmission Modes and Beamforming,” *White Paper,* 2011.

[73] T. J. A. Marques, Cooperation Schemes between Base Stations for LTE on the Downlink, Master Thesis, Aveiro, 2013.

[74] “LTE-advanced: next-generation wireless broadband technology [Invited Paper],” *Wireless Communications, IEEE,* vol. 17, no. 3, pp. 10-22, June 2010.

[75] S. Georgoulis, “Testing carrier aggregation in LTE-Advanced network infrastructure,” Aeroflex Test Solutions, 20 June 2012. [Online]. Available: http://edn.com/design/test-and-measurement/4375804/Testing-carrier-aggregation-in-LTE-Advanced-network-infrastructure.

[76] Agilent Technologies, “Introducing LTE-Advanced,” *White Paper,* 2011.

[77] D. Gesbert, S. Antipolis, S. Hanly, H. Huang and S. S. Shitz, “Multi-Cell MIMO Cooperative Networks: A New Look at Interference,” *IEEE Journal on Selected Areas in Communications,* vol. 28, no. 9, pp. 1380-1408, Dec. 2010.

[78] Y. Birk and T. Kol, "Informed-Source Coding-On-Demand (ISCOD) over Broadcast Channels," in *Proceedings of the Seventeenth Annual Joint Conference pf the IEEE Computer and Communications Societies*, IEEE INFOCOM'98, 1998.

[79] S. A. Jafar and S. Shamai, “Degrees of Freedom Region for the MIMO X Channel,” *IEEE Transactions on Information Theory,* vol. 54, no. 1, pp. 151-170, 11 May Jan 2008.

[80] T. Gou and S. A. Jafar, “Degrees of Freedom of the K User M × N MIMO Interference Channel,” *IEEE Transactions on Information Theory,* vol. 56, no. 12, 31 August 2008.

[81] J. Proakis and M. Salehi, Digital Communications, 5th edn, Mc-Graw Hill, 2005.

[82] R. Dinis, A. Gusmão e N. Esteves, “On Broadband Block Transmission over Strongly Frequency-Selective Fading Channels,” *Proc. Wireless,* July 2003.

[83] N. Benvenuto and S. Tomasin, “Block iterative dfe for single carrier modulation,” *Electronics*

Letters, vol. 38, no. 19, pp. 1144 -1145, Sep 2002.

[84] A. Silva, J. Assunção, R. Dinis and A. Gameiro, "Performance evaluation of IB-DFE-based strategies for SC-FDMA systems," *EURASIP Journal on Wireless Communications and Networking,* Dec. 2013.

[85] F. C. Ribeiro, Multicell Cooperation for Future Wireless Systems, Master Thesis, Lisboa, Set. 2012.

[86] F. Ganhão, Energy-efficient Diversity Combining for Different Access Schemes in a Multi-Path Dispersive Channel, Doctoral Thesis, Lisboa, Jan. 2014.

[87] R. Dinis, P. Silva and A. Gusmão, "IB-DFE Receivers with Space Diversity for CP-Assisted DS-CDMA and MC-CDMA Systems," *European Transactions on Telecommunications,* vol. 18, no. 7, pp. 791-802, June 2007.

[88] F. Zabini, B. M. Masini, A. Conti and L. Hanzo, "Partial equalization for MC-CDMA systems in non-ideally estimated correlated fading," *IEEE Transactions on Vehicular Technology,* vol. 59, no. 8, pp. 3818 - 3830, October Oct. 2010.

[89] R. Dinis, A. Gusmão and N. Esteves, "Iterative Block-DFE Techniques for Single-Carrier-Based Broadband Communications with Transmit/Receive Space Diversity," in *1st International Symposium on Wireless Communication Systems*, Sep. 2004.

[90] R. Dinis, R. Kalbasi, D. Falconer and A. Banihashemi, "Iterative Layered Space-Time Receivers for Single-Carrier Transmission over Severe Time-Dispersive Channels," *IEEE Communications Letters,* vol. 9, no. 8, pp. 579-581, Sep. 2004.

[91] R. Dinis, P. Silva and T. Araújo, "Turbo Equalization with Cancelation of Nonlinear Distortion for CP-Assisted and Zero-Padded MC-CDMA Schemes," *IEEE Transactions on Communications,* vol. 57, no. 8, pp. 2185-2189, Sep. 2009.

[92] H. Shen, B. Li, M. Tao and X. Wang, "MSE-based transceiver designs for the MIMO interference channel," *IEEE Transactions on Wireless Communications,* vol. 9, no. 11, pp. 3480-3489, Nov. 2010.

[93] S. W. Peters and R. W. Heath Jr., "Cooperative algorithms for MIMO interference channels," *IEEE Transactions on Vehicular Technology,* vol. 60, no. 1, pp. 206-218, Jan. 2011.

[94] C. M. Yetis, S. A. Jafar and A. H. Kayran, "Feasibility conditions for interference alignment," in *IEEE Global Telecommunications Conference (GLOBECOM)*, 2009.

[95] O. El Ayach, S. W. Peters and J. R. W. Heath, "The practical challenges of interference alignment," *IEEE Wireless Communications,* vol. 20, no. 1, pp. 35-42, Fev. 2012.